Feasibility of increasing the pedestal height on the J-class lift vessel by 10 meters

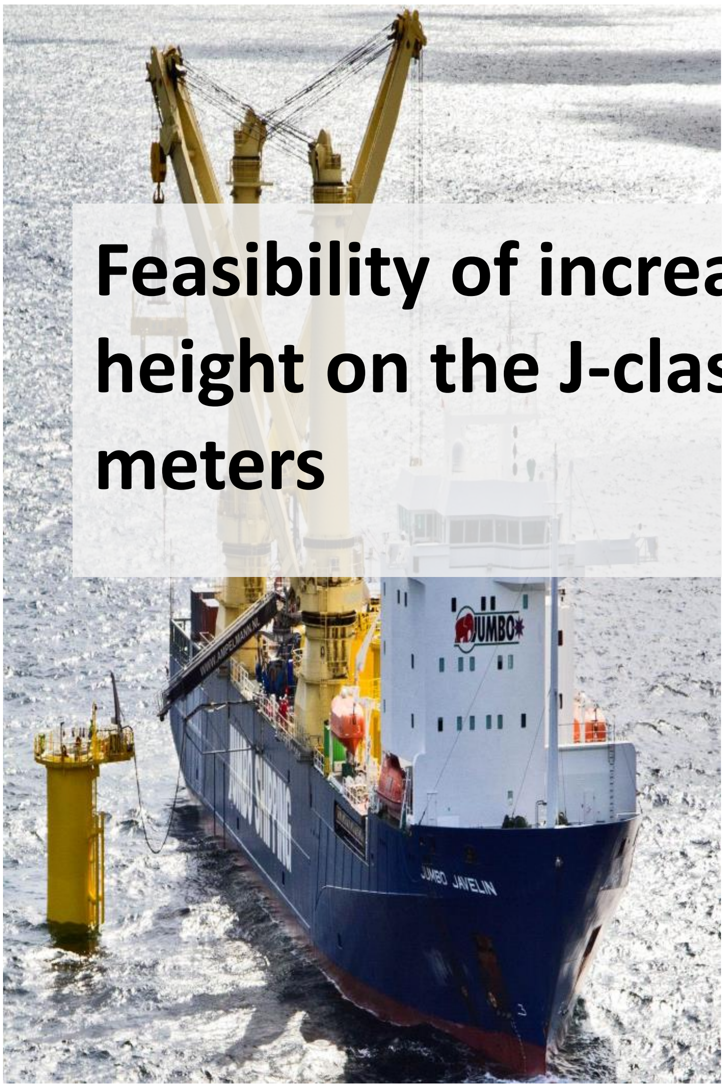

Moonhee Lee

Master thesis

Delft, May 2016

JUMBO

TU Delft Delft University of Technology

Master of Science Thesis

Feasibility of increasing the pedestal height on the J-class lift vessel by 10 meters

Moonhee Lee

May, 2016

DELFT UNIVERSITY OF TECHNOLOGY

SPONSOR: JUMBO MARITIME

Graduation committee

Prof. dr. ir. A.V. Metrikine	TU Delft
Dr. ir. J. De Oliveira Barbosa	TU Delft
Ir. K. van der Heiden	Jumbo
Dr. ir. K.N. van Dalen	TU Delft

Preface

In this report the work done for my final thesis is presented for the completion of the master study "Offshore and Dredging Engineering" at Delf University of Technology. This is done in coöperation with Jumbo Maritime, a company based in Schiedam specialized in shipping and heavy lift operations.

I would like to thank Jumbo Maritime for the opportunity to perform this work. It was an enjoyable experience in which I learned a lot about the inner workings of vessels and heavy lift processes. Also my graditude to my company supervisor Kasper van der Heiden for his support and insights, but also for his focus on the individual learning experience and growth.

At the University my thanks goes to the graduation committee. The guidance and advise from Joao De Oliveira Barbosa was helpful. The meetings with the committee were effective and always clear.

Lastly, my family who always rooted for me and friends who were interested and listened to what I had to say.

May, 2016

Abstract

In order for Jumbo to stay competitive in the offshore market, it's heavy lift vessels should be able to take on a wide range of lifting purposes. This can range from installation of transition pieces for wind turbines to installing modules of fpso's and platforms. One of the demands from the offshore market requires large lifting heights. It is proposed to increase the lifting height on existing mast cranes by increasing the pedestal by 10 meters. In this thesis it is tried to answer the question whether this is feasible. The pedestal should be increased such that it complies with geometric constraints, stability, vessel motions and structural integrity. This feasibility study is divided in two parts. In the first part it is investigated how the enhanced pedestal influences the vessel with regards to hydrostatic characteristics and vessel motions. This information is used to obtain the changed workability of the vessel.

Stability characteristics were slightly worse compared to the original vessel layout. As a result of this the maximum offshore lifting capacity decreased from 648 ton to 580 ton at an outreach of 36.5m as measured from the centerline of the vessel. For three crane configurations the hydrostatic values were obtained and served as input for the vessel motion analysis. Since the Jumbo Javelin heavy lift vessel is equipped with a DP-2 system, only first order motions needed to be taken into account. The motions, or Response Amplitude Operators (RAO's) express the ratio of the vessel motion amplitudes with the amplitudes of the incoming waves. In all crane configurations, the natural period shifted upwards. From all six degrees of freedom, the roll motion was the largest which is explained by the fact that roll has very little potential damping (energy transfer from ship motion to fluid motion). The final evaluation consisted of a workability study, expressed by the percentage of time that the vessel is able to operate in different sea states. Workability remained similar to the workability of the original vessel in cases where Jumbo performed operations before. A check for North sea circumstances led to an increased workability. This is due to the fact that the natural frequency of the enhanced vessel went further away from the most common sea states.

In the second part of this study the pedestal is evaluated structurally. A pedestal geometry is chosen such that it resists normal bending stresses by using the least amount of material. The Fatigue limit stress was taken as the limiting value. In this way an optimal tapered pedestal shape was chosen with varying wall thicknesses ranging from 6.25cm till 4.85cm along the height of the pedestal. The obtained shape is further processed by studying the natural frequencies of the pedestal including the mast and jib. Ship motions should not interfere with natural frequencies of the crane structure due to the effects of resonance which could lead to disproportionate stresses. To study this a finite element model is created using MATLAB that can include the effects of pedestal taper, crane components and DOF's for different jib angles. Planar motions for a plane frame are considered. 6 DOF's for each element are considered and hence represent elements that take both bending and compression. Natural frequencies for two operating conditions and one stowed condition with tip mass are investigated. The lowest observed frequency has a value of 1.39 rad/s. While the lowest natural frequency of vessel motions considered in the workability study is 1.25 rad/s. This led to the conclusion that the improved pedestal geometry and stiffness are sufficient and hence workable.

Abbreviations

RAO	Response Amplitude Operator
DP-2	Dynamic Positioning 2
DOF	Degree Of Freedom
JONSWAP	Joint North Sea Wave Project
EOM	Equation Of Motion
VCG	Vertical Center Of Gravity

List of Figures

List of Tables

Contents

Chapter 1

Introduction

Amongst offshore activities, heavy lift capabilities of installation vessels play a vital role when it comes to achieving safe and reliable results during the construction of offshore installations. Maintaining the safety of the involved personnel and the operation can only be achieved when the vessel and mast cranes are able to withstand harsh environments caused by wind and waves. The installation of components is done by using mast cranes and fly jibs that are able to move from a fixed position on the vessel towards the location of interest after which objects can be lifted or lowered. In this thesis, it will be investigated if the J-class vessel is able to operate with an increased pedestal height on which the mast crane is mounted. This is done in two parts. In the first part the influence of the pedestal increase on the vessel in terms of stability, motions and workability is investigated. In the second part, an initial analysis is done on the mast crane in terms of structural feasibility in which the static and dynamic properties are calculated.

1.1 Thesis Objective

The objective of this thesis is to investigate the possibility of increasing the height of the pedestal by 10 meters.This will lead to various changes with regards to vessel motions and stability. Initial stability is necessary in order to proceed any further analysis since it determines the vessel motion behavior, hence needs to be evaluated carefully. These vessel motions (expressed in RAO's) will be used to obtain the vessel's operability/workability. Furthermore, increasing the pedestal height will lead to a mast crane that deals with altered working loads. Initial dimensions will be designed as a result from this difference in working load(s) during lifting operations. The dynamic properties of the increased pedestal including the mast and jib need to be assessed in order to stay away from potentially dangerous excitation frequencies. This eventually leads to a conceptual design.

Chapter 2

Vessel Intro & Stability

In this research, the focus will be on the J-class vessels. This type of vessels have the capability to lift up to 1800 ton in dual crane configuration. The Jumbo Javelin is equipped with DP2 station keeping and anti-heeling systems. The main dimensions are given in figure 2.1

Principal Dimensions/Tonnage	
Length o.a.	144.1 m
Length b.p.p	133.8 m
Breadth moulded	26.7 m
Depth to Main Deck	14.1 m
Draft (bottom keel)	6.0 m / 8.1 m
Displacement (at 7.5m)	20,120 Te
Deadweight (at 7.5m)	10,942 Te
GRT	15,022 Te
NRT	4,506 Te

Figure 2.1: Principle dimensions and properties

For some operations it is possible to extend the capabilities of the vessel. If it is required, the lifting height can be increased by means of so called fly-jibs. The fly-jib is an optional addition which allows the J-class to adapt to project specific requirements. An example of a fly jib can be seen in figure 2.2.

Figure 2.2: Fly-jib

2.1 Lifting operations

Heaviest lift		
Cargo on board	2010.5	t
Max lift	574.0	t
Typical lift		
Cargo on board	1625.0	t
Max lift	130.5	t

Figure 2.3: Typical offshore lift

Typical values for lifting loads can be seen as represented in table 2.3. The Jumbo Javelin is used as an offshore heavy lift vessel equipped with two mast cranes with a safe working load of 900t each. Furthermore it is fitted with a fully redundant DP2 system enabling it to maintain its position during offshore lifting activities. In calm water it is able to lift 1800t, while offshore the maximum capacity is 1000t. At this moment, Jumbo is focussing on the installation of [1]:

- Loading/unloading buoys
- Mooring spreads and piles
- Transport of umbilicals and flexible flowlines
- Spool pieces, suction piles
- Jumpers and subsea structures
- Small offshore platforms with piece weights<1100Ts
- Buoyancy cans and riser towers

A pedestal mounted mast crane has some advantages over other types of lifting cranes:

- Low center of gravity
- Small footprint on deck
- Large outreach
- Low construction weight

2.2 static stability

Placing a different lifting crane configuration on the deck of the J-class vessel will lead to a different mass distribution on the vessel's deck. Weight will be added by placing the mast cranes on top of pedestals that are 10 meters heigher than the original. This leads to a change in stability. Stability is defined as the ship's ability to return to its original position once it has been subjected to a disturbing moment or force. A floating structure is said to be in a state of equilibrium or balance when the resultant of all forces and resulting moments is zero. This chapter gives a short description how to evaluate a vessel's stability.

2.2.1 Initial Stability

A vessel's intitial stability can be expressed in terms of mass, shape and buoyancy. A simple example of how these terms are related can be seen in figure 2.4 and 2.5. Note that this represents a situation as approximated by small angles up to 10 degrees. (The vertical shift of the center of buoyancy is ignored). This is a valid assumption since only small angles are allowed during lifting operations.

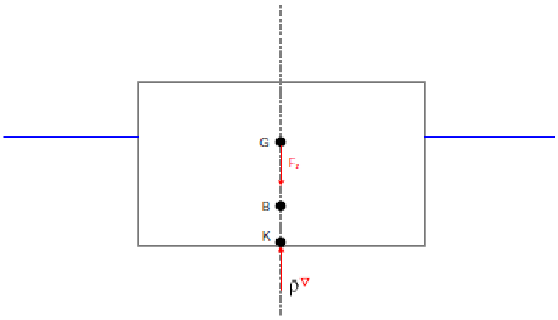

Figure 2.4: Equilibrium situation

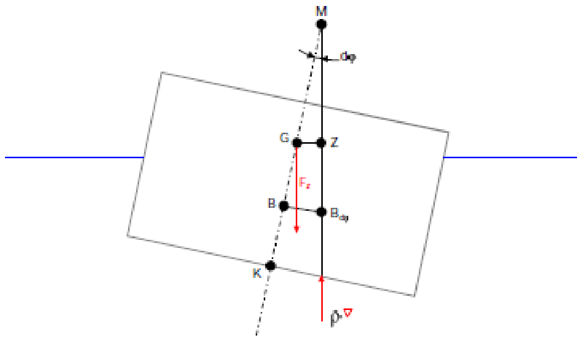

Figure 2.5: Heeled equilibrium

In figure 2.5 M is the metacenter, G the center of gravity, B the center of buoyancy, K is the keel and $B_{d\phi}$ the center of buoyancy at heel. The metacentric height is calculated as follows:

$$\overline{GM} = \overline{KB} + \overline{BM} - \overline{KG} \tag{2.1}$$

$$\overline{BM} = \frac{I_T}{\nabla} \tag{2.2}$$

With KB and KG the distance between the keel and center of buoyancy and gravity respectively, BM is the metacentric radius, I_T the transverse moment of inertia and ∇ the submerged volume of the body. The vessel is in a state of equilibrium when the righting stability moment caused by the force through the center of buoyancy, M_s equals the (external) heeling moment M_H:

$$M_s = M_H \tag{2.3}$$

$$M_s = \rho g \nabla \overline{GZ} \tag{2.4}$$

Furthermore, as can be seen in figure 2.5, $\overline{GZ}$ represents the righting arm over which the righting moment acts through the center of buoyancy. For practical reasons it is very convenient to present the stability in terms of this righting arm since it determines the magnitude of the stability moment. It is defined as:

$$\overline{GZ} = \overline{GM} sin\phi \tag{2.5}$$

The static stability curve visualizes the relation between $\overline{GZ}$ and angle of heel ϕ is given below 2.6.

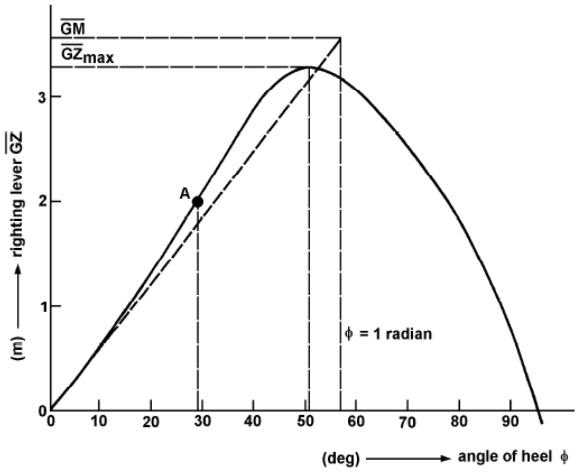

Figure 2.6: Static stability curve

From the stability curve, a few important characteristics can be derived:

- Slope at the origin: The initial metacentric height $\overline{GM}$ can be essential for the shape of the curve, especially at smaller angles of heel and for the area under the curve. This can be shown by the following:

$$\frac{d}{d\phi}\{\overline{GZ}\} = \frac{d}{d\phi}\{\overline{GN}_{\phi} sin\phi\} = \frac{d}{d\phi}\{(\overline{GM} + \frac{1}{2}\overline{BM}tan^2\phi)sin\phi\} \tag{2.6}$$

  At zero heeling angle the heeling angle becomes $\overline{GM}$.

- Maximum $\overline{GZ}$ value: The largest heeling moment that the vessel can resist without capsizing.

- Range of stability: Range of angles for which $\overline{GZ}$ is positive.

- Area under the static stability curve: The necessary work that has to be done to reach a certain heeling angle ϕ.

$$P_{\phi} = \int_0^{\phi} M_s \cdot d\phi = \rho g \bigtriangledown \cdot \int_0^{\phi} \overline{GN}_{\phi} \cdot sin\phi \cdot d\phi \tag{2.7}$$

For completeness, if the vertical shift of the metacenter MN_{ϕ} is equal to the vertical shift of the buoyancy $B'_{\phi}B_{\phi}$, then the following relation holds:

$$\overline{B'_{\phi}B_{\phi}} = \overline{MN_{\phi}} = \frac{I_T}{\nabla}\frac{1}{2}\tan^2\phi \tag{2.8}$$

The metacentric radius (*Scribanti formula*) can be expressed as:

$$\overline{BN_{\phi}} = \overline{BM}(1 + \frac{1}{1}\tan^2\phi) \tag{2.9}$$

$$\overline{GN_{\phi}} = \overline{KB} + \overline{BN_{\phi}} - \overline{KG} \tag{2.10}$$

Since in this thesis, it is investigated what happens if the configuration of the lifting crane changes, it is important to pay some attention on the influence of changing loads on the vessel.

2.3 Moving Loads

The change in center of gravity on a vessel due to a shift in load m at distance d can be expressed as 2.11:

$$\overline{GG_1} = \frac{dm}{\Delta} \tag{2.11}$$

This is visualized in figure 2.7.

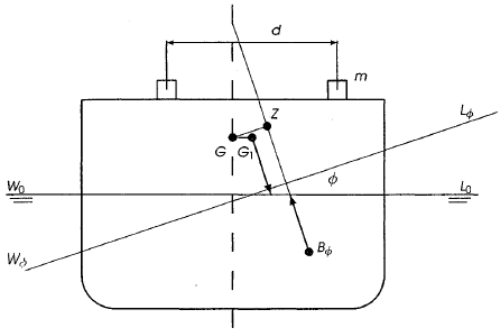

Figure 2.7: Destabilizing effect of mass moving transversely

To illustrate how a moving load can have an influence on the vessel's center of gravity, one needs to relate the heeling moment and the shift of center of gravity. Due to the shift in center of gravity $\overline{GG_1}$, the righting arm $\overline{GZ}$ will be reduced to an effective value $\overline{GZ}_{eff}$ 2.19.

$$\overline{GZ}_{eff} = \overline{GZ} - \frac{dm}{\Delta} cos\phi \tag{2.12}$$

2.4 Hanging Loads

During lifting operations, cargo will be hanging on wires that are connected to the lifting crane influence the overall stability due to heeling of the vessel. When for example the vessel heels with an angle ϕ due to an external moment, the hanging load will move transversely at a distance $h \cdot tan\phi$. As a result, the vessel will move in the same direction, hence:

$$\overline{GG_1} = \frac{hm}{\Delta} tan\phi \tag{2.13}$$

This is visualized in figure 2.8.
If the center of gravity moves to a higher position, the center of gravity will change vertically, GG_v is given as 2.14:

$$\overline{GG_V} = \frac{\overline{GG_1}}{tan\phi} = \frac{hm}{\Delta} \tag{2.14}$$

This leads to the effective metacentric height 2.15:

$$\overline{GM}_{eff} = \overline{GM} - \frac{hm}{\Delta} \tag{2.15}$$

Important to note here is that the mass can be considered to act at the hanging point. This is due to the fact that the metacentric height is reduced by the same amount as it would from lifting the load by a distance h.
Another type of load is moving load. A very common kind of moving load are liquids with free surfaces. Moving liquids can have a large influence of the vessel stability and hence should be disscussed.

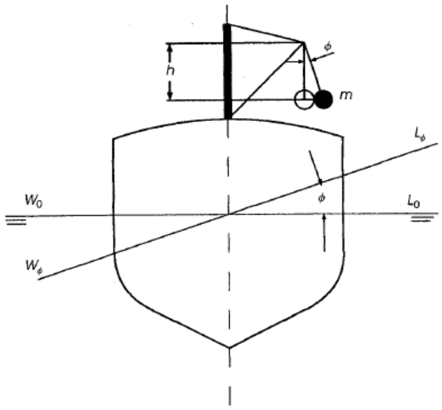

Figure 2.8: Hanging load

2.5 Free surface effects

Another common kind of moving loads are liquids with free surfaces. Free surfaces of liquids inside a vessel can have a large influence on the static stability. It reduces the righting moment or stability lever arm. If the tank filled with liquid is modelled as a ship hull and the free surface is considered, the center of gravity is the center of buoyancy of the liquid. Mostly there are more than one tank present in a vessel and hence need to be summed up to obtain the effective metacentric height. The heeling moment of this free liquid surface can be described by equation 2.16.

$$M_l = \rho i_B tan\phi \tag{2.16}$$

The heeling lever can in return be expressed as 2.17.

$$l_f = \frac{\rho i_B}{\Delta} \tag{2.17}$$

In general, the destabilizing effect of all tanks can be added and express the effective metacentric height and effective righting arm (2.18 and 2.19).

$$\overline{GM} = \overline{GM} - \frac{\sum_n^{k=1} \rho_k i_{Bk}}{\Delta} \tag{2.18}$$

$$\overline{GZ_{eff}} = \overline{GZ} - \frac{\sum_n^{k=1} \rho_k i_{Bk}}{\Delta} sin\phi \tag{2.19}$$

2.6 Stability criteria

Rules for lifting operations are generally created within the company. Mostly based on experience and empirical data. For offshore lifting the company has to satisfy the following rules:

- Intact stability during lifting
- The influence of wind on lifting: weather criterion
- Damage stability during lifting

These stability requirements are determined by a specified section for offshore crane vessels within DNV. A short description of each of these criterion will be discussed in the following sections.

2.6.1 Intact stability during lifting

The intact stability regulations of DNV for highest crane position as found in Pt.5 Ch.7 Sec.9, of which the following statements are the governing rules:

- Loading conditions with a maximum permissable crane load at highest position are to comply with the applicable stability requirements in operation mode.
- If counter ballast is used, the following additional requirements are to be met, with the vessel at the maximum allowable vertical center of gravity in operation mode, to provide adequate stability in case of sudden accidental loss of crane load.
  - Area A2 in figure 2.9 is not less than 40% in excess of area A1.
  - The angle of the first intercept between the righting lever curve after loss of crane load and the maximum permissable counter ballast lever curve is not more than 15 degrees; i.e. angle of equilibrium after loss of crane load.

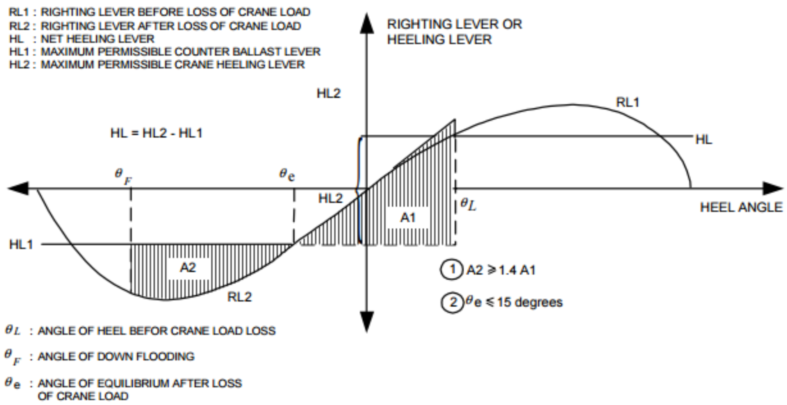

Figure 2.9: Loss of crane load DNV rule

The criteria regarding righting lever curve properties are obtained from IMO 2008 [2].

- For angles up to 30 degrees the area under the righting lever curve shall not be be less than 0.055 meter-radians.
- For angles up to 40 degrees the area under the righting lever curve shall not be less than 0.09 meter-radians.
- For angles between 30 and 40 degrees the area under the righting curve shall not be less than 0.03 meter-radians.
- For angles of heel equal or greater than 30 degrees the righting lever shall be at least $0.2m$.
- The initial metacentric height shall not be less than $0.15m$

2.6.2 Weather criterion

The weather criterion is defined as the vessel's ability to withstand the combined effects of beam winds and rolling. The following assumptions are made [2]:

- The ship is subjected to a steady wind pressure acting perpendicular to the vessel's centerline which results in a steady wind heeling lever l_{wl};

- From the resultant angle of equilibrium ϕ_0, the vessel is assumed to roll owing to wave action to an angle of roll ϕ_0 to windward. The angle of heel under action of steady wind ϕ_0 should not exceed 16^0 or 80% of the angle of deck edge immersion, whichever is less;
- The vessel is then subjected to a gust wind pressure which results in a gust wind heeling lever l_{w2}; and
- Under the circumstances, area b shall be equal to or greater than area a, as indicated in figure 2.10.

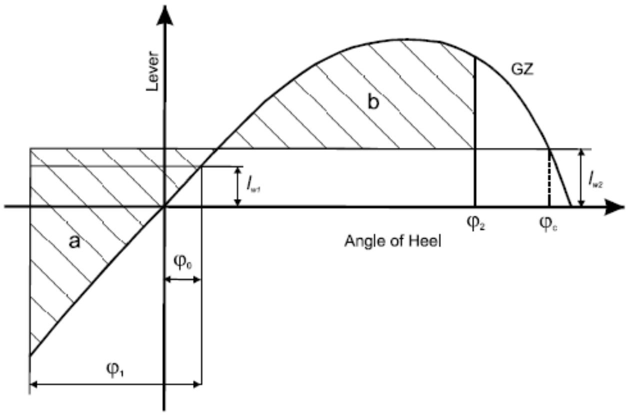

Figure 2.10: Weather criterion: IMO

2.6.3 Damage stability

When a damage occurs, the ship should still be able to float upright. If one or more compartments of the ship are damaged, two things can happen:

- Moving of the center of gravity
- Reduction of the stability ($\overline{GM}$) due to free surface effects

Chapter 3

Stability Analysis

The first step in this feasibility study is to investigate the stability effects of increasing the pedestal of the lifting crane on the J-class by ten meters. It will be checked if the vessel is able to meet the stability requirements.. If the requirements will not be met, the lifting loads need to be lowered iteravely until it does.
To be able to do the stability analysis, use is made of stability software package named *GStab*, by Seaway. It is used internally at Jumbo. *GStab* is a powerful and accuarate stability program for asessing the intact stability of a vessel.
The stability calculations will be done at different lift arrangements. Only tandem lifts will be considered as this arrangement is most likely to be used when lifting large objects. Critical crane positions will be evaluated that will lead to hydrostatic values that can be used for the workability analysis later on in this thesis.

3.1 Stability Calculations

In terms of stability and workability a few positions of the lifting crane are of importance. First, hydrostatic information about the stage before lift off should be obtained for the workability analysis later on. The other critical positions are when the load is at maximum height and at maximum outreach. In the case where the load is at maximum height, the $\overline{GM}$ will be smaller and at maximum outreach, the heeling moment will be the largest.
In order to determine the amount of total ballast water, the situation with the load at maximum outreach needs to be investigated. It should be noted that in *Gstab*, the lightweight conditions are already defined for the J-class vessel and can not be changed. In this lightweight, the lifting crane components are already taken into account and it is not possible to change these design values. In order to obtain the new center of gravity after increasing the pedestal height with ten meters, additional unit loads can be implemented to the existing configuration such that the total center of gravity will be shifted vertically. This additional load will be placed vertically in such a way that it resembles the situation as if the pedestal increase would shift the total center of gravity of the whole arrangement. For each lifting stage, the static stability will be evaluated by the stated criteria. The following information is needed in order to make a thorough static analysis:

- Density of steel used
- Radius of each section
- Thickness of mast and pedestal

The current pedestal dimensions are measured in Autocad and can be seen in figure 3.1 and table 3.1.

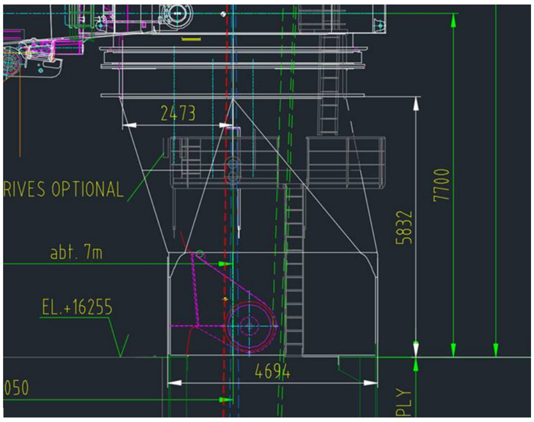

Figure 3.1: Current pedestal dimensions

Pedestal dimensions & properties	
$Length_{outer}$	6.4m
$Width_{outer}$	4.6m
$Height$	5.8 m
$Thickness$	0.035m
ρ_{steel}	7850 kg/m^3
σ_{yield}	250 Mpa

Table 3.1: Pedestal dimensions & properties

The pedestal will be increased by ten meters in height. The additional weight is calculated with the currrent dimensions for the width, length and thickness but with a height of 10m. with the dimensions and density of steel, the additional weight is calculated to be 75850kg per pedestal, hence the combined additional weight of the two pedestals becomes 151700kg, or 151 ton. With the obtained information, a stability analysis can be performed with G-stab. It will be investigated whether the increase in pedestal height will lead to a change of load capacity of the J-class vessels.

3.2 Standard Way Of Ballasting

The ballasting procedure that is used at Jumbo is done by filling the double bottom water tanks at 100% and then fill the wingtanks up to the required level. The total amount of ballast is determined at maximum outreach. It should be noted that the lifting stage before lift-off, the $\overline{GM}$ is highest since it should be able to deal with the shift of load. A consequence of this high $\overline{GM}$ value is that the natural roll period will be lowest during the lifting operation.

The compartments that make out the weight of the vessel consist out of the following masses:

- Lightweight
- Bunkers
- Hatchcover and miscelleneous
- Waterballast
- Load
- Moveable parts
- Coolwater inlet box

3.3 Stability Per Criterion

In this section, the hydrostatic values necessary for the motion analysis need to be obtained. The minimum $\overline{GM}_{min}$ value as used at Jumbo is:

$$\overline{GM}_{min} = 1 + (1.5 \cdot \frac{L}{800}) \tag{3.1}$$

With

L=Load in tonnes

Also information about the roll period needs to be included. The roll period can be expressed as indicated in equation 3.2. The natural roll period can indicate whether large motions will occur in the sea state of interest. Large motions will occur when the natural period and the peak period of the sea will be in the same range. If possible, the natural period should be far outside the peak period of the area in which the lifting operation takes place. The (tank) consumables will be filled up to 50% to take into acount free surface effects.

$$T_0 = \frac{2\pi k_{xx}}{\sqrt{g\overline{GM}}} \tag{3.2}$$

In here

$$k_{xx} = 0.4B$$

The vessel with the altered lifting cranes needs to comply with the stability requirements. Two critical crane arrangements will be investigated. The maximum load will be determined by increasing the loads iteratively until it does not comply with the stability regulations.

- The crane with the jib at maximum height.
- The crane at maximum outreach.

3.3.1 Jib at maximum outreach

In this section, it will be investigated what will be the maximum load when the jib is at its maximum outreach. This will be done by testing if after loss of load, the vessel will still satisfy the stability requirements. This process will be repeated until an optimal load is achieved. The loading condition at maximum outreach needs to satisfy the stability conditions as stated in chapter 2 figure 2.9. The steps necessary to check for dropping loads are stated below:

- At maximum outreach a load is hung in the crane and the ship is ballasted in such a way that the heeling is zero (or minimal).
- The stability requirements are checked (by G-Stab).
- The load is set to zero.
- The stability curve is checked to be within the requirements (area A2 is not less than 40% in excess of Area A1 ; angle of equilibrium after loss of load is not more than 15 degrees).

In case of a sudden drop of load at maximum outreach, the overturning moment will be the same as the heeling moment. Due to this, the transverse center of gravity will change. The $\overline{GZ}$ curve will be tested on the stability requirements. For a range of loads it is checked if at maximum outreach, the stability requirements are met. Also, when the load is removed, the static angle of inclination should be not more than 15 degrees. This is all done in the stability program G-stab. To determine the other drop of load requirement, the restoring energy should be bigger or equal to the net energy required to heel the ship by a factor 1.4 (Chapter 2,figure 2.9), a spread sheet is created and the areas under the GZ-curve ranging from zero to 15 degree angle and 15 till 40 degrees are determined using the trapezium rule. It should be noted that normally the range should be up to 50 degrees (flood point), but since in G-stab, the angles were limited to 40 degrees heeling, the maximum angle is taken up to 40 degrees as well. This has not lead to any problems since the limiting criterium turned out to be the static angle after loss of load. The area representing the restoring energy is 3.25 times the energy required to heel the ship. An example of a stability report from $G - Stab$ can be found in appendix A

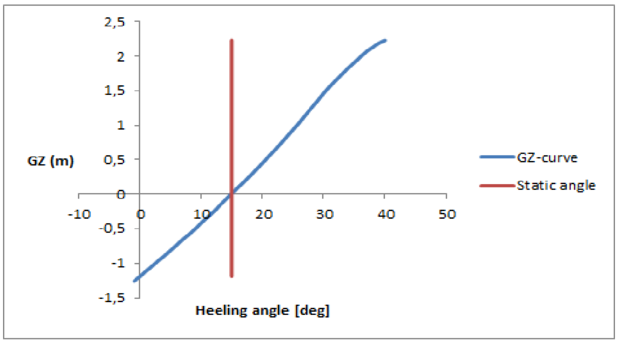

Figure 3.2: Loaddrop check

Following these steps, a maximum load of 580 t at an outreach of 26,5m is achieved. (tandem lift). The resulting hydrostatic values can be seen in table 3.8. The total amount of ballast used is 7179,8 ton. This is the maximum amount of ballast water that will be used during all stages of the lifting operation.

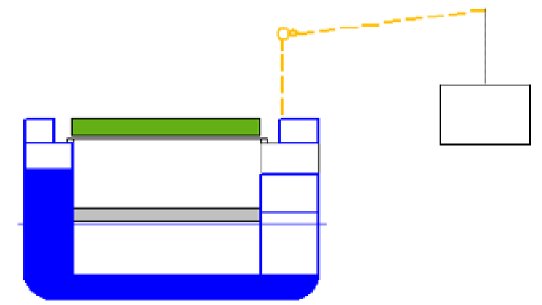

Figure 3.3: Ballast at maximum outreach

Maximum outreach	
Draft	6.94m
$\overline{GM}_{solid}$	3.34m
$\overline{GM}_{liquid}$	3.13m
VCG	9.58m
Displacement	18415t
T_{roll}	11.68s

Table 3.2: Hydrostatics at maximum outreach (increased pedestal)

Maximum outreach	
Draft	6.75m
$\overline{GM}_{solid}$	4.46m
$\overline{GM}_{liquid}$	4.24m
VCG	8.58m
Displacement	17837t
T_{roll}	10.14s

Table 3.3: Hydrostatics at maximum outreach (without increased pedestal)

3.3.2 Jib rigged up at maximum height

The other critical stage for stability is when the jibs are positioned such that the load is at its highest postition. In this stage, the center of gravity will be the highest, which will decrease the $\overline{GM}$ value. This is achieved when the radius of the jibs are at 6.5m radius. Figure 3.5 this position is shown. The criteria stated in G-stab are satisfied and can be seen in table 3.6.

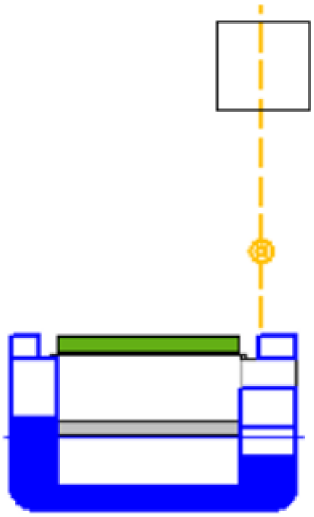

Figure 3.4: Ballast condition at maximum height

Maximum height	
Draft	6.94m
$\overline{GM}_{solid}$	2.82m
$\overline{GM}_{liquid}$	2.58 m
VCG	10.1m
Displacement	18415t
T_{roll}	12.71s

Table 3.4: Hydrostatics at maximum height (increased pedestal)

Maximum height	
Draft	6.75m
$\overline{GM}_{solid}$	3.88m
$\overline{GM}_{liquid}$	3.63 m
VCG	9.16m
Displacement	17837t
T_{roll}	10.88s

Table 3.5: Hydrostatics at maximum height (without increased pedestal)

Number	Criterion	Actual	Required
1	GM Upright >2.08m	2.578	2.08m
2	GZ(30°)>0.2m	1.609m	0.2m
3	V_m should be in range [30°,Vc]	40	30
4	V_m should be in range [25°,Vc]	40	25
5	GZ area in range [Vh,30°]> 0.055m rad	0.391	0.055
6	GZ area in range [Vh,40°]> 0.090m rad	0.719	0.090
7	GZ area in range [0.0°]> 0.090 m rad	0.719	0.090
8	GZ area in range [30°,40°] > 0.030 m rad	0.328	0.030
9	GZ area in range [30°,Vfl]> 0.030 m rad, unprotected	0.328	0.030
10	Weather criterion, Res. area in [Vf, min(Vfl,Vs, 50°)]/res. area [Vw,Vf]> 1.000,unprotected openings, Gust wind	4.530	1.000

Table 3.6: Intact stability criteria check

All the stability requirements are satisfied for the case with the jib at its highest position.

3.3.3 Jib position before liftoff

Before lift-off, the ship is ballasted such that it has the most stability during the whole lifting operation. The jib and load are not in its highest postion, but the ballast water will increase

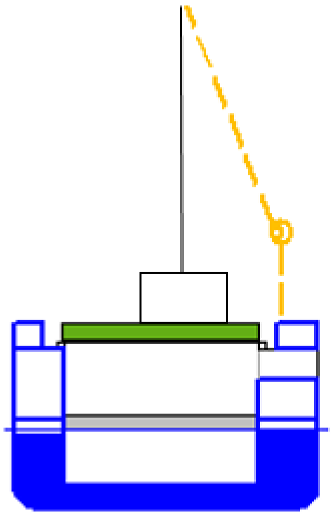

Figure 3.5: Ballast before lift-off

Before lift-off	
Draft	6.94m
$\overline{GM}_{solid}$	4.45m
$\overline{GM}_{liquid}$	4.09 m
VCG	8.58m
Displacement	18415t
T_{roll}	10.23s

Table 3.7: Hydrostatics before lift-off (inreased pedestal)

Before lift-off	
Draft	6.75m
$\overline{GM}_{solid}$	5.02m
$\overline{GM}_{liquid}$	4.77m
VCG	8.02m
Displacement	17837t
T_{roll}	9.56s

Table 3.8: Hydrostatics before lift-off (without increased pedestal)

3.4 Conclusions

In the stability analysis above a comparison has been made between the original and the enhanced vessel with regards to the hydrostatic properties. A general trend that can be observerd from this comparison is that, as expected the vertical center of gravity is shifted above. This has consequences for the natural roll period according to 3.2. A lower $\overline{GM}$ leads to a higher roll period. This has consequences for the motion and workability characteristics as will be explained in the next chapter.

Chapter 4

Waves & Vessel Motions

The J-class vessel will be subjected to waves in offshore environments. For this reason it is important to have a theory that describes waves. Offshore lifting operations take place in a matter of hours and hence are subjected to so called first order wind generated gravity waves. Second order wave effects such as drift forces are left out of consideration because of their large time scale and small magnitudes.
The first part of this chapter will describe the concepts around first order waves. The second part explains the relation between waves and vessel motions.

4.1 Wave Spectrum

The water surface elevation is chaotic and irregular. This irregularity can be modeled as a large summation of individual and independent sinusoidal wave components of which each component has its own frequency, amplitude and phase. To be more precise, the model that will be used here is long crested and unidirectional. This process is visualized in figure 4.1.

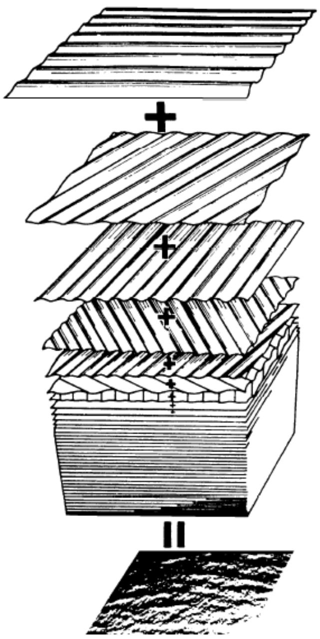

Figure 4.1: Large summation of waves [3]

The mathematical description of this summation is as follows 4.1

$$\eta(t) = \sum_{n=1}^{N} \zeta_{a,n} cos(\omega_n t + \epsilon_n) \tag{4.1}$$

In here

$\eta(t)$	=	water surface elevation as a function of time
N	=	number of wave components
$\zeta_{a,n}$	=	amplitude of wave component n $[m]$
ω_n	=	frequency of wave component n $[rad/s]$
t	=	time $[s]$
ϵ_n	=	phase angle of harmonic wave component n $[rad]$

This equation is also referred to as the random amplitude phase model.

4.1.1 Variance density and wave spectrum

The variance of a wave record is described as the surface elevation sqared (η^2). Also, the variance of a harmonic wave with an amplitude $\zeta_{a,n}$ is $\frac{1}{2}\zeta_{a,n}^2$. With this variance density spectrum, wave properties in a certain sea state can be described statistically. Equation 4.2 shows the relation between the variance density and wave spectrum. The wave spectrum describes the distribution of the variance of wave elevations as a function of frequency:

$$S_\zeta(\omega) d\omega = \frac{1}{2}\zeta_a^2(\omega) \tag{4.2}$$

With:

$S_\zeta(\omega)$	=	Variance density spectrum of wave $[m^2 s/rad]$
ω	=	Angular frequency $[rad/s]$
ζ_a	=	Wave amplitude $[m]$
$\frac{1}{2}\zeta_a^2$	=	Variance of wave elevation $[m^2]$

Many studies have been performed in the past to describe variance density spectra. The two most commonly used wave spectra are the $Pierson - Moskowitz$ spectrum and the $JONSWAP$ spectrum. The $Pierson - Moskowitz$ spectrum describes a fully developed sea state meaning that there is an infinite fetch. In other words, the distance over which wind generates waves. Waves travel at the same velocity as the wind.
The $JONSWAP$ spectrum is based on measurements performed during the Joint North Sea wave project in the north sea. It is a modified $Pierson - Moskowitz$ spectrum in which the peak is modified.

$$S_{PM}(\omega) = \frac{A}{\omega^5} exp\{-\frac{B}{\omega^4}\} \tag{4.3}$$

With:

$$\begin{aligned} A &= \frac{4\pi^3 H_s^2}{T_z^4} \\ B &= \frac{16\pi^3}{T_z^4} \end{aligned} \tag{4.4}$$

Where:

S_{PM} = Pierson-Moskowitz variance density spectrum $[m^2s/rad]$
ω = Angular frequency $[rad/s]$
H_s = Significant wave height $[m]$
T_z = Mean zero wave-crossing period $[s]$

And:

$$S_{JS}(\omega) = \frac{320H_s^2}{T_p^4}\omega^{-5}exp\{-\frac{1950}{T_p^4}\omega^{-4}\}\gamma^A \tag{4.5}$$

With:

$$\begin{aligned} A &= exp(-(\frac{\omega/\omega_p - 1}{\sigma\sqrt{2}})^2) \\ \omega_p &= \frac{2\pi}{T_p} \end{aligned} \tag{4.6}$$

σ is a step function of ω:

$\sigma = \sigma_a$ for $\omega \leq \omega_p$
$\sigma = \sigma_b$ for $\omega \geq \omega_p$

The measurements taken from the Joint North Sea Wave Project lead to average values for the spectrum's peak shape and numerical parameters:

$\gamma = 3.3$
$\sigma_a = 0.07$
$\sigma_b = 0.09$

In the figure below 4.2, an example of the difference between the $Pierson - Moskowitz$ and $JONSWAP$ spectrum is visualized.

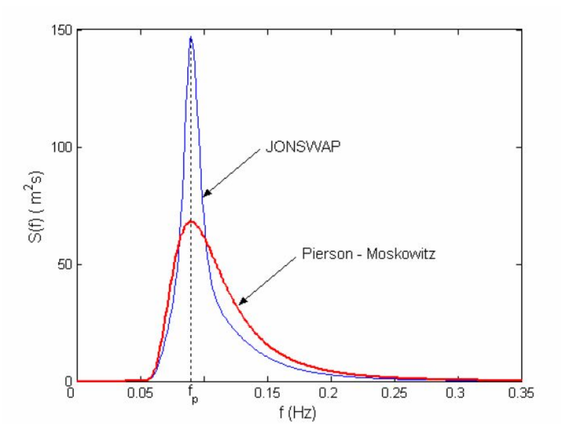

Figure 4.2: JONSWAP & Pierson-moskowitz spectrum [4]

For further calculations in this thesis, $JONSWAP$ will be selected because this spectrum gives a good estimation of area's of limited fetch. At Jumbo, most lifting activities take place in coastal waters. Also it contains the most energy and hence, design calculations will be on the conservative side.
With the above description of the behavior of waves, it is time to proceed to look how the vessel's motions will be influenced by these waves. This will be described in the next section.

4.2 Ship Motions

During offshore lifting, the vessel will experience motions in six degrees of freedom. These motions are induced by environmental loads such as wind and waves. In marine engineering, these motions are expressed in so called RAO's (response amplitude operators). An RAO expresses the relation between the motion of the vessel per one meter wave amplitude, for each wave component and frequency. From these RAO's, frequency response characteristics can be obtained and analysed. In other words, it can be seen at which frequencies (or periods) the vessel will have the largest motions. The most critical motions that will be investigated for workability are pitch and roll, as determined internally at Jumbo. workability is defined as the probability that a certain seastate will not be exceeded while the ship is able to perform the lift, expressed in percentage of time. In this section, a theoretical description of vessel motions will be presented.

4.3 Motions and Waves

In this report the motions of six degrees of freedom are analysed. Linear theory is used, so there is a linear relation between wave motions and ship motions. These relations are expressed in RAO's, expressed in a ratio between ship and wave amplitudes. A visualization of this is given in figure 4.3.

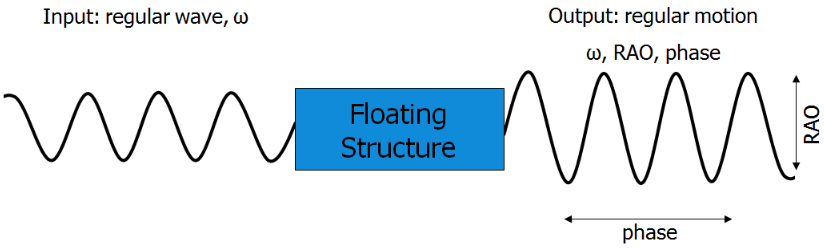

Figure 4.3: Relation between motions and waves

A motion analysis software tool called MaxSurf is used that is able to compute vessel responses. The motions are acquired by solving the equation of motion for 3 translational and 3 rotational degrees of freedom 4.7. From potential theory the forces and moments are calculated. Potential theory gives a mathematical description of flows.

$$(M + A(\omega))\ddot{x} + B(\omega)\dot{x} + Cx = F(\omega) \tag{4.7}$$

In which:

M	=	Mass matrix
$A(\omega)$	=	Added mass matrix
$B(\omega)$	=	Damping matrix
$C(\omega)$	=	Stiffness matrix
$F(\omega)$	=	Wave forces or moments

4.3.1 Roll Motion

From the motions in all degrees of freedom, the roll motion should be treated seperately. This is because the J-class vessel has a slender shape. This shape leads to high sailing speeds, however due to a very small amount of potential damping it is almost entirely dependent on frictional damping.

4.4 Motions Of Center of Gravity

First, the vessel motions will be illustrated as can be seen in figure 4.4. Vessel motions can be devided in three translations and three rotations, in or around the x-, y- and z-axes.

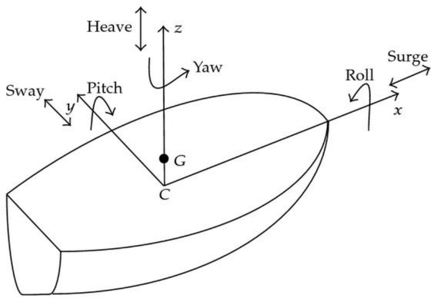

Figure 4.4: Motion definition in six DOF's

The translations of the vessel's center of gravity are defined as:

- Surge in x-direction, positive forwards
- Sway in y-direction, positive towards portside
- Heave in z-direction, positive upwards

The rotations about these axes are:

- Roll about the x-axis
- Sway about the y-axis
- Yaw about the z-axis

With these definitions of rotations and translations, *response* motions can be described. When a vessel is harmonically excited by waves, the vessel will have a certain harmonic response. The response to harmonic waves can be written as 4.8:

$$\begin{array}{ccl} \text{Surge} & : & x(t) = x_a \cos(\omega t + \varepsilon_{x\zeta}) \\ \text{Sway} & : & y(t) = y_a \cos(\omega t + \varepsilon_{y\zeta}) \\ \text{Heave} & : & z(t) = z_a \cos(\omega t + \varepsilon_{z\zeta}) \\ \text{Roll} & : & \phi(t) = \phi_a \cos(\omega t + \varepsilon_{\phi\zeta}) \\ \text{Pitch} & : & \theta(t) = \theta_a \cos(\omega t + \varepsilon_{\theta\zeta}) \\ \text{Yaw} & : & \psi(t) = \psi_a \cos(\omega t + \varepsilon_{\psi\zeta}) \end{array} \tag{4.8}$$

In here

$x_a, y_a, z_a, \phi_a, \theta_a, \psi_a$	=	motion amplitudes [m] and [rad]
ω	=	wave and response frequency [rad/s]
$\epsilon_{x\zeta}, \epsilon_{y\zeta}, \epsilon_{z\zeta}, \epsilon_{\phi\zeta}, \epsilon_{\theta\zeta}, \epsilon_{\psi\zeta}$	=	phase shift with respect to the harmonic wave at the CoG [rad]

To obtain the velocities and accelerations, the motions as defined in 4.8 should be differentiated over time once and twice respectively. The amplitudes of the vessel motions are assumed to be linearly proportional to the harmonic wave amplitudes. A way to relate the wave amplitude and the vessel motion is by means of a (motion) response amplitude operator (RAO). It is defined as the ration between the vessel amplitude and the amplitude of a regular wave. Below the motion RAO's are expressed as a function of wave frequency in each degree of freedom:

$$\begin{aligned} Surge: RAO_x(\omega) &= \frac{x_a}{\zeta_a}(\omega)\ [\frac{m}{m}] & Roll &: RAO_\phi(\omega) = \frac{\phi_a}{\zeta_a}(\omega)\ [\frac{\text{rad}}{m}] \\ Sway: RAO_y(\omega) &= \frac{y_a}{\zeta_a}(\omega)\ [\frac{m}{m}] & Pitch &: RAO_\theta(\omega) = \frac{\theta_a}{\zeta_a}(\omega)\ [\frac{\text{rad}}{m}] \\ Heave: RAO_z(\omega) &= \frac{z_a}{\zeta_a}(\omega)\ [\frac{m}{m}] & Yaw &: RAO_\psi(\omega) = \frac{\psi_a}{\zeta_a}(\omega)\ [\frac{rad}{m}] \end{aligned} \tag{4.9}$$

4.4.1 Relative motions

If small ship angles are assumed, linearized forms of absolute harmonic linear and angular motions at an arbitrary point $P(x_b, y_b, z_b)$ on the ship can be written as 4.10:

$$\begin{aligned} x_p &= x - y_b\psi + z_b\theta \\ y_p &= y + x_b\psi - z_b\phi \\ z_p &= z - x_b\theta + y_b\phi \end{aligned} \tag{4.10}$$

An example of an elaboration of the relative heave motion h is given below 4.11:

$$\begin{aligned} h &= z - x_b\theta + y_b\phi \\ &= z_a cos(\omega t + \varepsilon_{z,\zeta}) - x_b\theta_a cos(\omega t + \varepsilon_{\theta,\zeta}) + y_b\phi_a cos(\omega t + \varepsilon_{\phi,zeta}) \end{aligned} \tag{4.11}$$

Splitting the cos and sin terms in equation 4.11 leads to:

$$\begin{aligned} h = &\left(z_a cos(\varepsilon_{z\zeta}) - x_b\theta_a cos(\varepsilon_{\theta\zeta}) + y_b\phi cos(\varepsilon_{\phi\zeta})\right) cos(\omega t) + \\ &\left(-z_a sin(\varepsilon_{z\zeta} + x_b\theta_a sin(\varepsilon_{\theta\zeta}) - y_b\phi cos(\varepsilon_{\phi\zeta}))\right) sin(\omega t) \end{aligned} \tag{4.12}$$

Applying the goniometric rule:

$$cos(a+b) = cos(a)cos(b) - sin(a)sin(b) \tag{4.13}$$

Leads to:

$$h = h_a cos(\omega t + \varepsilon_{h\zeta}) = h_a cos(\varepsilon_{h\zeta})cos(\omega t) - (h_a sin(\varepsilon_{h\zeta}))sin(\omega t) \tag{4.14}$$

The in-phase and out-phase terms of h are obtained by equating the $cos(\omega t)$-parts and $sin(\omega t)$-parts of equations 4.14 and 4.12 respectively:

$$h_a cos(\varepsilon_{h\zeta}) = z_a cos(\varepsilon_{z\zeta}) - x_b\theta_a cos(\varepsilon_{\theta\zeta}) + y_b\phi cos(\varepsilon_{\phi\zeta}) \tag{4.15}$$

And

$$h_a sin(\varepsilon_{h\zeta}) = z_a sin(\varepsilon_{z\zeta}) - x_b\theta_a sin(\varepsilon_{\theta\zeta}) + y_b\phi sin(\varepsilon_{\phi\zeta}) \tag{4.16}$$

When equations 4.15 and 4.16 are first squared and added, h_a can be obtained.

$$h_a = \sqrt{z_a^2 - 2z_a x_b\theta_a cos(\varepsilon_{z\zeta} - \varepsilon_{\theta\zeta}) + 2z_a y_b\phi_a cos(\varepsilon_{z\zeta} - \varepsilon_{\phi\zeta}) + x_b^2\theta_a^2 - 2x_b\theta_a y_b\phi_a cos(\varepsilon_{\theta\zeta} - \varepsilon_{\phi\zeta}) + y_b^2\phi_a^2} \tag{4.17}$$

The phase $\varepsilon_{h\zeta}$ can be obtained by deviding equation 4.16 by equation 4.15:

$$\varepsilon_{h\zeta} = arctan\left\{\frac{z_a sin(\varepsilon_{z\zeta}) - x_b\theta_a(\varepsilon_\theta\zeta) + y_b\phi_a sin(\varepsilon_{\phi\zeta})}{z_a cos(\varepsilon_{z\zeta}) - x_b\theta_a cos(\varepsilon_{\theta\zeta}) + y_b\phi_a cos(\varepsilon_{\phi\zeta})}\right\} \tag{4.18}$$

The same can be done for surge and sway.
Note that dividing the motion amplitudes by the wave component amplitude leads to the expression for the RAO of that component and degree of freedom.

Next to RAO's, phase differences are also a function of wave frequency and wave direction. The vessel response for irregular waves can be written as the sum of regular response components 4.19. As an example, heave can be expressed as:

$$z(t) = \sum_{n=1}^{N} z_a cos(\omega_n t + \varepsilon_n + \varepsilon_z\zeta, n) \tag{4.19}$$

In which:

z_a	=	Heave [m]
n	=	Wave index number [-]
N	=	Number of wave frequencies [-]
ω_n	=	Angular frequency [rad/sec]
$z_{a,n}$	=	Heave amplitude [m]
ε_n	=	Phase shift of wave n [rad]
$\varepsilon_z\zeta, n$	=	Phase difference between wave elevation n and heave [rad]

It should also be noted that the heave amplitude z_a is denoted by $RAO_z(\omega_n) \cdot \zeta_{a,n}$.

4.5 Vessel Response Spectra

In chapter 4 the variance density spectrum of a wave record was described according to 4.2. The vessel motion spectra can be described in a similar fashion because the harmonic waves and vessel motions are assumed to be linear proportional in all degrees of freedom. As an example, the heave response spectrum is given as:

$$S_z(\omega)d\omega = \frac{1}{2}z_a^2(\omega) \tag{4.20}$$

with:

$S_z(\omega)$	=	Variance density spectrum of heave response $[m^2 s/rad]$
$\frac{1}{2}z_a^2$	=	Variance of heave motion $[m^2]$

The motion amplitude in any degree of freedom can be directly obtained from the motion RAO (heave example):

$$z_a(\omega) = RAO_z\zeta_a \tag{4.21}$$

From this relation and the fact that the response specra and wave spectrum are proportional to the amplitude squared, the response spectrum can be obtained by taking the square of the RAO:

$$S_z(\omega) = RAO_z^2 S_\zeta(\omega) \tag{4.22}$$

The expression of equation 4.22 is convenient in the sense that it can be relatively easy to check the vessel response spectra and behavior in any given sea state. The n^{th} order moment m_n for the heave response spectrum is defined as:

$$m_n = \int_0^\infty \omega^n S_z(\omega)d\omega \tag{4.23}$$

The significant response height and mean zero-crossing period response can be determined by:

$$H_{z1/3} = 4\sqrt{m_{0z}} \tag{4.24}$$

And

$$T_{zz} = 2\pi\sqrt{\frac{m_{0z}}{m_{2z}}} \tag{4.25}$$

Chapter 5

Motion Analysis

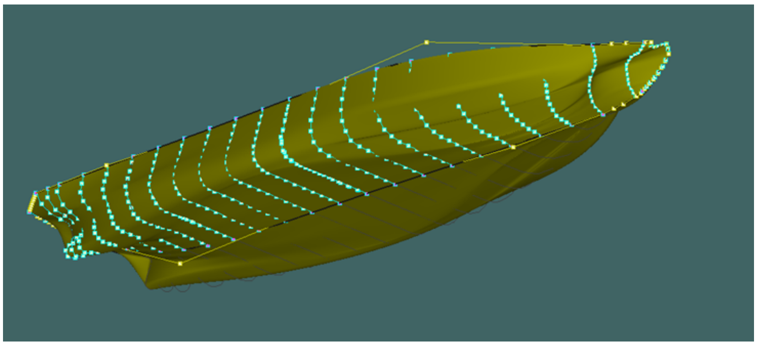

The vessel will be subjected to environmental forces such as wind and waves and will cause the vessel to move in six degrees of freedom. Additional forces will also be present at the crane tip which are caused by accelerations from the lifted mass and from supports. These additional forces will lead to a decrease in safe working loads of the cranes. Also, in order to avoid repeated clashing between lifting load and other objects, the vertical hoisting velocity is limited. Furthermore, from the sidelead criterium the maximum roll and pitch can be determined. In the following sections the process of obtaining the limiting values for maximum vertical crane tip acceleration, velocity and sidelead are described.

5.1 Limiting criteria

As indicated in the brochure of crane manufacturer *Huisman* [5], offshore lift cranes need to be designed for static and dynamics loads. The dynamic loading can be expressed in three main factors and consists of the duty factor, horizontal loads and hoisting factor. These terms are related as:

$$F_z = F_d \cdot F_H \cdot Load \tag{5.1}$$

In which

F_z	=	Vertical hook load
F_d	=	Duty factor
F_H	=	Hoisting factor

For offshore lifts, the Lloyds register indicates a duty factor of 1.20, however, these are meant for cranes on platforms that are used regularly with smaller working loads. For bigger offshore loads, more calculations will be done beforehand, reducing the risk of the lifting operation. A duty factor of 1.05 suffices in order to make calculations for lifts above water. Furthermore the *Huisman* cranes are designed with a hoisting factor of 1.1. A hoisting factor is defined as the ratio of the maximum dynamic load and static load. With the cranes capable of lifting 1800 ton the engineered strength of the cranes is calculated from equation 5.1 and turns out to be $900 \cdot 1.1 \cdot 1 = 990ton$. However, when working offshore, ship motions and accelerations will be larger and are determined by dynamic factors that have an influence on the crane due to lifting loads from supports and accelerations of the lifted mass. These factors are defined as F_{h1}, which represents the factor of influence on the crane due to lifting loads from the supports and F_{h2}, which is representative for the factor due to the acceleration of the lifted mass.

$$F_{h1} = 1 + \frac{V_s + V_d + V_c}{g}\sqrt{\frac{C}{M}} \quad or \quad F_{h1} = 1 + \frac{V_R}{g}\sqrt{\frac{C}{M}} \tag{5.2}$$

V_s	=	Hoisting (steady state) velocity [m/s]
V_d	=	Instantaneous velocity of the load support structure just before lift-off
V_c	=	Instantaneous cranetip velocity just before lift-off [m/s]
V_R	=	The maximum velocity of $\sqrt{V_d^2 + V_c^2}$ [m/s]
C	=	Crane stiffness [KN/m]
M	=	Mass of the load [t]

The increased offshore duty factor of 1.05, the engineered strength and the maximum offshore load as calculated in chapter 3 (580ton), the new hoisting factor can be determined from equation 5.1 and turns out to be $F_h = 3.25$ This maximum hoisting factor is the limiting value for both F_{h1} and F_{h2}, from which the limiting crane tip velocity and acceleration can be determined respectively. Both F_{h1} and F_{h2} should be smaller or equal to 3.25.
When the load is lifted and fully supported by the lifting crane, one needs to account for the remaining dynamics. The hoisting factor F_{h2} is fully dependent on the crane tip acceleration and is calculated by the following equation;

$$F_{h2} = 1 + \frac{a_z}{g} \tag{5.3}$$

From equation 5.3, a limiting cranetip acceleration of $a_z = 22.07m/s^2$. a_z is defined as the most probable maximum during 3 hours. The significant relative acceleration is defined as $a_{max}/1.86$ which leads to a significant cranetip acceleration of $a_{sign} = 11.87m/s^2$.
The crane stiffness C is determined to be 2850 KN/m, the hoisting velocity V_h for 900 ton is $3.1m/min$, or $0.052m/s$. V_R can be determined from F_{h1}:

$$V_R = \frac{(F_{h1} - 1)g}{\sqrt{\frac{C}{M}}} \tag{5.4}$$

Filling in the determined values into equation 5.4, a V_R of $2.25m/s$ is reached. The minimum required hoisting speed is determined by $V_s = 0.25\sqrt{(V_d^2 + V_c^2)}$. For internal lifts V_d is zero, so $V_s = 0.25V_c$. Also, the relative crane tip velocity becomes $V_R = V_s + V_c$, hence $1.25V_c \leq 2.25$. This means that the maximum (instantaneous) cranetip velocity is $1.8m/s$. The instantaneous cranetip velocity is taken to be maximal once in every four waves. Since the wave amplitudes obey a Rayleigh distribution, the significant maximum cranetip velocity is expressed within:

$$1/4 = EXP\Big(-2\Big(\frac{1.8}{V_{1/3}}\Big)^2\Big) \tag{5.5}$$

The maximum significant crane tip velocity $V_{1/3}$ is then $2.16m/s$.
Lastly the amplitude criteria due to the crane's side and offlead limitations need to be determined. The maximum offload and sidelead are 1 and 4 degrees respectively. These values are fixed values that are found in the user manual for the 900ton heavy lift mast crane from $Huisman-Itrec$.

Offlead is defined as the transverse load motion while the sidelead is the motion of the load in longitudinal direction. Since the offlead criterium can be accounted for by an increase of the radius which leads to a lower SWL (safe working load), it is not determining. However, the sidelead criterium of 4 degrees is expressed by pitch and roll of the ship:

$$MaximumSidelead = \sqrt{\theta^2 + \phi^2} \tag{5.6}$$

The maximum significant amplitudes are then defined as $4/1.86 = 2.15 degrees$, or $\sqrt{\theta^2 + \phi^2} \leq 2.15 degrees$.

5.1.1 Conclusion

The calculations above have been done to obtain the limiting criteria for the workability of the ship. It turned out that the cranetip velocity, acceleration and sidelead are the governing limitations for the workability analysis. The values can be seen in the following table:

Criterium	**Value**
Significant maximum vertical acceleration	$11.87 m/s^2$
Significant maximum vertical velocity	$2.16 m/s$
Significant maximum amplitudes	$\sqrt{\theta^2 + \phi^2} \leq 2.15 degrees$

Table 5.1: Motion Criteria

5.2 Ship motions

The motions of the vessel will be expressed in RAO's for six degrees of freedom. To obtain these RAO's, the ship motions program $MAXSURF$ is used. In order to calculate the motions, a panel model of the J-1800 vessel is created. The linear potential theory is used to calculate the external forces and moments and the following assumptions are made:

- Wave height and steepness are assumed to be small
- The fluid is assumed to be inviscid and incompressible
- Irrotational fluid flows

5.2.1 Roll motion

Of motions in all degrees of freedom, the uncoupled motion in roll is the most governing one. This is because the roll motion has very little potential damping. Potential damping is defined as the transfer of energy from the motion to the fluid which radiates away from the vessel. The uncoupled equation of motion, as computed by $MaxSurf$ is given as:

$$(I_4 + A_{44})\ddot{\phi} + B_{44}\dot{\phi} + C_{44}\phi = F_4 e^{i\omega_e t} \tag{5.7}$$

In $Maxsurf$, the following terms are defined:

I_4	=	Roll moment of inertia $I_4 = {k_{xx}}^2 \Delta\rho$
A_{44}	=	Roll added inertia coefficient $A_{44} = 0.3I_4$
B_{44}	=	Roll damping coefficient
C_{44}	=	Roll hydrostatic restoring coefficient $C_{44} = \overline{GM}\nabla\rho g$
F_4	=	Roll exciting moment at encounter frequency ω_e
ϕ	=	Instantaneous roll displacement
$\dot{\phi}$	=	Instantaneous roll velocity
$\ddot{\phi}$	=	Instantaneous roll acceleration

The roll motion is given by:

$$\phi = \frac{F_4}{\sqrt{(C_{44} - (I_4 + A_{44})(\omega_e)^2)^2 + B^2(\omega_e)^2}} cos(\omega_e t + \varepsilon) \tag{5.8}$$

Here ε represents the phase lag relative to the forcing function. Furthermore, the (non dimensional) damping ratio is $\eta_{44} = \frac{B_{44}}{2\sqrt{C_{44}(I_4 + A_{44})}}$, the natural frequency, $\omega_0 = \sqrt{\frac{C_{44}}{(I_4 + A_{44})}}$ and the tuning factor $\lambda = \frac{\omega_e}{\omega_0}$. The response function for roll is is calculated by:

$$RAO_\phi = \frac{\phi C_{44}}{F_4} = \frac{1}{\sqrt{(1-\lambda^2)^2 + 4\eta_{44}\lambda^2}} \tag{5.9}$$

Lastly, some important motion behaviour is pointed out in figure 5.1

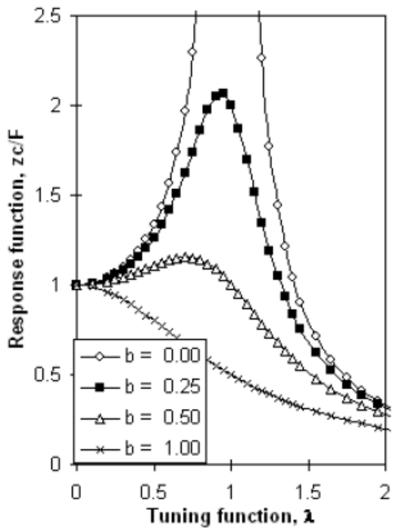

Figure 5.1: Frequency response

In this figure, three areas are distinguished:

- Low frequency area, $\omega^2 \ll \frac{C_{44}}{I_{44} + A_{44}}$, with motions dominated by the hydrostatic restoring coefficient. The motions will follow the waves. The RAO tends to 1 and the phase lag tends to zero.
- Natural frequency area, $\omega^2 \approx \frac{C_{44}}{I_{44} + A_{44}}$, with motions dominated by the damping term. Here resonance occurs.
- High frequency area, $\omega^2 \gg \frac{C_{44}}{I_{44} + A_{44}}$, with motions dominated by the inertia or mass (hydrodynamic) terms.

5.2.2 Roll damping

Before proceeding with the motion analysis, the damping coefficient needs to be determined as damping can have a significant influence on the ship motions, mostly at the natural frequencies. Like explained before, there is very little radiation damping due to the slender shape of the J-class vessel. The motion is almost completely dependent on frictional damping. Frictional damping is quadratically related to the velocity. This is why an equivalent linear damping needs to be found. This equivalent linear damping is obtained by free decay test data of a scale model, performed at Marin. In these tests the damping coefficients are derived by the decay of two successive motion amplitudes. This data is used to plot the decrease of the motion amplitude devided by the mean amplitude, versus the mean amplitude as can be seen in figure 5.2 and 5.3. This damping coefficient consists of two parts; linear potential damping and quadratic frictional damping. This equivalent linear damping coefficient is defined as the total energy lost, both linear and quadratic, during one period.

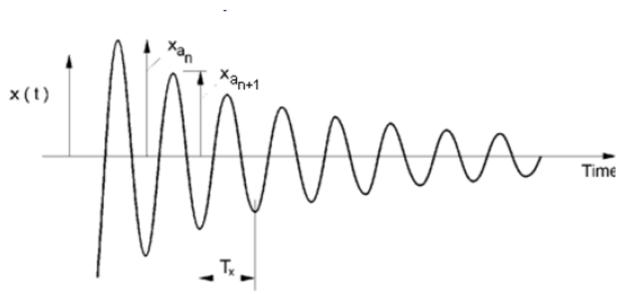

Figure 5.2: Motion decay

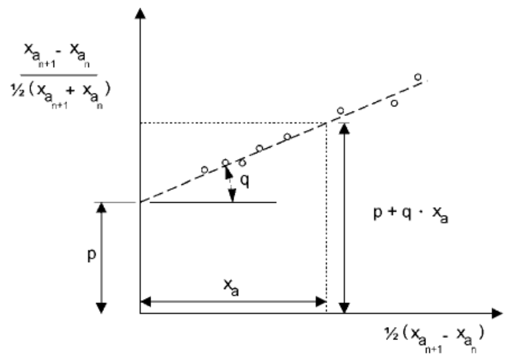

Figure 5.3: Determination of damping coefficients

with reference to the $Marin$ test report [6], the equivalent damping coefficient is determined:

$$b_{equivalent} = 2(p + qx_a)\frac{a_x}{T_x} = 2(p + qx_a)a_x\frac{\omega_n}{2\pi} \tag{5.10}$$

In which

x_a	=	Mean motion amplitude
a_x	=	Total ship mass (ship mass+added mass), expressed as ${k_{xx}}^2\Delta + a_{xx}$
T_x	=	Natural rolll period, defined as $2\pi\sqrt{\frac{{k_{xx}}^2\Delta + a_{xx}}{g\overline{GM}\Delta}}$
ω_n	=	Natural frequency

This leads to the following expression:

$$b_{equivalent} = \frac{(p + qx_a)}{2\pi}2({k_{xx}}^2\Delta + a_{xx})\sqrt{\frac{\Delta g\overline{GM}}{k_{xx}\Delta + a_{xx}}} \tag{5.11}$$

Or:

$$b_{equivalent} = \frac{p + qx_a}{2\pi^2}g\overline{GM}\Delta\sqrt{\frac{{k_{xx}}^2\Delta + a_{xx}}{g\overline{GM}\Delta}}2\pi = \frac{(p + qx_a)}{2\pi^2}g\overline{GM}\Delta T \tag{5.12}$$

Filling in the parameters as obtained from the Marin scale model free decay tests in 5.12, the expression for $b_{equivalent}$ is described by equation 5.13. The used parameters can be found in the table below.

Parameter	Value
Δ	$18300ton$
p	$0.066[-]$
q	$0.029[1/deg]$
T_{roll}	$13.98s$
g	$9.81m/s^2$

Table 5.2: Used parameters

$$b_{equivalent} = 26562 + 11671\phi \tag{5.13}$$

Note that only one equivalent damping coefficient can be determined per period and hence per one roll amplitude and natural roll frequency. The limiting roll amplitude as determined in section 5.1 is chosen as the governing one (2.15 degrees). From equation 5.13 it can be seen that the equivalent damping coefficient consists of a part that represents the linear damping (potential and linear) and the quadratic part. Also, the calculated equivalent damping coefficient is valid only for the natural frequency as was determined from the scale model free decay tests at $Marin$. This frequency has a value of $0.44rad/s$. Since the viscous damping is quadratically related to the velocity, a ratio needs to be added that relates the natural frequency to the quadratic part of the equivalent damping. This ratio is defined as $w_n/0.44$, with 0.44 the eigenfrequency determined at $Marin$. The final equivalent damping then becomes:

$$b_{equivalent} = 26562 + 57029\omega_n \tag{5.14}$$

The equivalent damping coefficient as described in equation 5.14 is used for the critical situations as determined in chapter 3.

5.2.3 Motion behaviour

What should be done next is compare motion responses for different lifting configurations with different VCG's. The radius of gyration is kept constant for all configurations since the mass distribution on the vessel is not fully known. The maximum allowable wave height will be determined by analysing the result of different pairs of wave peak period and encounter angle. The limiting (design) wave height is set at two meters. In this section the motion results from $Maxsurf$ will be discussed. First, the RAO's of the different lifting arrangements will be compared. This is done in order to determine the lifting situation that leads to the highest average motions in the frequency domain. Also, in this way the amount of $Maxsurf$ runs will be limited by one limiting RAO. As can be seen in figure 5.4 the configuration before lift-off, the area under the curve is the largest, hence this RAO will be used as the limiting response. The reason that the loading condition 'before liftoff' has the largest frequency response is due to the high required stability ($\overline{GM}$). In the expression for the non-dimensional damping ratio, defined as $\eta_{44} = \dfrac{b_{equivalent}}{2\sqrt{c_{44} \cdot (I_4 + a_{44})}}$ the actual damping is further away from the critical damping when the ship has a high initial stability expressed in $\overline{GM}$. This can be explained by equation 5.8, where at the low frequency range, the hydrostatics are dominating, around the natural frequencies the damping is dominating and finally at the high frequencies the added mass and inertia effects are dominating the motion. Besides decreasing the amount of necessary runs in $Maxsurf$, this also leads to an analysis that is more on the conservative side. For clarification, the encounter frequencies as shown on the horizontal axis of figure 5.4 are converted to period in seconds in table 5.4. Frequency and period are related by $\omega = \dfrac{2\pi}{\omega}$.

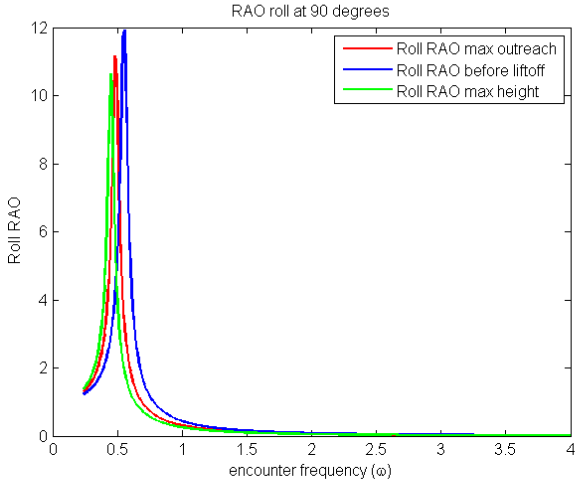

Figure 5.4: Comparison Roll

Areas under curve	
$RAO_{roll_{Maxoutreach}}$	1.57
$RAO_{roll_{Beforeliftoff}}$	1.94
$RAO_{roll_{Maxheight}}$	1.32

Table 5.3: Areas under curves

$\omega[rad/s]$	$T[s]$
0.5	12.57
1	6.28
1.5	4.19

Table 5.4: Conversion

Now that the limiting (most conservative) motions have been determined, expressed as RAO's for a range of incoming wave angles at zero ship velocity, the position of the crane-tip that leads to the largest velocities and accelerations need to be determined. In order to do this, two extreme crane positions will be evaluated, being the crane-tip postition just before lift-off and the crane tip position at maximum outreach. These positions with their cordinates can be seen in the figure below.

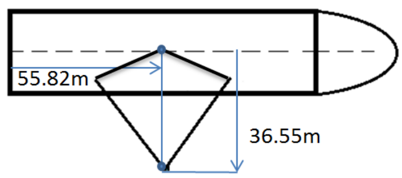

Figure 5.5: Crane-tip positions

Crane-tip coordinates		
Position	**x**	**y**
Maximum outreach	55.82m	36.55m
Before lift-off	55.82m	0m

Table 5.5: Crane-tip positions

The J-class vessels are relatively slender, meaning that the ships are narrow concerning the width/length ratio. This is beneficial for the sailing speeds, but the damping ratio will be low. Due to this the roll motion is the limiting motion in most cases as will be shown in this remaining chapter.

Next, the maximum wave height will be determined for a range of combinations of peak period and encounter angles. This is done for each limiting criterium as determined in the preceeding section. The maximum allowable significant wave height will be determined by looking for combinations between different sea states and ship motion RAO's that lead to the response spectrum for each criterium. Then the maximum wave height for each specific heading and wave peak period will be determined by using the following relation:

$$H_{max} = \frac{Maximum\ amplitude}{Significant\ amplitude} \cdot H_{sign} \tag{5.15}$$

The limiting motion criteria are based on the maximal crane-tip vertical acceleraton, velocity and sidelead. First, the acceleration criterium will be checked, followed by the crane-tip velocity and sidelead. These criteria are repeated in the table below:

Criterium	Value
Significant maximum vertical acceleration	$11.87m/s^2$
Significant maximum vertical velocity	$2.16m/s$
Significant maximum amplitudes	$\sqrt{\theta^2 + \phi^2} \leq 2.15 degrees$

Crane-tip acceleration check

In order to check the maximum allowable crane-tip accelerations, first for different outreaches, the acceleration-RAO's will be compared. The situation with the largest motions will be used as the limiting configuration to be used for further analysis. The acceleration-RAO's for two extreme positions as can be seen in figure 5.5 are plotted below.

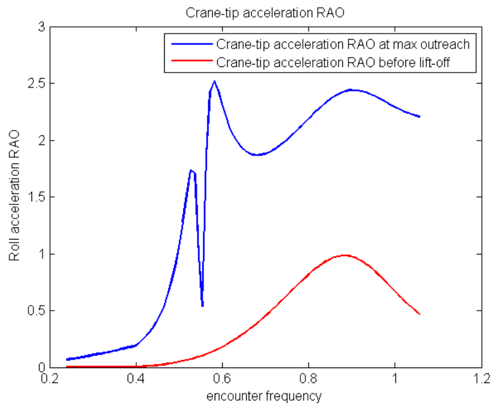

Figure 5.6: Acceleration RAO's

From this graph it can be seen that the situation with the crane-tip at maximum outreach, the motions acceleration will be the largest. For this crane-tip position, the maximum allowable wave heights will be determined for different peak periods and accelerations. This can be seen in the table below for a wave heading of 90 degrees. As expected, the acceleration criterium is of non concern since the magnitudes are far below the maximum allowable acceleration. This criterium is also checked for all other headings and it can already be concluded that crane-tip accelerations will not cause any problems.

Crane-tip velocity check

The maximum velocity criterium will be checked in a similar fashion as the acceleration criterium. First it will be checked which crane-tip position will lead to the largest velocities. This can be seen in figure 5.7. In this graph it can be seen that again, the position at maximum outreach is the governing position, hence this position will be used to check the velocity criterium.
Now the maximum allowable wave height is determined again for each combination of peak wave period and ship significant velocity. The relations between the roll RAO, wave spectrum for different peak periods (Tp's) and roll response spectra at 90 degree heading can be seen below.

Acceleration Criterium			
$T_p(s)$	**acceleration** (m/s^2)	$H_{sign}(m)$	$H_{max}(m)$
5	$3.74/s^2$	2	6.33
6	3.13	2	7,59
7	2.82	2	8.43
8	2.58	2	9.20
9	2,48	2	9,57
10	2,575	2	9,22
11	2,829	2	8,39
12	2,60	2	8,39
13	2,09	2	11,36
14	1,75	2	13,55
15	1,57	2	15,16
16	1,42	2	16,73
17	1,29	2	18,45
18	1,17	2	18,45

Table 5.6: Acceleration criterium

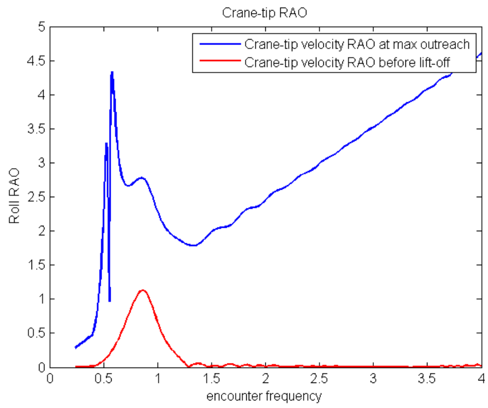

Figure 5.7: Velocity RAO's at different crane-tip positions

Sidelead Check

Lastly, the sidelead will be checked. The sidelead consists of the combined square root of the roll and pitch motion squared. From the results it can be seen that the roll motion is the governing motion for all wave headings except for 0 and 180 degrees. In the figures below, the relations between roll RAO, wave spectrum and response for a wave heading of 165 degrees. The limiting wave heights for a range of significant pitch and roll motion are obtained as well.

Velocity criterium			
$T_p(s)$	**velocity** (m/s)	$H_{sign}(m)$	$H_{max}(m)$
5	2.11	2	2.10
6	2.15	1.93	1.94
7	2.16	1.73	1.73
8	2.15	1.57	1.57
9	2.15	1.38	1.38
10	2.16	1.15	1.15
11	2.16	0.94	0.94
12	2.16	0.99	0.99
13	2.16	1.24	1.24
14	2.16	1.47	1.47
15	2.16	1.65	1.65
16	2.16	1.81	1.80
17	2.16	1.97	1.97
18	2	2	2.16

Table 5.7: Velocity criterium

Tp(s)/Theta(deg)	0	15	30	45	60	75	90	105	120	135	150	165	180
5	44,08	7,97	4,21	3,03	2,49	2,16	2,05	2,17	2,45	3,02	4,27	8,18	56,84
6	26,18	8,59	4,77	3,45	3,34	2,14	1,94	2,22	2,73	3,34	4,88	9,15	35,41
7	16,18	10,02	5,31	3,54	3,49	1,92	1,73	1,94	2,52	3,49	5,27	10,75	21,71
8	16,94	8,37	4,36	2,89	2,9	1,7	1,57	1,72	2,14	2,9	4,4	8,87	21,49
9	18,62	6,13	3,27	2,25	2,26	1,47	1,38	1,48	1,75	2,26	3,3	6,35	25,26
10	15,16	4,49	2,47	1,74	1,75	1,21	1,15	1,21	1,39	1,75	2,5	4,65	22,04
11	12,9	3,41	1,91	1,37	1,39	0,98	0,94	0,99	1,12	1,39	1,95	3,59	18
12	11,9	3,44	1,95	1,41	1,44	1,03	0,99	1,03	1,17	1,44	2,03	3,7	15,71
13	11,49	4,17	2,42	1,76	1,9	1,03	1,24	1,29	1,47	1,9	2,54	4,57	14,55
14	11,4	4,86	2,88	2,1	2,16	1,53	1,47	1,53	1,75	2,16	3,04	5,38	14,07
15	11,52	5,35	3,2	2,34	2,41	1,71	1,65	1,73	1,96	2,41	3,37	5,89	13,76
17	11,74	5,75	3,49	2,56	2,63	1,87	1,81	1,89	2,14	2,63	3,67	6,33	13,8
17	12,03	6,18	3,79	2,78	2,87	2,05	1,97	2,07	2,33	2,87	3,99	6,81	14,03
18	12,38	6,62	4,09	3,02	3,13	2,23	2,15	2,25	2,54	3,13	4,32	7,31	14,35

Figure 5.8: Maximum wave heights per $Tp - \theta$ combination

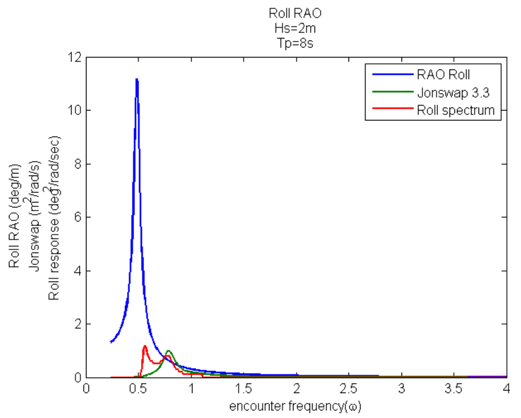

Figure 5.9: Roll RAO, Jonswap spectrum, Roll response

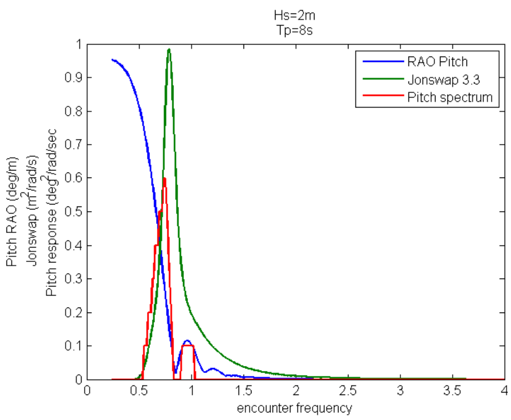

Figure 5.10: Pitch RAO, Jonswap spectrum, Pitch response

Figure 5.9 and 5.10, lead to a maximum significant wave height of $H_{max} = \frac{2.15}{\sqrt{\theta^2 + \phi^2}} H_{sign} =$

$$\frac{2.15}{\sqrt{1.04^2 + 0.65^2}} = 3.5m.$$

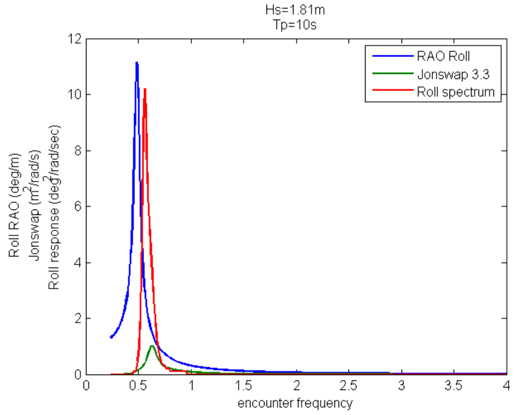

Figure 5.11: Roll RAO, Jonswap spectrum, Roll response

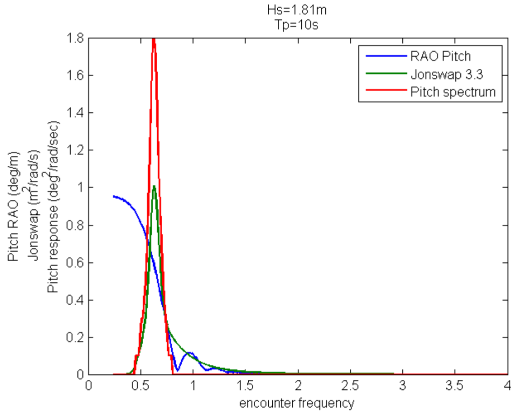

Figure 5.12: Pitch RAO, Jonswap spectrum, Pitch response

$$H_s = \frac{2.15}{\sqrt{\theta^2 + \phi^2}} H_{sign} = \frac{2.15}{\sqrt{1.91^2 + 0.99^2}} \cdot 2 = 1.81m$$

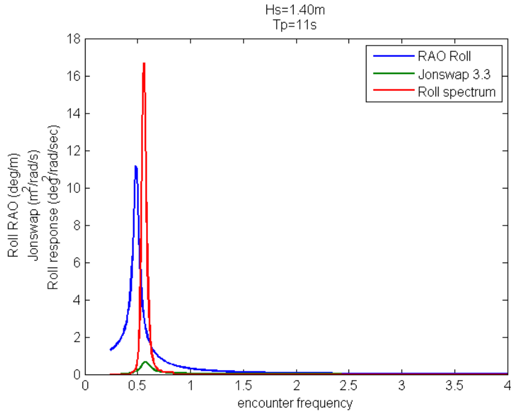

Figure 5.13: Roll RAO, Jonswap spectrum, Roll response

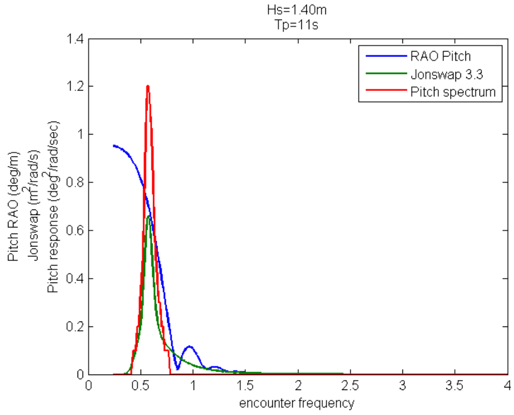

Figure 5.14: Pitch RAO, Jonswap spectrum, Pitch response

$$H_s = \frac{2.15}{\sqrt{\theta^2 + \phi^2}} H_{sign} = \frac{2.15}{\sqrt{2^2 + 0.8^2}} \cdot 2 = 1.40m$$

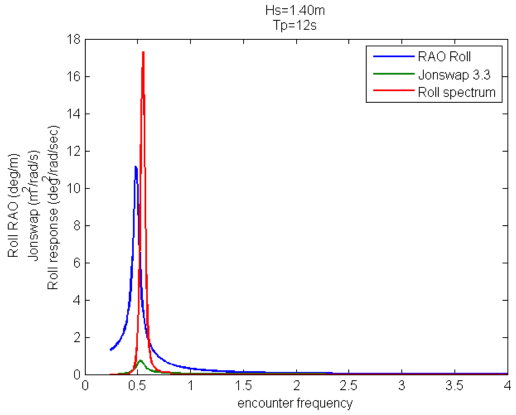

Figure 5.15: Roll RAO, Jonswap spectrum, Roll response

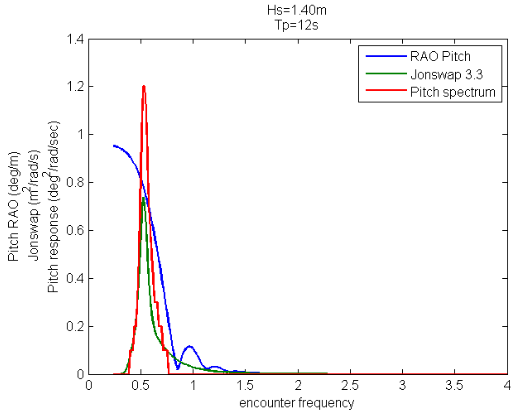

Figure 5.16: Pitch RAO, Jonswap spectrum, Pitch response

$$H_s = \frac{2.15}{\sqrt{\theta^2 + \phi^2}} H_{sign} = \frac{2.15}{\sqrt{2^2 + 0.8^2}} \cdot 2 = 1.40m$$

The process above is repeated for every wave heading (0 to 180 degrees) and the resulting maximum allowable significant wave heights are summarized in figure 5.17.

Tp(s)/Theta(deg)	0	15	30	45	60	75	90	105	120	135	150	165	180
5	19,55	7,19	3,92	2,79	1,94	2,02	2	2,03	2,29	2,8	3,89	7,23	21,5
6	11,62	5,96	3,4	2,43	1,94	1,72	1,78	1,76	1,97	2,45	3,4	6	12,29
7	7,54	4,54	2,71	1,92	1,53	1,42	1,48	1,46	1,59	1,99	2,81	4,89	9,35
8	5,12	3,1	1,89	1,37	1,14	1,06	1,07	1,08	1,17	1,43	2	3,51	6,83
9	3,39	2,13	1,32	0,98	0,82	0,75	0,74	0,76	0,84	1,01	1,4	2,44	4,73
10	2,81	1,87	0,98	0,71	0,59	0,71	0,53	0,54	0,6	0,73	0,91	1,81	3,98
11	2,64	1,3	0,65	0,54	0,46	0,4	0,39	0,4	0,45	0,55	0,77	1,4	3,77
12	2,64	1,31	0,75	0,54	0,45	0,41	0,39	0,41	0,45	0,55	0,77	1,41	3,77
13	2,72	1,55	0,92	0,67	0,56	0,5	0,49	0,51	0,56	0,68	0,95	1,71	3,87
14	2,87	1,78	1,09	0,8	0,67	0,6	0,59	0,61	0,67	0,82	1,14	1,99	4,06
15	3,05	1,96	1,22	0,9	0,75	0,68	0,66	0,68	0,76	0,92	1,27	2,21	4,26
16	3,23	2,11	1,33	0,98	0,82	0,74	0,72	0,75	0,83	1,01	1,39	2,39	4,53
17	3,44	2,29	1,45	1,08	0,89	0,81	0,79	0,81	0,9	1,09	1,51	2,6	4,83
18	3,44	2,48	1,57	1,17	0,97	0,88	0,86	0,89	0,99	1,2	1,64	2,81	5,12

Figure 5.17: Maximum wave heights per $Tp - \theta$ combination

Comparison

Now that the criteria have been tested against the maximum allowable significant wave height for a range of $Tp - \theta$, the limiting one can be obtained by determining which criterium leads to the lowest amount of acceptable significant wave heights within this range. In the tables below the tables are compared.

Velocity criterium

Tp(s)/Theta(deg)	0	15	30	45	60	75	90	105	120	135	150	165	180
5	44,08	7,97	4,21	3,03	2,49	2,16	2,05	2,17	2,45	3,02	4,27	8,18	56,84
6	26,18	8,59	4,77	3,45	3,34	2,14	1,94	2,22	2,73	3,34	4,88	9,15	35,41
7	16,18	10,02	5,31	3,54	3,49	1,92	1,73	1,94	2,52	3,49	5,27	10,75	21,71
8	16,94	8,37	4,36	2,89	2,9	1,7	1,57	1,72	2,14	2,9	4,4	8,87	21,49
9	18,62	6,13	3,27	2,25	2,26	1,47	1,38	1,48	1,75	2,26	3,3	6,35	25,26
10	15,16	4,49	2,47	1,74	1,75	1,21	1,15	1,21	1,39	1,75	2,5	4,65	22,04
11	12,9	3,41	1,91	1,37	1,39	0,98	0,94	0,99	1,12	1,39	1,95	3,59	18
12	11,9	3,44	1,95	1,41	1,44	1,03	0,99	1,03	1,17	1,44	2,03	3,7	15,71
13	11,49	4,17	2,42	1,76	1,9	1,03	1,24	1,29	1,47	1,9	2,54	4,57	14,55
14	11,4	4,86	2,88	2,1	2,16	1,53	1,47	1,53	1,75	2,16	3,04	5,38	14,07
15	11,52	5,35	3,2	2,34	2,41	1,71	1,65	1,73	1,96	2,41	3,37	5,89	13,76
17	11,74	5,75	3,49	2,56	2,63	1,87	1,81	1,89	2,14	2,63	3,67	6,33	13,8
17	12,03	6,18	3,79	2,78	2,87	2,05	1,97	2,07	2,33	2,87	3,99	6,81	14,03
18	12,38	6,62	4,09	3,02	3,13	2,23	2,15	2,25	2,54	3,13	4,32	7,31	14,35

Figure 5.18: Maximum wave heights per $Tp - \theta$ combination

Sidelead criterium

Tp(s)/Theta(deg)	0	15	30	45	60	75	90	105	120	135	150	165	180
5	19,55	7,19	3,92	2,79	1,94	2,02	2	2,03	2,29	2,8	3,89	7,23	21,5
6	11,62	5,96	3,4	2,43	1,94	1,72	1,78	1,76	1,97	2,45	3,4	6	12,29
7	7,54	4,54	2,71	1,92	1,53	1,42	1,48	1,46	1,59	1,99	2,81	4,89	9,35
8	5,12	3,1	1,89	1,37	1,14	1,06	1,07	1,08	1,17	1,43	2	3,51	6,83
9	3,39	2,13	1,32	0,98	0,82	0,75	0,74	0,76	0,84	1,01	1,4	2,44	4,73
10	2,81	1,87	0,98	0,71	0,59	0,71	0,53	0,54	0,6	0,73	0,91	1,81	3,98
11	2,64	1,3	0,65	0,54	0,46	0,4	0,39	0,4	0,45	0,55	0,77	1,4	3,77
12	2,64	1,31	0,75	0,54	0,45	0,41	0,39	0,41	0,45	0,55	0,77	1,41	3,77
13	2,72	1,55	0,92	0,67	0,56	0,5	0,49	0,51	0,56	0,68	0,95	1,71	3,87
14	2,87	1,78	1,09	0,8	0,67	0,6	0,59	0,61	0,67	0,82	1,14	1,99	4,06
15	3,05	1,96	1,22	0,9	0,75	0,68	0,66	0,68	0,76	0,92	1,27	2,21	4,26
16	3,23	2,11	1,33	0,98	0,82	0,74	0,72	0,75	0,83	1,01	1,39	2,39	4,53
17	3,44	2,29	1,45	1,08	0,89	0,81	0,79	0,81	0,9	1,09	1,51	2,6	4,83
18	3,44	2,48	1,57	1,17	0,97	0,88	0,86	0,89	0,99	1,2	1,64	2,81	5,12

Figure 5.19: Maximum wave heights per $Tp - \theta$ combination

From figures 5.18 and 5.19 it can be seen that the sidelead criterium, consisting of roll and pitch are limiting with regards to the maximum allowable significant wave height during a lifting operation. For the workablity analysis in the next section, a design wave height of 2 meters will be used. This wave height is chosen to prevent any problems such as the vertical vessel motions and heave compensator system.

5.3 Workability

Since heavy lift operations take place in a time window in the order of a few hours, combined with the statement from DNV that "Marine operations with a reference period less than 72 hours may be called weather restricted", an operability analysis is necessary. The workability is defined as the percentage of time that the sea circumstances are good enough for the ship to operate. In order to perform the workability analysis, information about the location of interest is necessary in the form of so called scatter diagrams. Scatter diagrams show the probability of the joint occurrance of certain seastates in terms of significant wave height and peak period. They are location and season dependent which means that the workability is dependent on these same factors. To evaluate and compare the J-class vessel with the increased pedestal and the original vessel in terms of workability, a representative scatter diagram is needed. Metocean data of Northwest Australia is used since this is a region in which Jumbo has recently operated. Also, a workability analysis will be done under North sea circumstances to check for more difficult sea states.

The maximum significant wave height that is used for the operability analysis is set to two meters. This is because otherwise problems can occur with for example the heave compensator or other effects. DNV states that since there are some uncertainties in weather forecasts, operational limits of environmental parameters shall be lower than design values. That is why the maximum allowable significant wave heights in the previous section need to be multiplied by alpha factors as specified in [7], or $H_{s_{op}} = \alpha \cdot H_s$. Here, $H_{s_{op}}$ is the operable significant wave height. The alpha factor is based on the weather forecast level B, which applies to environmental sensitive operations of significant importance with regard to value and consequences. Offshore lifts are typical cases of a type B operation. The table of α values is shown in the figure below.

As can be seen from figure 5.20, alpha values for significant wave heights between 1 and 2 meters are linearly interpolated between 0.68 and 0.8. alpha values for wave heights below 1 meter are not defined, but for the workability calculations taken as 0.68. The workability in percentage of time is calculated for wave encounter angles ranging from 0 to 180 degrees, in steps of 15 degrees. The workability is calculated by adding the amount of occurrances a certain sea state is within the

Table 4-2 α-factor for waves, Level B highest forecast							
Operational Period [h]	*Design Wave Height [m]*						
	$H_s = 1$	$1 < H_s < 2$	$H_s = 2$	$2 < H_s < 4$	$H_s = 4$	$4 < H_s < 6$	$H_s \geq 6$
$T_{POP} \leq 12$	0.68	Linear Interpolation	0.80	Linear Interpolation	0.83	Linear Interpolation	0.84
$T_{POP} \leq 24$	0.66		0.77		0.80		0.82
$T_{POP} \leq 36$	0.65		0.75		0.77		0.80
$T_{POP} \leq 48$	0.63		0.71		0.75		0.78
$T_{POP} \leq 72$	0.58		0.66		0.71		0.76

Figure 5.20: alpha values, from DNV [8]

acceptable operational criteria, for each period. This is done by combining information gathered from the motion analysis with the scatter diagrams. Scatter diagrams give statistical data about the amount of times a certain sea state occurs, expressed for each combination of significant wave height and peak period. Below, the workability of the ship with the increased pedestal is be compared with the workability of the original ship. In both cases the most critical lifting phase is evaluated with the crane at maximum outreach (36.55m from centerline).

Workability-Increased pedestal [%]													
Wave direction [deg]													
Location	**0**	**15**	**30**	**45**	**60**	**75**	**90**	**105**	**120**	**135**	**150**	**165**	**180**
North sea	39	32	18	13	11	8	9	9	12	14	20	31	39
n-w Australia	82	55	17	8	3	3	3	3	3	8	16	76	82

Table 5.8: Workability for ship with increased pedestal

Workability-Original ship [%]													
Wave direction [deg]													
Location	**0**	**15**	**30**	**45**	**60**	**75**	**90**	**105**	**120**	**135**	**150**	**165**	**180**
North sea	25	14	9	7	6	6	6	6	7	10	16	27	39
n-w Australia	82	54	17	8	3	3	3	3	3	8	16	76	82

Table 5.9: Workability for original ship

Some general trends that can be observed from the workability analysis is that for the original ship, the workability in the north sea is higher in the case of the ship with increased pedestal height. This is due to the fact that the natural roll period is at around 11 seconds, while the natural period for the original ship is at around 10 seconds. When looking at the scatter diagram for the north sea, it can be seen that the most likely sea-states that occur have a peak period of 6-10 seconds and a significant wave height of 1-2 meters. Since the workability is mostly dependent on the roll motion, it can be concluded that in the case of the original ship with a natural roll period around 10 seconds is closer to the most common sea states and hence results in a lower workability compared to the case with increased pedestal.
When looking at the workability results of N-W Australian region, it can be seen that the workability between the original and enhanced ship are almost the same. This, again can be explained by comparing the natural roll period with the peak periods of the most common sea states of this region. The most likely sea states occur at peak periods between 10-14 seconds. Since the natural roll periods of both ship-layouts (with increased pedestal and without) are right in between 10-14 seconds, the workability of both cases is similar. The last observation from the workability results

is that in the north sea region, the workability is less dependent on the wave encounter angle. From the workability calculations it can be concluded that increasing the pedestal height has a slight beneficial effect due to the higher natural roll period. Furthermore it should also be noted that the difference of damping does not change much in both vessel layouts.

Conclusion

From the first part of the analysis, which was focussed on the influence of the increased pedestal on the vessel, the following was observed.

- Workability is similar
- Less stability
- Less lifting capacity (from 648 to 580 ton)

The decrease of ship stability due to the increased pedestal leads to a lower lifting capacity, however a typical offshore lift consists of a load of 130 ton. From the above it can be said that the enhanced pedestal on the vessel is quite limited. Given that the type of loads are similar to the lifted loads of the crane with the original pedestal it can be concluded that increasing the lifting height of the pedestal by ten meters in this part of the analysis is feasible. In the second part of this feasibility study it is investigated how this pedestal should be constructed such that the structural integrity is guaranteed both statically and dynamically.

Chapter 6

Structural analysis

The pedestal will be subjected to several forces during lifting operations. To get more insight of the load-structure interaction, an initial sizing of the pedestal is be done. The size of the pedestal will be dependant on the critical material properties. In this chapter, first the current pedestal is described. After this the stresses that occur due to the pedestal increase are analysed. The loads are determined by the maximum load at maximum outreach, wind forces and structural weight.

6.1 Current Pedestal Mast Crane

The pedestal mounted mast crane that is currently used on the J-class vessels are two Huisman cranes designed to lift 900 ton per crane. The cranes are designed such that the load moment is carried by the mast and hence the slew bearing is not a critical construction item. Also, the main boom and auxiliary hoist winches are installed inside the wing section of the vessel. The structure is made of a high tensile steel and the crane does not require ballast weight. These combined design elements lead to a small required foundation, low center of gravity and a low own construction weight.

Figure 6.1: Currently pedestal mounted mast cranes

6.2 Available deck space

Before further analysing the pedestal, it is necessary to look at the space that is available on the deck. This, in order to prevent a pedestal design that exceeds the limits of maximum allowable footprint. In figure 6.2, the amount of space from the edge of the ship until the start of the start of the tweendeck is indicated. The pedestal may not reach to the tweendeck since cargo needs to be fitted inside this available space.

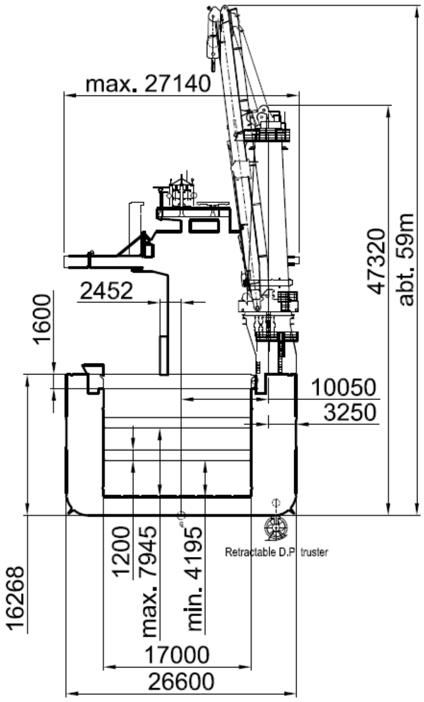

Figure 6.2: Available deck space

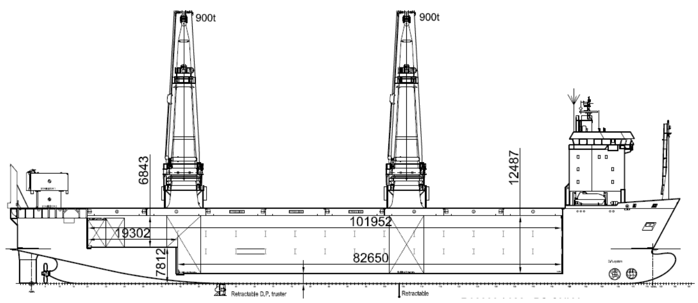

Figure 6.3: Available deck space in longitudinal direction

From this, it can be seen that the limiting pedestal dimension is in the direction of the width of the ship. In the longitudinal direction, the pedestal is not expected to be limited.

6.3 Pedestal Sizing

The pedestal of the crane construction will take in part of the moment that is caused by the loads hanging in the cranes. How this moment is created can be seen in figure 6.5 and 6.6. It should be noted that the jib is attached to the mast by roll bearings. Since these roll bearings do not take any moments, a big part of the moment is taken by the mast. At the pedestal, a net horizontal force and moment will be present at the tip resulting in normal stresses through the structure towards the bottom. Besides loading forces, wind forces will be taken into account as well. The maximum moment that the crane is subjected to is determined by the load curve as seen in figure 6.4. For this initial design it is assumed that the load curve is the same as in the crane with the increased pedestal. The maximum moment is determined at an outreach of 25m with a safe working load of 900 ton. The resulting moment is $900000 \cdot 25 \cdot 9.81 = 220.7MNm$. The maximum allowable stress is based on a paper which describes crack formation due to fatigue stress of high tensile steal [9] and has a value of $110Mpa$. In this paper it is stated that for high tensile steel in a welded state, for a certain stress range (till $110Mpa$) and a number of cycles, crack initiation occurs.

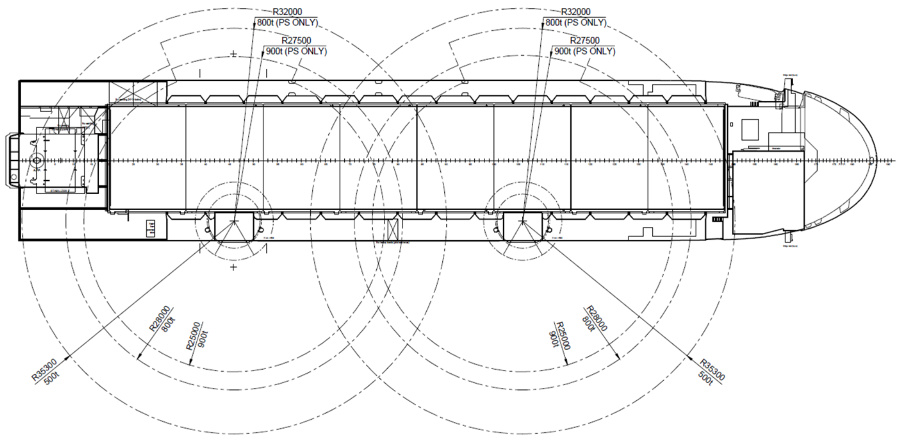

Figure 6.4: Loadcurve

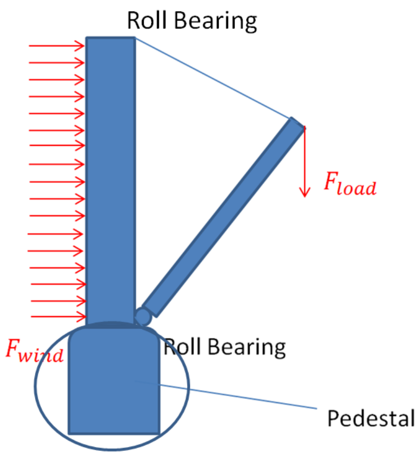

Figure 6.5: Pedestal mounted mast crane

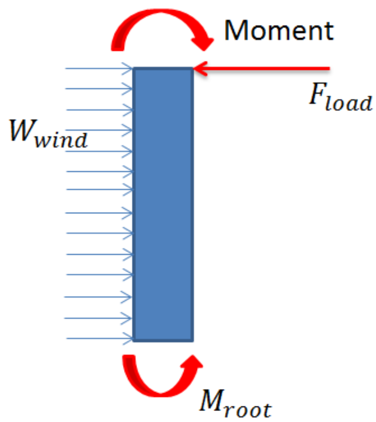

Figure 6.6: Pedestal loading

To optimize the geometry of the enhanced pedestal, some starting parameters are determined first. These can be found in the table below:

Parameter	Value
Pedestal height	15.8 m
Wall thickness	35 mm
Material	High tensile steel A514
Fatigue stress	110 Mpa
E-modulus	210 Gpa
Density	7800 kg/m^3

Table 6.1: Material properties

With these known material properties, the optimum cross section is determined. If the excisting pedestal is examinated, it can be seen that the footprint of the pedestal is around 4.7m wide, while the dimension in longitudinal direction is 6.4m as can be seen in figure 6.7. Because the width can not be extended due to the twindeck area, only the geometry in the longitudinal direction can be changed. (if necessary).
In this process of determining the geometry, first it will be investigated how the moments and forces will change from the top to the bottom of the pedestal. This is checked because the

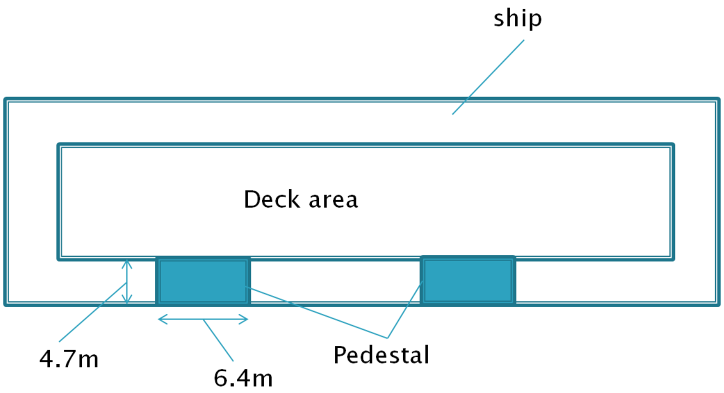

Figure 6.7: Pedestal footprint

dimensions should increase to withstand these changing moments and forces. For this initial design, it is assumed that the most governing stresses are caused by normal stresses due to bending moments. These normal stresses are calculated with the flexural formula 6.4. In the numerical model the beam is divided in n-elements. Each element is assumed to have a constant diameter, shear force and internal moment. The representation of an element with length dx can be seen in figure 6.8. In this way, for each element the forces and moments are evaluated.

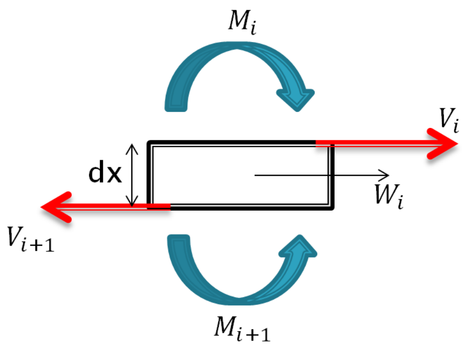

Figure 6.8: Beam element

Wind loads are calculated according to regulations [10] in which, if no purchaser specified information is available, the wind velocity to use for all in service conditions shall be 40mph (17.6m/s) up to an H_{sign} of 3 meters. These wind velocities include the effects of elevation and gust loads for the crane location. The wind area acting on the projected area of the crane components and lifted load shall be calculated as: $P_{wind} = 0.00256 C_s U^2$, in which U is the wind velocity, C_s the member shape coefficient and P_{wind} the wind pressure in N/m^2. The shape coefficient for a square tube is defined as 1.5. To obtain the wind force, this pressure is multiplied by the element area A_i.The area of the first element is found by using a guess diameter. This leads to the following element expression:

$$W_i = P_{wind} \cdot A_i \tag{6.1}$$

With the obtained wind force, the shear force can be calculated as:

$$V_i = V_{i-1} + W_i \tag{6.2}$$

Equation 6.3 evaluates the moment of the element by summing the contribution of the internal moment of the previous element, the wind force on the current element and the previous shear force.

$$M_i = M_{i-1} + 0.5 \cdot W_i \cdot dx + V_{i-1}dx \tag{6.3}$$

This leads to the distribution of shear and moment and will be applied to the flexural formula [11]:

$$\sigma_z = \frac{I_{xx}M_y - I_{xy}M_x}{I_{xx}I_{yy} - {I_{xy}}^2}x + \frac{I_{yy}M_x - I_{xy}M_y}{I_{xx}Iyy - {I_{xy}}^2}y \tag{6.4}$$

The expression in equation 6.4 can be reduced due to symmetry around the x and y axis in which I_{xy} simplifies to zero.

$$\sigma_z = \frac{M_y}{I_{yy}}x + \frac{M_x}{I_{xx}}y \tag{6.5}$$

Using the above relations and material properties it is observed that the moment does not change towards the root of the pedestal. This is due to the small contribution of the horizontal forces caused by wind. Also, with the skin thickness used of 35mm, the pedestal dimensions are larger than the necessary attachement points at the top and bottom. Therefore it is checked how large the skin thickness should be in order to obtain reasonable dimensions. First, the top part of the pedestal is checked. This part is restricted by the bottom diameter of the mast crane itself. From drawings it is determined that this diameter is 5m. This means that the top of the pedestal has a minimum length of 5×5 meters in longitudinal and lateral. Spacially, it is desirable to have the same footprint as the current pedestal. In order to achieve this, there are two possibilities. The first option is to increase the diameter in longitudinal direction from the top part of the pedestal to the dimensions of the footprint. The second option is to linearly increase the pedestal diameter longituninally from the top of the pedestal to the bottom footprint.

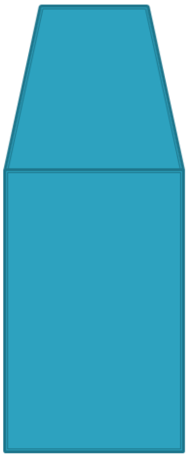

Figure 6.9: Pedestal shape straight

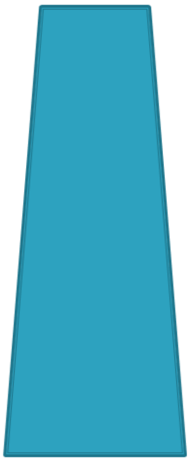

Figure 6.10: Pedestal shape linear

which shape will be selected is dependent on the constructional complexity and structural weight. Also, the shape that leads to eigenfrequencies the furthest away from excitation frequencies will be chosen.

Wall thickness along the pedestal height

Since it is determined that the geometrical constraints are the decisive factor for the pedestal outer shape, it is necessary to obtain the wall thickness along the height. This optimal thickness is calculated for each section along the height using finite elements, in a similar fashion as described previously. The pedestal can be loaded in both around the x-axis as well as around the y-axis, as can be seen in figure 6.11.

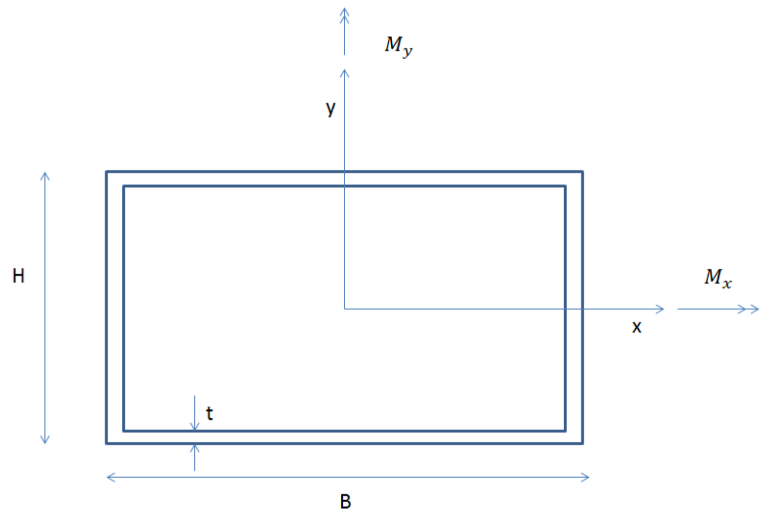

Figure 6.11: Moment around x and y

Both moments around the x and y-axis were checked and it turned out that the moment around the x-axis is governing because it leads to the highest distribution of thickness for each section along the pedestal height.. The thickness distribution is computed by first increasing the thickness of both side B and side H simultaneously until the normal stress as defined in equation 6.4 reaches a value below the material yields stress. Then, for more accuacy the thickness of side B is increased until the normal stress due to the external moment equals the material fatigue limit stress. In this way the thickness for each section along the z-axis (height) is calulated. The moment of ineria along each section around the x- axis can be seen in equation 6.6 and 6.7. It is calculated by subtracting the moment of inertia of the outer dimensions with the moment of inertia of the inner dimensions.

$$I_{xx} = (\frac{1}{12})BH^3 - \frac{1}{12}(B - 2t_B)(H - 2t_H)^3 \tag{6.6}$$

Or with thicknesses expressed in percentage of the wall dimensions. t^3 terms are ignored due to its small contribution:

$$I_{xx} = \frac{1}{12}BH^3 - \frac{1}{12}B(1 - \frac{2t}{B})(H^3(1 - \frac{6t}{H}) + 12H^3(\frac{t}{H})^2) \tag{6.7}$$

Shape 1

In this way, the final thickness distribution is determined. Side B of the pedestal has a thickness distribution of $0.0625m$ while the thickness of the H side of the pedestal runs from $0.0625m$ at the top till a minimum value of $0.0485m$ at the lower part of the pedestal. In this way, the least amount of material is used and hence designing has been done on the verge of the material fatigue limit stress. The thickness distribution for the first pedestal shape can be seen in figure 6.12.

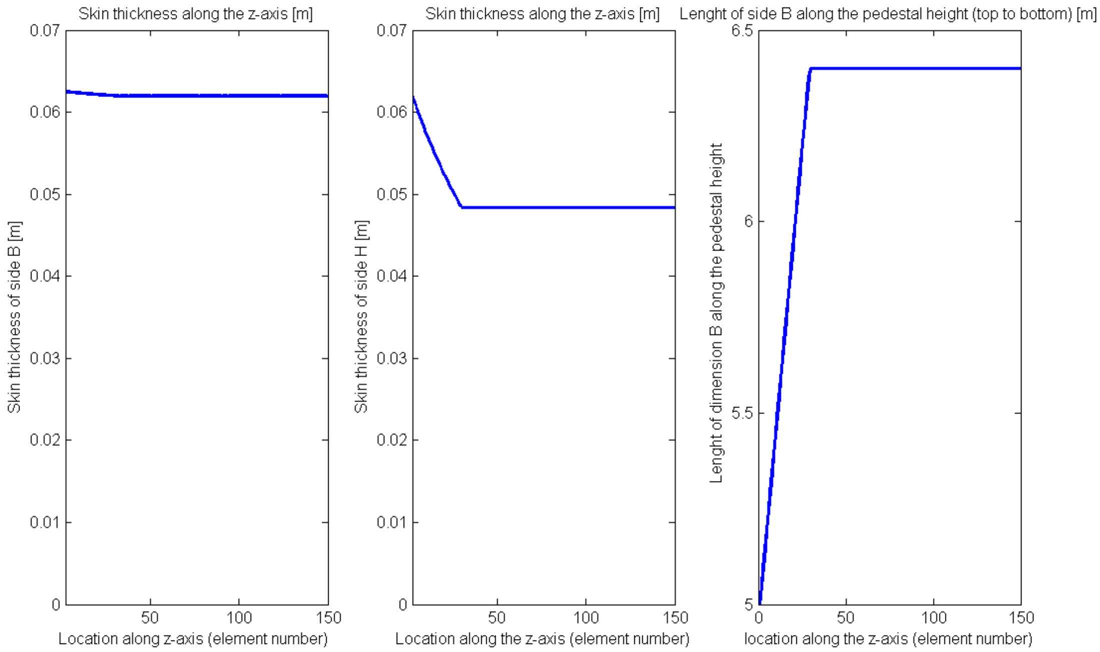

Figure 6.12: Thickness distribution and dimensions of lenght B

Shape 2

The thickness distribution of the second shape has a thickness distribution of $0.0625m$ from top till bottom. The thickness distribution of the H side of the pedestal runs from $0.0625m$ at the top till $0.0485m$ at the bottom. These results can be seen in figure 6.13.

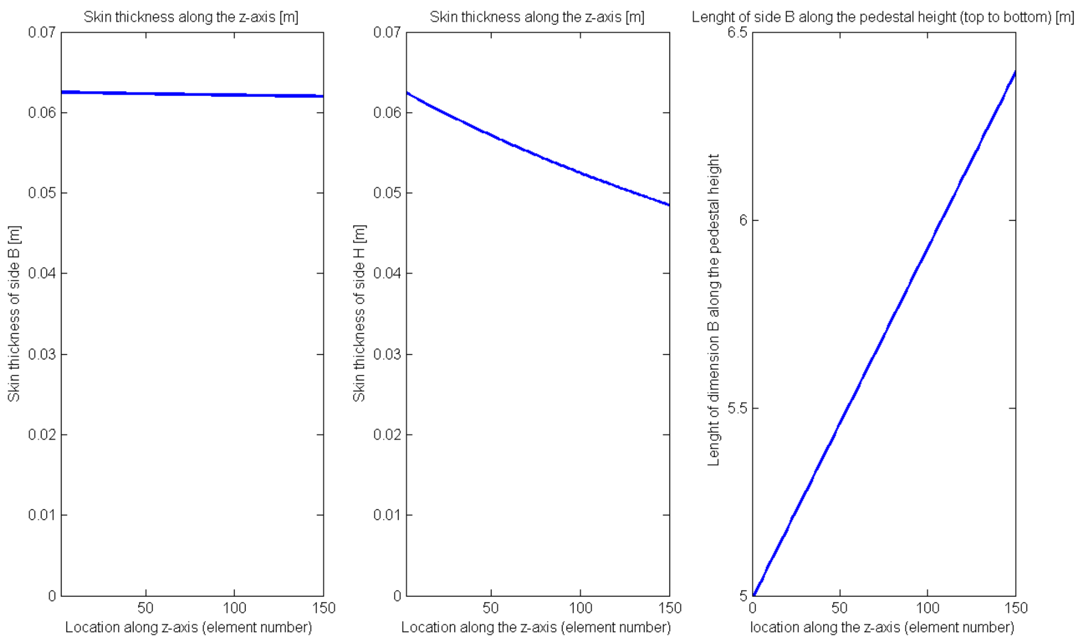

Figure 6.13: Thickness distribution and dimensions of lenght B

For completeness, the thickness distribution due to the moment around the y-axis of the pedestal cross section is shown in appendix B. The total weight of both shape one and two are shown in table 6.2. From this it can be concluded that from a weight perspective, the pedestal with shape 2 has a lower weight and hence is chosen as the shape to be further analysed.

Pedestal total weight [ton]	
Shape 1	154.46
Shape 2	152.33

Table 6.2: Weight comparison

6.4 Dynamic Crane Properties

Once the geometry of the pedestal is obtained, one should perform a dynamic analysis. During the early design stages it is important to predict in which range the natural frequencies of the design are located. Also, it is convenient to see how much the natural frequencies of the enhanced pedestal differ from the natural frequencies of the original pedestal design. However, it is expected that the natural frequencies of the pedestal, isolated from the mast and boom section, are very high and thus outside the regions of any excitation frequencies of interest. For this reason it is necessary to include the mast and boom in order to obtain sensible dynamic behaviour of the whole crane system (due to the pedestal increase). In this chapter the theoretical principles to obtain the dynamic behaviour of the pedestal-crane system is layed out, after which a numerical analysis is performed to obain the natural frequencies of this crane system. First, the principle of the **Euler Bernoulli beam** is explained to show the behaviour of a bending beam. Secondly, the equation of motion of **Rods** under axial loading are explained. This is done due to the fact that the pedestal-mast-boom system is modeled as a combination of rigid jointed frames that resist the combined effects of horizontal and vertical loads. The strength of the frames are derived from moment interactions between the beams and the columns at the rigid joints. This means that the elements are subjected to bending but also axial forces. The combined effects are referred to as **beam-column** elements, described in the third part of this chapter.

Euler Bernoulli-beam

To investigate the dynamic properties of the pedestal, it is assumed that it is slender enough to act like a beam. The equation of motion for this beam can be described by considering the free-body diagram of an element beam, which can be seen in figure 6.14. Here $f(x,t)$ is the external force applied to the beam, A(x) is the cross sectional area, V(x,t) is the shear force and M(x,t) is the bending moment. The relationship between bending moment and deflection can be expressed as:

$$M(x,t) = EI(x)\frac{\partial w}{\partial x^2}(x,t) \tag{6.8}$$

Where E is the Young's modulus and I(x) is the moment of inerita of the beam cross section about the y-axis.
Furthermore the force equation of motion in the z-direction is

$$-(V+dV) + f(x,t)dx + V = \rho A(x)dx\frac{\partial^2 w}{\partial t^2}(x,t) \tag{6.9}$$

where ρ is the density of mass and $A(x)$ is the cross sectional area of the beam. Next, the moment equilibrium is given by

$$(M+dM) - (V+dV)dx + f(x,t)dx\frac{dx}{2} - M = 0 \tag{6.10}$$

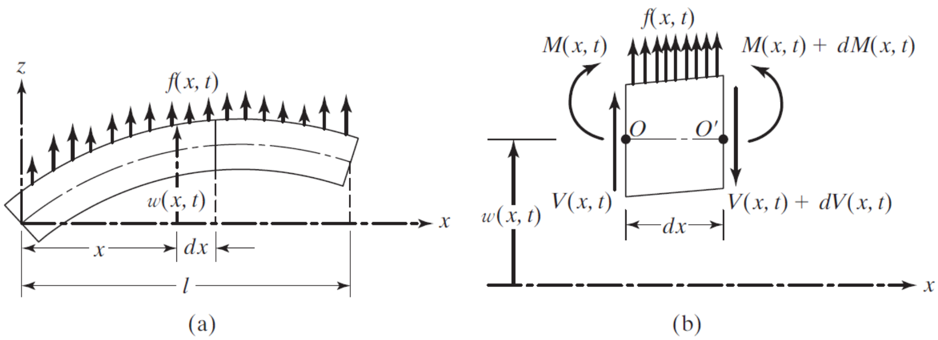

Figure 6.14: Beam element in bending [12]

dV and dM are expressed by $dV = \dfrac{\partial V(x,t)}{\partial x}dx$ and $dM = \dfrac{\partial M(x,t)}{\partial M}dx$. If this is substituted in equation 6.9 and 6.10 and also disregarding terms that involve second powers in dx, then these expressions can be written as

$$-\frac{\partial V}{x}(x,t) + f(x,t) = \rho A(x)\frac{\partial^2 w}{\partial t^2}(x,t) \tag{6.11}$$

$$\frac{\partial M}{\partial x}(x,t) - V(x,t) = 0 \tag{6.12}$$

From the relation $V = \dfrac{\partial M}{\partial x}$, equation 6.11 becomes

$$-\frac{\partial^2 M}{\partial x^2}(x,t) + f(x,t) = \rho A(x)\frac{\partial^2 w}{\partial t^2}(x,t) \tag{6.13}$$

Finally, when substituting equation 6.8 into equation 6.13 the equation of motion for a non-uniform beam subjected to a forced viibration in lateral direction is obtained:

$$\frac{\partial^2}{\partial x^2}\left[EI(x)\frac{\partial^2 w}{\partial x^2}(x,t)\right] + \rho A(x)\frac{\partial^2 w}{\partial t^2}(x,t) = f(x,t) \tag{6.14}$$

In the case of a uniform beam, equation 6.14 reduces to

$$EI\frac{\partial^4 w}{\partial x^4}(x,t) + \rho A\frac{\partial^2 w}{\partial t^2}(x,t) = f(x,t) \tag{6.15}$$

If no external force is applied $f(x,t) = 0$ the equation of motion for a free vibration becomes

$$c^2\frac{\partial^4 w}{\partial x^4}(x,t) + \frac{\partial^2 w}{\partial t^2}(x,t) = 0 \tag{6.16}$$

Here

$$c = \sqrt{\frac{EI}{\rho A}} \tag{6.17}$$

Rods

The governing equation to describe a longitudinal motion of an axial bar (rod) is introduced next and from the second law of Newton the EOM is described by 6.18 and figure 6.15:

$$\rho A dx \frac{\partial^2 u}{\partial t^2} = (P + \frac{\partial P}{\partial x}) - P \tag{6.18}$$

Where u is the axial displacement along the rod direction and x and t are the spatial and time terms.

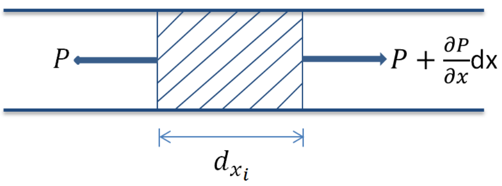

Figure 6.15: Free body diagram for axial member

From Hooke's law, the following relation between stress and strain is obtained:

$$\frac{P}{A} = E\epsilon \tag{6.19}$$

$$\epsilon = \frac{\partial u}{\partial x} \tag{6.20}$$

Substituting equation 6.19 and 6.20 into equation 6.18, the final expression is obtained:

$$\rho A \frac{\partial^2 u}{\partial t^2} = \frac{\partial}{\partial x}(AE\frac{\partial u}{\partial x}) \tag{6.21}$$

For rods with non uniform cross sections equation 6.21 changes to:

$$\rho A(x) \frac{\partial^2 u}{\partial t^2} = \frac{\partial}{\partial x}(EA(x)\frac{\partial u}{\partial x}) \tag{6.22}$$

6.4.1 Analytical Expressions: Planar Motions

Now that the EOM's of a bending beam and rod are described, these expressions are used to analyse the motions of the individual crane-members. It should be stated that the crane system is simplified and only compressive bending beams and rigid joints are investigated. This plane frame model is used to get an impression of the present natural frequencies. It should provide sufficient enough information to evaluate the system's natural frequencies for the initial stage of the design.
In the figure below the analysis model for the simplified crane system is shown. The beam-parts are rigidly connected to each other. The vertical beam is connected to a clamped support. The EOM's for translational and longitudinal motions are expressed by equation 6.23 and 6.24 which were derived in the previous sections of this chapter. If straight sections are assumed, the following can be obtained:

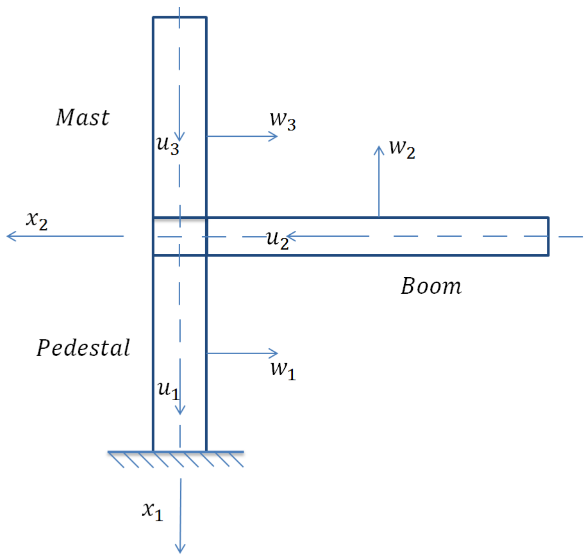

Figure 6.16: Free body diagram of the crane

$$\textit{EOM bending beam} \qquad \rho A \frac{\partial^2 w}{\partial t^2} + EI \frac{\partial^4 w}{\partial x^4} = 0 \tag{6.23}$$

$$\textit{EOM rod} \qquad \rho A \frac{\partial^2 u}{\partial t^2} + EA \frac{\partial^2 u}{\partial x^2} = 0 \tag{6.24}$$

There are in total six EOM's. Three in lateral direction and three in longitudinal direction. Note that the pedestal and mast share the same axis (x_1). These motions for the three parts of the crane are described as follows:

Lateral motion

Pedestal section

$$\rho A_1 \frac{\partial^2 w_1}{\partial t^2} + EI_1 \frac{\partial^4 w_1}{\partial x_1^4} = 0 \tag{6.25}$$

Boom section

$$\rho A_2 \frac{\partial^2 w_2}{\partial t^2} + EI_2 \frac{\partial^4 w_2}{\partial x_2^4} = 0 \tag{6.26}$$

Mast section

$$\rho A_3 \frac{\partial^2 w_3}{\partial t^2} + EI_3 \frac{\partial^4 w_3}{\partial x_1^4} = 0 \tag{6.27}$$

Longitudinal motion

Pedestal section

$$\rho A_1 \frac{\partial^2 u_1}{\partial t^2} + EA_1 \frac{\partial^2 u_1}{x_1^2} = 0 \tag{6.28}$$

Boom section

$$\rho A_2 \frac{\partial^2 u_2}{\partial t^2} + EA_2 \frac{\partial^2 u_2}{x_2^2} = 0 \tag{6.29}$$

Mast section

$$\rho A_3 \frac{\partial^2 u_3}{\partial t^2} + EA_3 \frac{\partial^2 u_3}{x_1^2} = 0 \tag{6.30}$$

Next to these sets of motion equations, boundary and interface conditions need to be described at the root of the pedestal and the location of the rigid joint that links the pedestal with the mast and boom section. The interface conditions consist of kinematic (displacement and rotation balance) and dynamic expressions (moment and force balance):

Interface conditions (at rigid joint)

Kinematic conditions: displacements

$$u_1 = -w_2 = u_3 \tag{6.31}$$

$$w_1 = -u_2 = w_3 \tag{6.32}$$

Kinematic conditions: rotations

$$\frac{\partial w_1}{\partial x_1} = -\frac{\partial w_2}{\partial x_2} = \frac{\partial w_3}{\partial x_1} \tag{6.33}$$

Dynamic conditions: moment balance

$$\frac{\partial^2 w_1}{\partial x_1^2} = -\frac{\partial^2 w_2}{\partial x_2^2} = \frac{\partial^2 w_3}{\partial x_1^2} \tag{6.34}$$

Dynamic conditions: force balance

$$-EA\frac{\partial u_1}{\partial x_1} = EI\frac{\partial^3 w_2}{\partial x_2^3} = -EA\frac{\partial u_3}{\partial x_1} \tag{6.35}$$

$$EI\frac{\partial^3 w_1}{\partial x_1^3} = -EA\frac{\partial u_2}{\partial x_2} = EI\frac{\partial^3 w_3}{x_3^3} \tag{6.36}$$

Boundary conditions

Pedestal root: displacements and rotations

$$w_1 = 0 \qquad u_1 = 0 \qquad \frac{\partial w_1}{\partial x_1} = 0 \tag{6.37}$$

Boom free-end

$$\frac{\partial^2 w_2}{\partial x_2^2} = \frac{\partial^3 w_2}{\partial x_2^3} = 0 \tag{6.38}$$

$$EA\frac{\partial u_2}{\partial x_2} = 0 \tag{6.39}$$

Mast free-end

$$\frac{\partial^2 w_3}{\partial x_1^2} = \frac{\partial^3 w_3}{\partial x_1^3} = 0 \tag{6.40}$$

$$EA\frac{\partial u_3}{\partial x_1} = 0 \tag{6.41}$$

Added tip-mass

The last thing to consider is a case when a mass is added to the tip of the crane. This leads to changes in the boom boundary conditions (kinematic and dynamic) and the free body diagram is shown in figure 6.17. Equation 6.38 and 6.39 change to:

Boom free-end

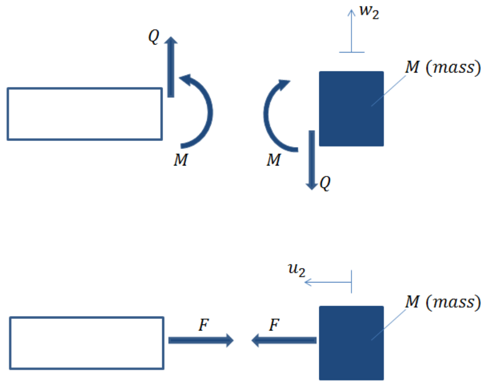

Figure 6.17: Free body diagram Tip mass

$$EI_2\frac{\partial^2 w_2}{\partial x_2^2} = 0 \tag{6.42}$$

$$EA_2\frac{\partial u_2}{\partial x_2} = M\frac{\partial^2 u_2}{\partial t^2} \tag{6.43}$$

$$EI_2\frac{\partial^3 w_2}{\partial {x_2}^3} = M\frac{\partial^2 w_2}{\partial t^2} \tag{6.44}$$

6.4.2 Numerical Analysis

The natural frequencies are dependent on the fundamental characteristics and are a product of the chosen geometry, density and material choice or stiffness. These characteristics can be implemented in a finite element model. In this way the natural modes and corresponding frequencies can be obtained. Information about natural frequency characteristics is important since external force excitations could exist that resonate with one of the natural frequencies of the pedestal. This in turn can lead to large stresses and stains. If no damping is present, the dynamic characteristics are described by:

$$\omega^2[M]\{v_i\} = [K]\{v_i\} \tag{6.45}$$

In here $[K]$ is the stiffenes matrix, $[M]$ is the mass matrix, ω is the angular frequency for a given mode and $\{v_i\}$ is the vector that corresponds to that mode shape. With the finite element method a set of natural frequencies and mode shapes are determined.

Beam element: Euler-Bernoulli

In the following figure an element of an Euler-Bernoulli beam is visualized. v_1 and v_2 represent displacements while θ_1 and θ_2 are rotational displacements of each end point. This vector is expressed as:

$$V = \begin{bmatrix} v_1 \\ v_2 \\ \theta_1 \\ \theta_2 \end{bmatrix} \tag{6.46}$$

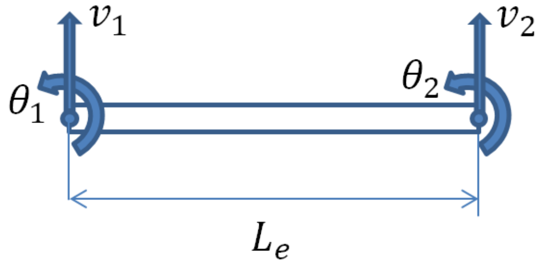

Figure 6.18: Euler-Bernoulli beam element

$w(x,t)$ is described by four boundary conditions, being $w(0,t) = v_1(t)$, $\dfrac{\partial w(0,t)}{\partial x} = \theta_1(t)$, $w(L,t) = v_2(t)$ and $\dfrac{\partial w(L,t)}{\partial x} = \theta_2(t)$. $w(x,t)$ is defined as:

$$w(x,t) = a(t) + b(t)x + c(t)x^2 + d(t)x^3 \tag{6.47}$$

When the four boundary conditions are implemented one finds that:

$$\begin{aligned} a(t) &= v_1(t) \\ b(t) &= \theta_1(t) \\ c(t) &= \frac{1}{L^2}(-3v_1(t) - 2L\theta_1(t) + 3v_2(t) - L\theta_2(t) \\ d(t) &= \frac{1}{L^2}(2v_1 + L\theta_1(t) - 2v_2(t) + L\theta_2(t)) \end{aligned}$$

By making use of so called shape-functions 6.49, the transverse motion $w(x,t)$ can be written as:

$$w(x,t) = N_1(x)v_1 + N_2(x)\theta_1(t) + N_3(x)v_2(t) + N_4(x)\theta_2(t) \tag{6.48}$$

From equation 6.47 the shape functions are defined as:

$$\begin{aligned} N_1(x) &= 1 - 3(\frac{x}{L})^2 + 2(\frac{x}{L})^3 \\ N_2(x) &= x - 2L(\frac{x}{L})^2 + L(\frac{x}{L})^3 \\ N_3(x) &= 3(\frac{x}{L})^2 - 2(\frac{x}{L})^3 \\ N_4(x) &= -L(\frac{x}{L})^2 + L(\frac{x}{L})^3 \end{aligned} \tag{6.49}$$

The kinetic energy of the beam can be expressed as:

$$KE = \frac{1}{2}\int_0^L \rho A(\frac{\partial w}{\partial t})^2 dx = \frac{1}{2}\rho A\int_0^L [N_1(x)\dot{v}_1(t) + N_2(x)\dot{\theta}_1(t) + N_3(x)\dot{v}_2(t) + N_4(x)\dot{\theta}(t))2dx] \tag{6.50}$$

Evaluating this integral gives:

$$KE = \frac{\rho AL}{420}\dot{v}^T M\dot{v} \tag{6.51}$$

The mass matrix for each element is defined as:

$$M^e = \frac{\rho AL}{420}\begin{bmatrix} 156 & 22L & 54 & -13L \\ 22L & 4L^2 & 13L & -3L^2 \\ 54 & 13L & 156 & -22L \\ -13L & -3L^2 & -22L & 4L^2 \end{bmatrix} \tag{6.52}$$

Lastly, the stiffness matrix is derived from the potential energy :

$$PE = \frac{1}{2}EI\int_0^L (\frac{\partial^2 v}{\partial x^2})^2 dx = v^T K v \tag{6.53}$$

The element stiffness matrix is then given as:

$$K^e = \frac{EI}{L^3}\begin{bmatrix} 12 & 6L & -12 & 6L \\ 6L & 4L^2 & -6L & 2L^2 \\ -12 & -6L & 12 & -6L \\ 6L & 2L^2 & -6L & 4L^2 \end{bmatrix} \tag{6.54}$$

Truss element: Plane truss

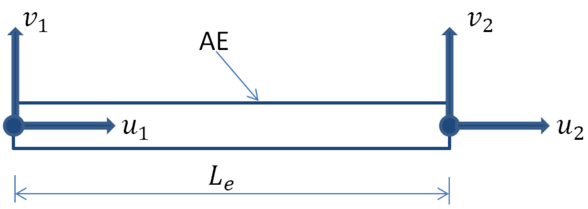

Figure 6.19: Truss element (2D)

In the figure above a bar element is shown. When a linear displacement function along the x-axis of the bar is assumed, then:

$$u = a_1 + a_2 x \tag{6.55}$$

Equation 6.55 can also be expressed as:

$$u(x,t) = (\frac{d_{2_x} - d_{1_x}}{L})x + d_{1_x} \tag{6.56}$$

Or:

$$u = [N_1(x)\; N_2(x)]\begin{bmatrix} d_{1_x} \\ d_{2_x} \end{bmatrix} \tag{6.57}$$

With the shape functions defined as:

$$\begin{aligned} N_1(x) &= 1 - \frac{x}{L} \\ N_2(x) &= \frac{x}{L} \end{aligned} \tag{6.58}$$

From the weak form as descibed in [13], the stiffness and mass matrices of a two dimensional truss are shown in equation 6.60 and 6.61 respectively. Also the nodal degrees of freedom of each truss element are expressed in equation 6.59

$$d^e = [u1\, v1\, u2\, v2]^T \tag{6.59}$$

$$K^e = \begin{bmatrix} \frac{AE}{L} & 0 & -\frac{AE}{L} & 0 \\ 0 & 0 & 0 & 0 \\ -\frac{AE}{L} & 0 & \frac{AE}{L} & 0 \\ 0 & 0 & 0 & 0 \end{bmatrix} \tag{6.60}$$

$$M^e = \frac{\rho AL}{6} \begin{bmatrix} 2 & 0 & 1 & 0 \\ 0 & 0 & 0 & 0 \\ 1 & 0 & 2 & 0 \\ 0 & 0 & 0 & 0 \end{bmatrix} \tag{6.61}$$

In here A and E are the cross sectional area and elastic modulus, respectively while L represents the length of the element. Note that the second and fourth rows and columns are zero since these are associated with transverse motions (rod only has axial deformations).

Beam-column element

Finally, beam column elements are described. Their nodal displacements consist of of translations and rotations. These displacements can be seen in 6.62. In total there are six degrees of freedom for each element.

$$[d^e] = [u_1\, v_1\, \theta_1\, u_2\, v_2\, \theta_2]^T \tag{6.62}$$

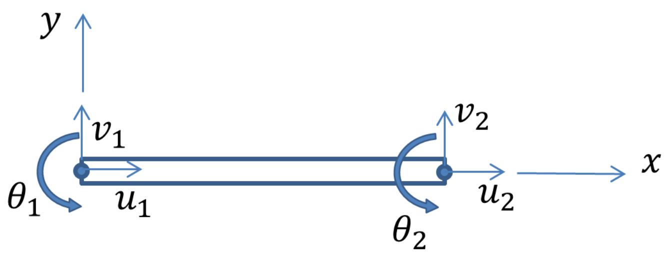

Figure 6.20: Beam-column element

If deformations are small, coupling between axial displacements do not interact with the bending deformations. In this way, the stiffness and mass matrix for a 2D- frame element can be constructed by using the principle of superposition. This is done by simply adding the matrices of a beam element 6.52 and 6.54 to the matrices of a truss element 6.60 and 6.61. Both the mass and stiffness matrix are expressed in terms of

$$K^e = \frac{E}{L^3} \begin{bmatrix} AL^2 & 0 & 0 & -AL^2 & 0 & 0 \\ 0 & 12I & 6IL & 0 & -12I & 6IL \\ 0 & 6IL & 4IL^2 & 0 & -6IL & 2IL^2 \\ -AL^2 & 0 & 0 & AL^2 & 0 & 0 \\ 0 & -12I & -6IL & 0 & 12I & -6IL \\ 0 & 6IL & 2IL^2 & 0 & -6IL & 4IL^2 \end{bmatrix} \tag{6.63}$$

$$M^e = \begin{bmatrix} 2ma & 0 & 0 & ma & 0 & 0 \\ 0 & 156mm & 22Lmm & 0 & 54mm & -13Lmm \\ 0 & 22Lmm & 4L^2mm & 0 & 13Lmm & -3L^2mm \\ ma & 0 & 0 & 2ma & 0 & 0 \\ 0 & 54mm & 13Lmm & 0 & 156mm & -22Lmm \\ 0 & -13Lmm & -3L^2mm & 0 & -22Lmm & 4L^2mm \end{bmatrix} \tag{6.64}$$

with $ma = \dfrac{\rho AL}{6}$ and $mm = \dfrac{\rho AL}{420}$.
In order to transform the beam column elements from local to the global coordinate system for inclined members a planar transformation is necessary. The relation between local and global displacements is:

$$\begin{bmatrix} u_1 \\ v_1 \\ \theta_1 \\ u_2 \\ v_2 \\ \theta_2 \end{bmatrix} = \begin{bmatrix} cos(\theta) & sin(\theta) & 0 & 0 & 0 & 0 \\ -sin(\theta) & cos(\theta) & 0 & 0 & 0 & \\ 0 & 0 & 1 & 0 & 0 & 0 \\ 0 & 0 & 0 & cos(\theta) & sin(\theta) & 0 \\ 0 & 0 & 0 & -sin(\theta) & cos(\theta) & 0 \\ 0 & 0 & 0 & 0 & 0 & 1 \end{bmatrix} \begin{bmatrix} \overline{u}_1 \\ \overline{v}_1 \\ \overline{\theta}_1 \\ \overline{u}_2 \\ \overline{v}_2 \\ \overline{\theta}_2 \end{bmatrix} \tag{6.65}$$

Matrix 6.65 can be written as:

$$\{d^e\} = [T]\{\overline{d}^e\} \tag{6.66}$$

From the concept of strain energy [13] the frame element can be expressed in the global coordinate system as follows:

$$[\overline{K}^e] = [T]^T[K^e][T] \tag{6.67}$$

$$[\overline{M}^e] = [T]^T[M^e][T] \tag{6.68}$$

With $\overline{K^e}$ and $\overline{M^e}$ expressing the stiffness and mass matrix in global coordinates.

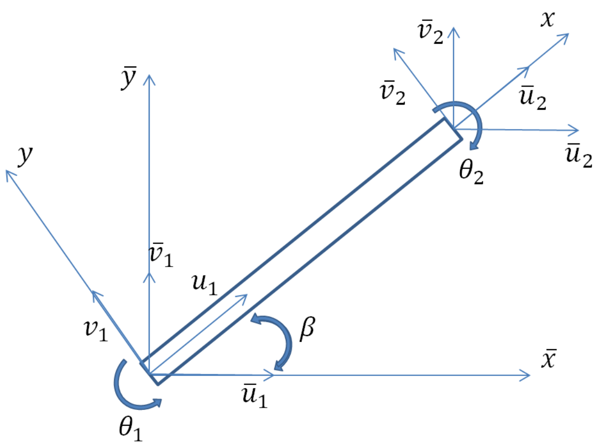

Figure 6.21: Beam-column element and relation between global and local coordinates

These beam-column elements are used to perform a numerical analysis for the dynamic properties of the pedestal-crane system. In the numerical model, the pedestal taper is taken into account by discretizing the model into finite (beam-column) elements with uniform cross sectional shape and mass distribution. In this way, the geometry is approximated by piecewise constant cross-sections. Additional explanation about the finite element model can be found in appendix C.

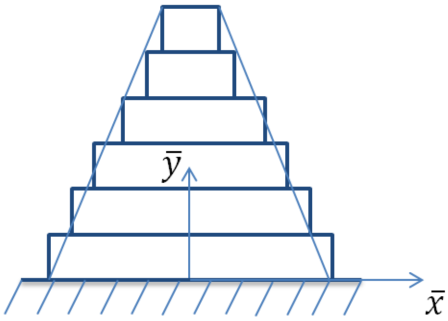

Figure 6.22: Idealized tapered pedestal geometry

6.5 System Natural Frequencies

The natural frequencies of the crane with the increased pedestal are investigated in this section. The material properties of the individual members are listed in table6.4 and the dimensions in6.3. First the system natural frequencies without the influence of the tip mass are investigated. After this a mass of 900 ton is attached to the tip of the boom to see how this influences the system natural frquencies. Lastly, a check is done in the case of a pedestal with constant wall thickness of 6.25cm along the height of the pedestal.

Pedestal	**Value**
Width top (B)	5m
Width bottom (B)	5m
Length top (H)	5m
Length bottom (H)	6.4m
Height	15.8 m
Thickness top	0.063m
Thickness bottom	0.049m
Mast	**Value**
Radius	2.5m
Height	18.8m
Wall thickness	0.06 m
Jib (Boom)	**Value**
Area cross section	0.52m^2
Height	34m
Wall thickness	0.06m

Table 6.3: Crane-component dimensions

Parameters	**Value**
Fatigue stress	110 Mpa
E-modulus	210 Gpa
Density	7800 kg/m^3

Table 6.4: Material properties

No crane-tip mass

The dynamic properties expressed in natural frequencies for the enhanced crane pedestal are obtained from the numerical model for different jib positions. These positions consist of two operating conditions and one in stowed (rest) position. The results for a range of mode numbers can be seen in the tables below.

Natural Frequencies		
Mode number	Freq. [Hz]	Freq. [rad/s]
1	0.26	1.66
2	2.41	15.11
3	4.91	30.88
4	8.01	50.37
5	9.23	58.01

Table 6.5: Natural frequencies in dropped down operating condition

Natural Frequencies		
Mode number	Freq. [Hz]	Freq. [rad/s]
1	0.22	1.39
2	2.22	13.94
3	5.46	33.96
4	8.18	51.40
5	10.18	63.95

Table 6.6: Natural frequencies in upright operating condition

Natural Frequencies		
Mode number	Freq. [Hz]	Freq. [rad/s]
1	0.21	1.34
2	2.14	13.47
3	6.12	38.47
4	8.54	53.67
5	11.26	70.73

Table 6.7: Natural frequencies in stowed condition

As can be seen from table 6.5 till 6.7, the lowest frequencies are between 1.34 and 1.66 rad/s. In DNV [14] it is stated that calculation of natural-frequencies and eigenmodes is normally not covered. However dynamic amplification of the crane displacements may occur when the ship movement has the same period as the the natural period of the crane. This is why the lower and upper limit are determined from the scatter diagram as shown in the ship workability calculations in chapter 5. These values are at the limits of the scatter diagram being in between wave frequencies of 0.34 and 1.25 rad/s. The natural frequencies of the crane with the increased pedestal are higher than this value and hence the stiffness of the pedestal does not need to be stiffened in both x-or y-direction.

Added crane-tip mass

Next, the mass of 900 ton is added to the tip of the boom.This is done by adding the magnitude of this mass to the node corresponding to the tip of the boom. Since the shape of the cargo is not known, the moment of inertia is not included. The concentrated mass is added to the global system mass matrix as defined by equation 6.64 and the total mass matrix is shown below.

$$[M] = [M] + \begin{array}{c} \begin{array}{ccc} u_i & v_i & \theta_i \end{array} \\ \begin{bmatrix} m_c & 0 & 0 \\ 0 & m_c & 0 \\ 0 & 0 & 0 \end{bmatrix} \end{array} \begin{array}{c} \\ u_i \\ v_i \\ \theta_i \end{array} \qquad (6.69)$$

In which m_c is the additional concentrated mass at node i (at boom tip position).
With this, the natural frequencies with tip mass are determined for operating conditions. The results are listed below.

Natural Frequencies		
Mode number	Freq. [Hz]	Freq. [rad/s]
1	0.23	1.46
2	1.01	6.35
3	2.41	15.12
4	3.76	23.63
5	7.81	49.08

Table 6.8: Natural frequencies in dropped down operating condition with tip mass

Natural Frequencies		
Mode number	Freq. [Hz]	Freq. [rad/s]
1	0.22	1.39
2	0.96	6.01
3	2.25	14.13
4	5.04	31.65
5	8.56	53.78

Table 6.9: Natural frequencies in upright operating condition with tip mass

Constant pedestal wall thickness

Lastly, the natural frequencies of the crane with constant wall thickness with tip mass are determined.

Natural Frequencies		
Mode number	Freq. [Hz]	Freq. [rad/s]
1	0.24	1.53
2	1.01	6.37
3	2.41	15.14
4	3.98	25.02
5	7.83	49.19

Table 6.10: Natural frequencies in dropped down operating condition constant thickness

Natural Frequencies		
Mode number	Freq. [Hz]	Freq. [rad/s]
1	0.22	1.39
2	0.97	6.08
3	2.25	14.11
4	5.25	32.99
5	8.54	53.63

Table 6.11: Natural frequencies in upright operating condition
constant thickness

It can be seen that the natural frequencies increase slightly when compared to the pedestal with varying skin thickness. This is due to the general increase of the moment of inertia along each cross section. The influence of this stiffening is however relatively small.

6.5.1 Conclusion

From the structural analysis in this chapter, a pedestal shape is achieved with the lowest possible weight. This is done by adding the right amount of stiffness to each pedestal cross section along the height to cope with the bending moments due to the load hanging in the crane at a certain distance. The statically determined tapered shape combined with the distribution of the wall thickness lead to total crane natural frequencies that are in an acceptable range situated just outside the regions of the ship frequencies that it may encounter in both sailing and operating conditions. With the mass attached to the tip of the crane, the system natural frequencies decrease. The combined effect of constant pedestal wall thickness and tip mass raises the natural frequencies slightly. For all three cases the system natural frequencies are well outside the frequencies of ship excitation.

Chapter 7

Discussion and Recommendations

The feasibility of raising the lifting height on the J-class heavy lift vessel by a pedestal increase has been studied in this thesis. This has been done in two parts. The first part focused on the changes to the vessel motion and stability characteristics. From this it was observed that with custom ballast conditions the draft increased and the stability expressed in $\overline{GM}$ decreased. This lowered the maximum load capacity. The overall effect caused an increase of the natural period for the roll motion. The roll displacements were the most critical for all crane configurations. Furthermore it was observed that a higher stability combined with larger draft led to lower (roll) damping ratios and hence larger RAO values near the natural periods. In this study the lifting capacity without the use of stabilizing pontoons, before the pedestal increase was determined at 648 ton while after the increase of pedestal the lifting capacity decreased by about 100 ton to a value of 580 ton. Using these hydrostatic and motion characteristics, the workability for two locations were calculated. Workability in the north-north sea would actually increase from 13.7% to 19.7%. The workability for the north western regions of Australia stayed constant at 27.6%. Vessel characteristics are negatively influenced by the enhanced pedestal. A decreased stability and lifting capacity were obtained, while workability was observed to be similar or the same compared to the original pedestal configuration. However a typical offshore lift at Jumbo has a weight of about 130 ton. From this it can be concluded that the negative influence of the increased pedestal is quite limited. A higher lifting capacity is gained in return.

The second part of this feasibility study focused on the structural integrity of the pedestal when increased by 10 meters in height. Bending stresses were governing limitations for this initial design. Dimensioning of the geometry was done such that the external loads did not lead to stresses higher than the fatigue limit stress of 110Mpa. In this way a tapered shape with a linear wall thickness distribution led to the optimal design in terms of weight (and cost). A weight of 152 ton was obtained. The obtained shape was subjected to a dynamic analysis. For sensible results, the tapered pedestal was connected to the mast and jib. A simplified dynamic model was created using finite elements in which planar motions were investigated. Natural frequencies for different crane configurations including a tip mass of 900 ton were evaluated. This resulted in a value of 1.39 rad/s as a lower limit. This value is higher than the lowest frequency of 1.25 rad/s of vessel motions as obtained from the workability study. No additional stiffening of the pedestal needs to be done. Within the assumptions made for the analysis, it is concluded that a pedestal increase is feasible.

Recommendations

The first recommendation is to investigate the possibility to increase the lifting capacity using stabilizing pontoons. These pontoons should be made such that static stability is increased while reaching a natural period that does not negatively influence the workability.
For a more detailed analysis of the structural integrity, compressive thick beams or Timoshenko beams can be investigated. With this, the effect of shear deformation causing rotation between the neutral-axis and the beam cross section and rotational inertia are taken into account. The effect of a finite shear modulus will lead to a more flexible model and hence lower natural frequencies which deliver a more conservative/realistic approach. In addition, when for a detailed analysis, finite element software can be used using different types of elements.

Bibliography

[1] [Online]. Available: http://www.ktf.no/fileadmin/Dokumenter/Kursdokumenter/2007/3-the-12th-north-sea-offshore-cranes-and-lifting-conference/22-transport-offshore-lifting.pdf

[2] ISO, "Adoptation of the international code on intact stability," 2008.

[3] J.M.JJournee and W.WMassie, *Offshore Hydromechanics*, 2001, vol. first edition.

[4] [Online]. Available: http://www.atmosferis.com/olas-oceanicas-calculo-de-su-energia/

[5] E. Delfos, "Huisman construction insights," 2003.

[6] M. B. Abeil, "J1800-class heavy lift vessel (134m); additional seakeeping tests," vol. volume 1, October, 2013.

[7] DNV-RP-H103, "Modelling and analysis of marine operations," *DNV*, April 2011.

[8] DNV-OS-H101, "Marine operations,general," 2011.

[9] A. F. B. R.J.M Pijpers, M.H. Kolenstein, "Fatigue experiments on very high strength steel base material and transverse butt welds," *Advanced Steel Construction Vol.5 No.1*, 2009.

[10] A. petroleum institute, "Specification for offshore pedestal mounted cranes," March, 2004.

[11] Megson, *Aircraft Structural analysis*. Elsevier Ltd., 2007.

[12] S. Rao, *Mechanical Vibrations*, T. Quinn, Ed. Prentice Hall, 2011.

[13] Y. W. Kwon and H. Bang, *The Finite Element Method Using Matlab*, F. A. Kulacki, Ed. Adrian Bejan, 1997.

[14] DNV, "Lifting appliances," *DNV*, June 2013.

Appendices

A Stability Report for maximum outreach

Weight Summary

Group Name	Weight	Long.Pos	TCG	VCG	F.S. Mom.
		Fwd of AP	SB:+	Above BL	
	t	m	m	m	t·m
WATER BALLAST TANKS	7180	68.85	-4.93	4.25	535
MARINE DIESEL OIL TANKS	103	18.09	-1.09	5.17	438
HEAVY FUEL OIL TANKS	635	54.20	-6.33	8.69	2593
LUBRICATING OIL TANKS	79	20.00	-0.15	2.47	70
FRESH WATER TANKS	70	117.37	-5.67	8.83	164
VARIOUS TANKS	66	85.03	1.71	5.49	130
MISCELLANEOUS TANKS	88	20.92	-0.57	1.21	63
STABILIIZER TANKS	0				0
CARGO	883	56.82	27.45	40.57	0
CRANES	0				0
STABILIZER POSITIONS	100	3.90	-0.00	20.87	0
HATCH COVERS	852	62.68	-0.55	15.57	0
TWEENDECK HATCH COVERS	604	72.78	-0.43	7.07	0
Deadweight	10660	65.22	-1.11	8.41	3992
Lightship	7755	61.07	1.61	11.20	
Displacement	18415	63.47	0.03	9.59	
Buoyancy	18414	63.46	0.03	3.75	

Loading Table

WATER BALLAST TANKS

Number	Description	DWT Type	Density	Max vol	% Full	Volume	Weight	VCG	FS mom.
								Above BL	
			t/m³	m³	%	m³	t	m	t·m
3013	FP CL WB	WB	1.025	586.2	0.00	0.0	0.0		0
115	DB 1 CL WB	WB	1.025	620.9	100.00	620.9	636.5	1.10	0
116	DB 1 SB WB	WB	1.025	297.8	100.00	297.8	305.3	1.20	0
114	DB 1 PS WB	WB	1.025	245.5	100.00	245.5	251.6	1.22	0
118	DB 2 CL WB	WB	1.025	430.0	100.00	430.0	440.8	1.08	0
119	DB 2 SB WB	WB	1.025	432.5	100.00	432.5	443.3	1.11	0
117	DB 2 PS WB	WB	1.025	389.3	100.00	389.3	399.1	1.12	0
122	DB 3 CL WB	WB	1.025	474.0	100.00	474.0	485.9	1.11	0
123	DB 3 SB WB	WB	1.025	490.5	100.00	490.5	502.7	1.12	0
121	DB 3 PS WB	WB	1.025	391.9	100.00	391.9	401.7	1.11	0
125	LW 1 SB WB	WB	1.025	501.9	0.00	0.0	0.0		0
131	UW 1 SB WB	WB	1.025	458.0	0.00	0.0	0.0		0
124	LW 1 PS WB	WB	1.025	361.9	100.00	361.9	370.9	5.30	0
130	UW 1 PS WB	WB	1.025	709.2	84.00	595.7	610.6	10.65	194
127	LW 2 SB WB	WB	1.025	499.5	0.00	0.0	0.0		0
133	UW 2 SB WB	WB	1.025	308.8	0.00	0.0	0.0		0
126	LW 2 PS WB	WB	1.025	561.0	100.00	561.0	575.1	4.98	0
132	UW 2 PS WB	WB	1.025	627.4	61.95	388.7	398.4	9.75	157
129	LW 3 SB WB	WB	1.025	505.7	0.00	0.0	0.0		0
135	UW 3 SB WB	WB	1.025	308.8	0.00	0.0	0.0		0
128	LW 3 PS WB	WB	1.025	537.4	100.00	537.4	550.8	5.29	0
134	UW 3 PS WB	WB	1.025	729.7	84.00	612.9	628.3	10.45	183
2014	AP PS WB	WB	1.025	174.5	100.00	174.5	178.9	8.39	0
136	TW 1 PS WB	WB	1.025	122.9	0.00	0.0	0.0		0
137	TW 2 PS WB	WB	1.025	125.4	0.00	0.0	0.0		0
139	TW 3 PS WB	WB	1.025	146.9	0.00	0.0	0.0		0
138	TW 2 SB WB	WB	1.025	121.2	0.00	0.0	0.0		0
140	TW 3 SB WB	WB	1.025	158.1	0.00	0.0	0.0		0
Total				**11317.1**	**61.89**	**7004.6**	**7179.8**	**4.25**	**535**

MARINE DIESEL OIL TANKS

Number	Description	DWT Type	Density	Max vol	% Full	Volume	Weight	VCG	FS mom.
2000	DB CL MDO	MDO	0.920	121.4	50.00	60.7	55.9	1.40	396
2017	DAY PS MDO	MDO	0.920	26.0	50.00	13.0	12.0	12.00	6
147	SB EDG MDO	MDO	0.920	2.2	50.00	1.1	1.0	14.64	0
20171	DAY PS MGO 1	MDO	0.920	26.1	50.00	13.1	12.0	12.00	3
2013	AP MGO SB	MDO	0.920	47.9	50.00	23.9	22.0	6.87	34
Total				**223.7**	**50.00**	**111.9**	**102.9**	**5.17**	**438**

HEAVY FUEL OIL TANKS

Number	Description	DWT Type	Density	Max vol	% Full	Volume	Weight	VCG	FS mom.
3007	DT SB HFO	HFO	0.985	137.6	50.00	68.8	67.8	8.85	164
3006	DT PS HFO	HFO	0.985	137.6	50.00	68.8	67.8	8.85	164
3003	OVERFLOW PS HFO	HFO	0.985	206.4	50.00	103.2	101.7	12.75	221
2012	AP CL HFO	HFO	0.985	184.6	50.00	92.3	90.9	6.00	1880
2015	PS HFO	HFO	0.985	317.6	50.00	158.8	156.4	7.72	86
2018	OVERFLOW PS HFO	HFO	0.985	73.5	50.00	36.7	36.2	5.24	27
2019	PRE SETTLING PS HFO	HFO	0.985	104.8	50.00	52.4	51.6	9.37	25

Numb er	Description	DWT Type	Density	Max vol	% Full	Volume	Weight	VCG	FS mom.
2021	DAY PS HFO	HFO	0.985	56.6	50.00	28.3	27.9	9.63	13
2020	SETTLING PS HFO	HFO	0.985	70.3	50.00	35.2	34.6	9.37	14
Total				**1289.0**	**50.00**	**644.5**	**634.8**	**8.69**	**2593**

LUBRICATING OIL TANKS

Numb er	Description	DWT Type	Density	Max vol	% Full	Volume	Weight	VCG	FS mom.
2007	SB LUB A.E.	LO .92	0.920	9.0	50.00	4.5	4.1	2.15	3
2008	SB LUB M.E.	LO .92	0.920	52.5	50.00	26.2	24.1	2.84	33
2005	DB SUMP PS	LO .92	0.920	16.1	50.00	8.0	7.4	0.76	2
2006	DB SUMP SB	LO .92	0.920	16.1	50.00	8.0	7.4	0.76	2
2022	LO ST GEAR BOX	LO .92	0.920	2.0	50.00	1.0	0.9	4.85	0
2023	HYD OIL ST CPP	LO .92	0.920	2.0	50.00	1.0	0.9	4.85	0
2024	HYD OIL ST GEAR	LO .92	0.920	0.6	50.00	0.3	0.3	9.05	0
2010	PS SEP SLUDGE	LO .95	0.950	27.0	50.00	13.5	12.8	3.09	6
2009	PS SLUDGE	LO .95	0.950	41.9	50.00	21.0	19.9	2.55	23
2025	OVERFLOW LUB A.E.	LO .92	0.920	1.2	50.00	0.6	0.6	2.46	0
148	SB LUB EDG	LO .92	0.920	0.3	50.00	0.2	0.2	14.98	0
Total				**168.8**	**50.00**	**84.4**	**78.7**	**2.47**	**70**

FRESH WATER TANKS

Numb er	Description	DWT Type	Density	Max vol	% Full	Volume	Weight	VCG	FS mom.
3009	PS 1 FW	FW	1.000	72.6	50.00	36.3	36.3	8.85	73
3010	PS 2 FW	FW	1.000	68.3	50.00	34.1	34.1	8.80	90
Total				**140.9**	**50.00**	**70.4**	**70.4**	**8.83**	**164**

VARIOUS TANKS

Numb er	Description	DWT Type	Density	Max vol	% Full	Volume	Weight	VCG	FS mom.
149	TH OIL EXPANSION TK	GREY 1.0	1.000	3.7	50.00	1.8	1.8	15.03	0
3005	DB CL GREY WATER	GREY 1.0	1.000	48.6	50.00	24.3	24.3	0.79	100
3008	CL SEWAGE	GREY 1.0	1.000	44.1	50.00	22.1	22.1	8.68	7
150	SANITARY TK	GREY 1.0	1.000	1.7	50.00	0.9	0.9	4.23	0
20131	AP T.O. SB	GREY 1.0	1.000	34.6	50.00	17.3	17.3	7.08	22
Total				**132.8**	**50.00**	**66.4**	**66.4**	**5.49**	**130**

MISCELLANEOUS TANKS

Numb er	Description	DWT Type	Density	Max vol	% Full	Volume	Weight	VCG	FS mom.
2011	DB PS TO DRAIN	MISC .92	0.920	13.5	50.00	6.7	6.2	3.38	4
2004	DB SB DIRTY WATER	MISC 1.0	1.000	28.4	50.00	14.2	14.2	0.76	6
2002	DB SB LUB DRAIN	MISC 1.0	1.000	23.5	50.00	11.7	11.7	0.76	20
2001	DB PS DIRTY/LEAK OIL	MISC .985	0.985	24.4	50.00	12.2	12.0	0.71	19
2003	DB PS TECH WATER	MISC 1.0	1.000	35.8	50.00	17.9	17.9	0.74	8
2026	PS SHAFT COOL WATER	MISC 1.025	1.025	25.7	50.00	12.9	13.2	1.69	3
2027	SB SHAFT COOL WATER	MISC 1.025	1.025	25.7	50.00	12.9	13.2	1.69	3
Total				**176.9**	**50.00**	**88.5**	**88.4**	**1.21**	**63**

Unit Cargo Table

CARGO

Name	Color	Description	Type	Amount	Auto	Weight	LCG	TCG	VCG	Length	Width	Height
							Fwd of AP	SB:+	Above BL			
						t	m	m	m	m	m	m
Pedestal1			(none)	1	OFF	152	32.82	10.05	38.40	2.0	2.0	2.0
Pedestal2			(none)	1	OFF	152	80.82	10.05	38.40	2.0	2.0	2.0
Unit Load (2)			(none)	1	OFF	580	56.82	36.55	41.70	2.0	2.0	2.0
Total				**3**		**883**	**56.82**	**27.45**	**40.57**			

CRANES

Name	Color	Description	Type	Amount	Auto	Weight	LCG	TCG	VCG	Length	Width	Height
							Fwd of AP	SB:+	Above BL			
						t	m	m	m	m	m	m
(Boom)			(none)	1	ON	100	38.42	16.50	23.88	0.0	0.0	0.0
(Boom - Lightship compensation)			(none)	1	ON	-100	32.82	6.98	31.17	0.0	0.0	0.0
(Hook)			(none)	1	ON	27	55.82	36.55	27.26	0.0	0.0	0.0
(Hook - Lightship compensation)			(none)	1	ON	-27	32.82	4.42	51.06	0.0	0.0	0.0
(Boom)			(none)	1	ON	100	68.70	24.01	24.85	0.0	0.0	0.0
(Boom - Lightship compensation)			(none)	1	ON	-100	80.82	5.59	41.07	0.0	0.0	0.0
(Hook)			(none)	1	ON	27	57.82	36.55	27.26	0.0	0.0	0.0
(Hook - Lightship compensation)			(none)	1	ON	-27	80.82	4.42	51.06	0.0	0.0	0.0
Total				**8**		**0**	**-1.#J**	**1.#J**	**-1.#J**			

STABILIZER POSITIONS

Name	Color	Description	Type	Amount	Auto	Weight	LCG	TCG	VCG	Length	Width	Height
							Fwd of AP	SB:+	Above BL			
						t	m	m	m	m	m	m
(PONTOON WEIGHT)		Pontoon 1	(none)	1	ON	69	3.91	-0.00	22.07	8.0	11.0	3.7
(PONTOON WEIGHT)		Pontoon 2	(none)	1	ON	30	3.89	-0.00	18.16	5.0	10.5	3.7
Total				**2**		**100**	**3.90**	**-0.00**	**20.87**			

HATCH COVERS

Name	Color	Description	Type	Amount	Auto	Weight	LCG	TCG	VCG	Length	Width	Height

							Fwd of AP	SB:+	Above BL			
						t	m	m	m	m	m	m
(HATCH COVER WEIGHT)		Hatch Cover No.1	(none)	1	O N	98	108.00	-0.55	15.57	12.8	17.1	1.6
(HATCH COVER WEIGHT)		Hatch Cover No.2	(none)	1	O N	99	95.20	-0.55	15.57	12.8	17.1	1.6
(HATCH COVER WEIGHT)		Hatch Cover No.3	(none)	1	O N	98	82.40	-0.55	15.57	12.8	17.1	1.6
(HATCH COVER WEIGHT)		Hatch Cover No.4	(none)	1	O N	120	69.61	-0.55	15.57	12.8	17.1	1.6
(HATCH COVER WEIGHT)		Hatch Cover No.5	(none)	1	O N	120	56.80	-0.55	15.57	12.8	17.1	1.6
(HATCH COVER WEIGHT)		Hatch Cover No.6	(none)	1	O N	120	44.00	-0.55	15.57	12.8	17.1	1.6
(HATCH COVER WEIGHT)		Hatch Cover No.7	(none)	1	O N	98	31.20	-0.55	15.57	12.8	17.1	1.6
(HATCH COVER WEIGHT)		Hatch Cover No.8	(none)	1	O N	99	18.40	-0.55	15.57	12.8	17.1	1.6
Total				**8**		**852**	**62.68**	**-0.55**	**15.57**			

TWEENDECK HATCH COVERS

Name	Col or	Description	Type	Am ount	Au to	Weight	LCG	TCG	VCG	Length	Width	Height
							Fwd of AP	SB:+	Above BL			
						t	m	m	m	m	m	m
(HATCH COVER WEIGHT)		Tweendeck Hatch Cover No.1	(none)	1	O N	45	111.16	-0.41	7.07	6.1	16.9	1.2
(HATCH COVER WEIGHT)		Tweendeck Hatch Cover No.2	(none)	1	O N	47	104.80	-0.45	7.07	6.4	16.9	1.2
(HATCH COVER WEIGHT)		Tweendeck Hatch Cover No.3	(none)	1	O N	47	98.40	-0.45	7.07	6.4	16.9	1.2
(HATCH COVER WEIGHT)		Tweendeck Hatch Cover No.4	(none)	1	O N	47	92.00	-0.45	7.07	6.4	16.9	1.2
(HATCH COVER WEIGHT)		Tweendeck Hatch Cover No.5	(none)	1	O N	47	85.60	-0.45	7.07	6.4	16.9	1.2
(HATCH COVER WEIGHT)		Tweendeck Hatch Cover No.6	(none)	1	O N	47	79.20	-0.45	7.07	6.4	16.9	1.2
(HATCH COVER WEIGHT)		Tweendeck Hatch Cover No.7	(none)	1	O N	47	72.80	-0.45	7.07	6.4	16.9	1.2
(HATCH COVER WEIGHT)		Tweendeck Hatch Cover No.8	(none)	1	O N	47	66.40	-0.45	7.07	6.4	16.9	1.2
(HATCH COVER WEIGHT)		Tweendeck Hatch Cover No.9	(none)	1	O N	47	60.00	-0.41	7.07	6.4	16.9	1.2
(HATCH COVER WEIGHT)		Tweendeck Hatch Cover No.10	(none)	1	O N	47	53.59	-0.41	7.07	6.4	16.9	1.2
(HATCH COVER WEIGHT)		Tweendeck Hatch Cover No.11	(none)	1	O N	46	47.19	-0.41	7.07	6.4	16.9	1.2
(HATCH COVER WEIGHT)		Tweendeck Hatch Cover No.12	(none)	1	O N	47	40.79	-0.41	7.07	6.4	16.9	1.2
(HATCH		Tweendeck	(none)	1	O	45	34.52	-0.41	7.07	6.0	16.9	1.2

Name	Color	Description	Type	Amount	Auto	Weight	LCG	TCG	VCG	Length	Width	Height
							Fwd of AP	SB:+	Above BL			
						t	m	m	m	m	m	m
COVER WEIGHT)		Hatch Cover No.13			N							
Total				**13**		**604**	**72.78**	**-0.43**	**7.07**			

Stability

Heeling direction: Starboard

Vh = 0.0°; Vc > 40.0°; Max GZ = 2.432 m; GZ Area = 0.849 m·rad

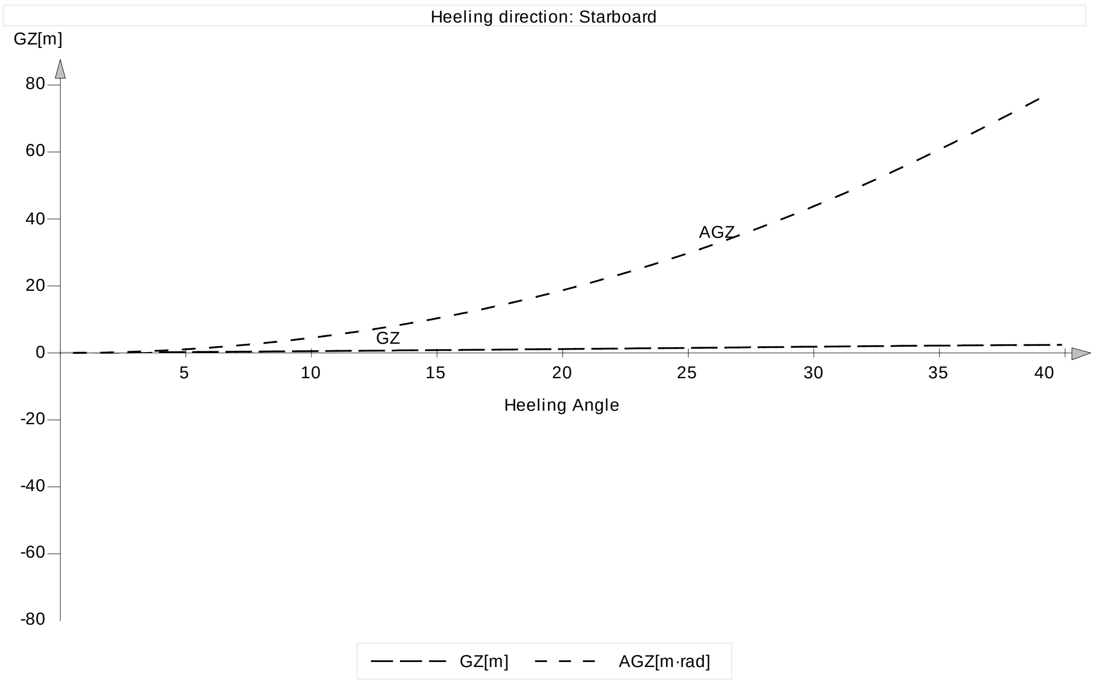

Heeling Angle	D.Mean	Trim	RM	GZ	AGZ	TCG	LCG	VCG
		ByBow:+				SB:+	Fwd of AP	Above BL
deg		m	t·m	m	m·rad	m	m	m
-1.00	6.94	-0.34	-1007	-0.05	0.000	0.03	63.47	9.59
0.00	6.94	-0.34	-2	-0.00	0.000	0.03	63.47	9.59
1.00	6.94	-0.34	1003	0.05	0.000	0.04	63.47	9.59
2.00	6.93	-0.32	2009	0.11	0.002	0.04	63.47	9.59
3.00	6.93	-0.31	3019	0.16	0.004	0.05	63.47	9.59
4.00	6.92	-0.30	4034	0.22	0.008	0.05	63.47	9.59
5.00	6.90	-0.29	5053	0.27	0.012	0.05	63.47	9.59
6.00	6.89	-0.28	6079	0.33	0.017	0.06	63.47	9.59
7.00	6.87	-0.26	7111	0.39	0.023	0.06	63.47	9.59
8.00	6.85	-0.24	8153	0.44	0.031	0.06	63.47	9.59
9.00	6.83	-0.22	9206	0.50	0.039	0.07	63.47	9.59
10.00	6.80	-0.20	10273	0.56	0.048	0.07	63.47	9.59
11.00	6.77	-0.18	11357	0.62	0.058	0.07	63.47	9.59
12.00	6.74	-0.16	12456	0.68	0.070	0.07	63.47	9.59
13.00	6.70	-0.14	13572	0.74	0.082	0.08	63.47	9.59
14.00	6.66	-0.11	14702	0.80	0.095	0.08	63.47	9.59
15.00	6.62	-0.08	15846	0.86	0.110	0.08	63.47	9.59
16.00	6.58	-0.05	17003	0.92	0.125	0.08	63.47	9.59
17.00	6.53	-0.02	18171	0.99	0.142	0.08	63.47	9.59
18.00	6.48	0.01	19351	1.05	0.160	0.09	63.47	9.59
19.00	6.43	0.04	20540	1.12	0.179	0.09	63.47	9.60
20.00	6.37	0.07	21738	1.18	0.199	0.09	63.47	9.60
21.00	6.31	0.11	22943	1.25	0.220	0.09	63.47	9.60
22.00	6.24	0.14	24162	1.31	0.242	0.09	63.47	9.60
23.00	6.18	0.17	25401	1.38	0.266	0.10	63.47	9.60
24.00	6.11	0.20	26667	1.45	0.290	0.10	63.47	9.60
25.00	6.03	0.23	27965	1.52	0.316	0.10	63.47	9.60

Heeling Angle	D.Mean	Trim	RM	GZ	AGZ	TCG	LCG	VCG
		ByBow:+				SB:+	Fwd of AP	Above BL
deg		m	t·m	m	m·rad	m	m	m
26.00	5.95	0.25	29299	1.59	0.344	0.10	63.47	9.60
27.00	5.87	0.27	30658	1.66	0.372	0.10	63.47	9.60
28.00	5.79	0.29	32027	1.74	0.402	0.10	63.47	9.60
29.00	5.70	0.31	33394	1.81	0.433	0.11	63.47	9.60
30.00	5.60	0.32	34743	1.89	0.465	0.11	63.47	9.60
31.00	5.51	0.33	36061	1.96	0.498	0.11	63.47	9.60
32.00	5.41	0.33	37337	2.03	0.533	0.11	63.47	9.61
33.00	5.30	0.34	38560	2.10	0.569	0.11	63.47	9.61
34.00	5.19	0.34	39721	2.16	0.606	0.11	63.47	9.61
35.00	5.08	0.34	40808	2.22	0.645	0.11	63.47	9.61
36.00	4.96	0.34	41811	2.27	0.684	0.11	63.47	9.61
37.00	4.84	0.34	42720	2.32	0.724	0.12	63.47	9.61
38.00	4.72	0.34	43525	2.37	0.765	0.12	63.47	9.61
39.00	4.59	0.35	44214	2.40	0.806	0.12	63.47	9.61
40.00	4.45	0.35	44777	2.43	0.849	0.12	63.47	9.61

Criteria Evaluation

Evaluated Stability Criteria Set "IMO A749 Standard Stability Criteria" is satisfied!

Heeling direction: Most Critical
GM Fluid: Minimum to satisfy this criteria set: 0.148 m, Actual: 3.126 m
KG Fluid: Maximum to satisfy this criteria set: 12.782 m, Actual: 9.804 m

Number	Criterion	Actual	Required	KG fluid req	GM fluid req	Heel
				m	m	
1	GM Upright > 0.15	3.127	0.150	12.78	0.15	Starboard
2	GZ(30.00°) > 0.200 m	1.887	0.200	12.93	0.00	Starboard
3	Vm should be in range [30.00°, Vc]	40.000	30.000	12.93	0.00	Starboard
4	Vm should be in range [25.00°, Vc]	40.000	25.000	12.93	0.00	Starboard
5	GZ area in range [Vh, 30.00°] > 0.055 m·rad	0.465	0.055	12.86	0.07	Starboard
6	GZ area in range [Vh, 40.00°] > 0.090 m·rad	0.849	0.090	12.93	0.00	Starboard
7	GZ area in range [0.00°,Vfl] > 0.090 m·rad, Unprotected openings	0.849	0.090	12.93	0.00	Starboard
8	GZ area in range [30.00°, 40.00°] > 0.030 m·rad	0.384	0.030	12.93	0.00	Starboard
9	GZ area in range [30.00°,Vfl] > 0.030 m·rad, Unprotected openings	0.384	0.030	12.93	0.00	Starboard
10	Weather criterion, Res. area in [Vf, min(Vfl, Vs, 50.00°)] / res. area in [Vw, Vf] > 1.000, Unprotected openings, Gust wind	4.236	1.000	12.93	0.00	Starboard

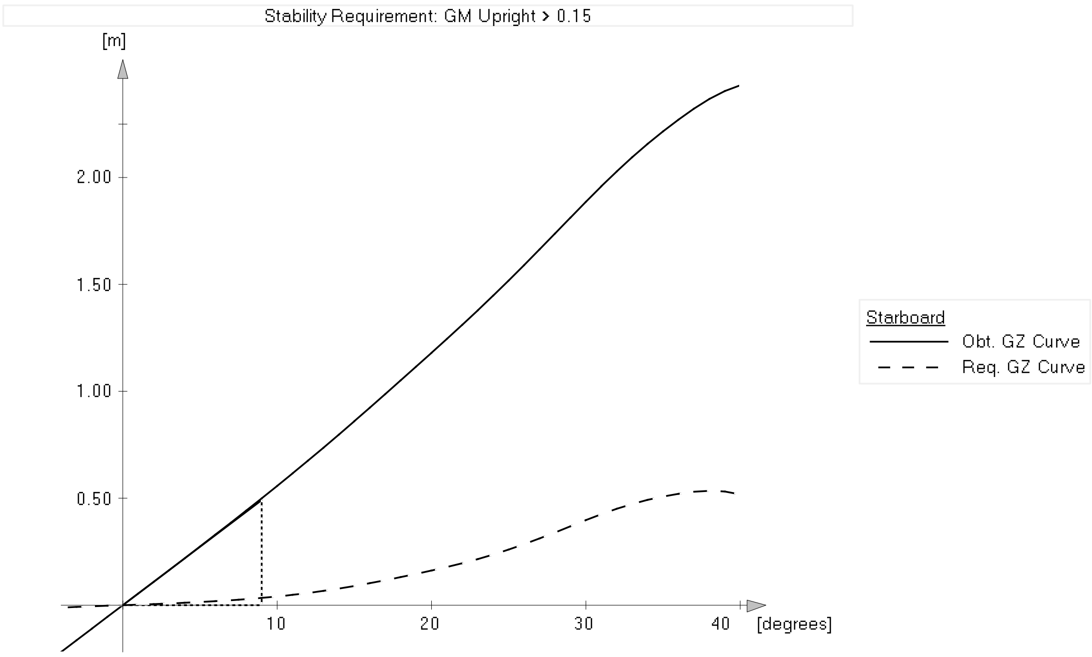

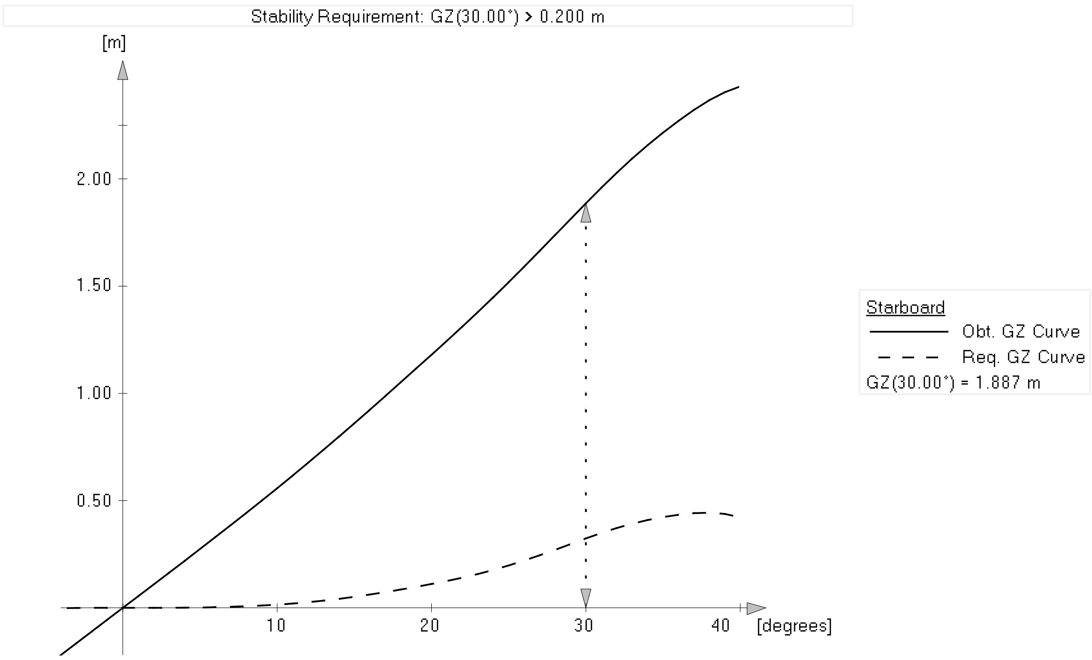
Stability Requirement: GZ(30.00°) > 0.200 m
[m]
2.00
1.50
1.00
0.50
10
20
30
40
[degrees]
Starboard
Obt. GZ Curve
Req. GZ Curve
GZ(30.00°) = 1.887 m

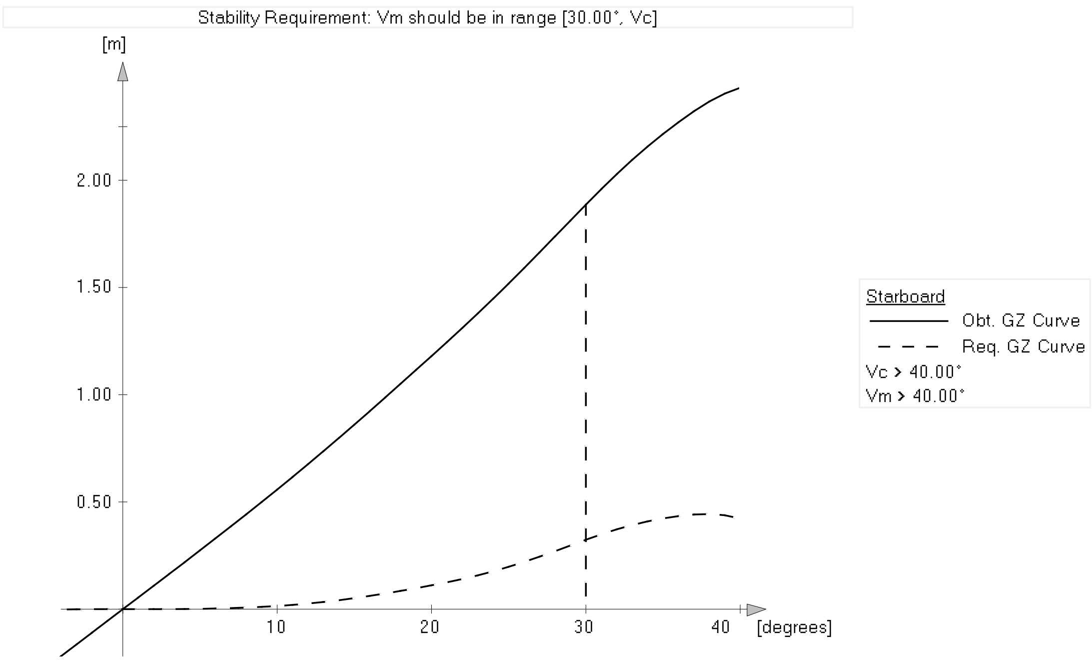
Stability Requirement: Vm should be in range [30.00°, Vc]
[m]
2.00
1.50
1.00
0.50
10
20
30
40
[degrees]
Starboard
Obt. GZ Curve
Req. GZ Curve
Vc > 40.00°
Vm > 40.00°

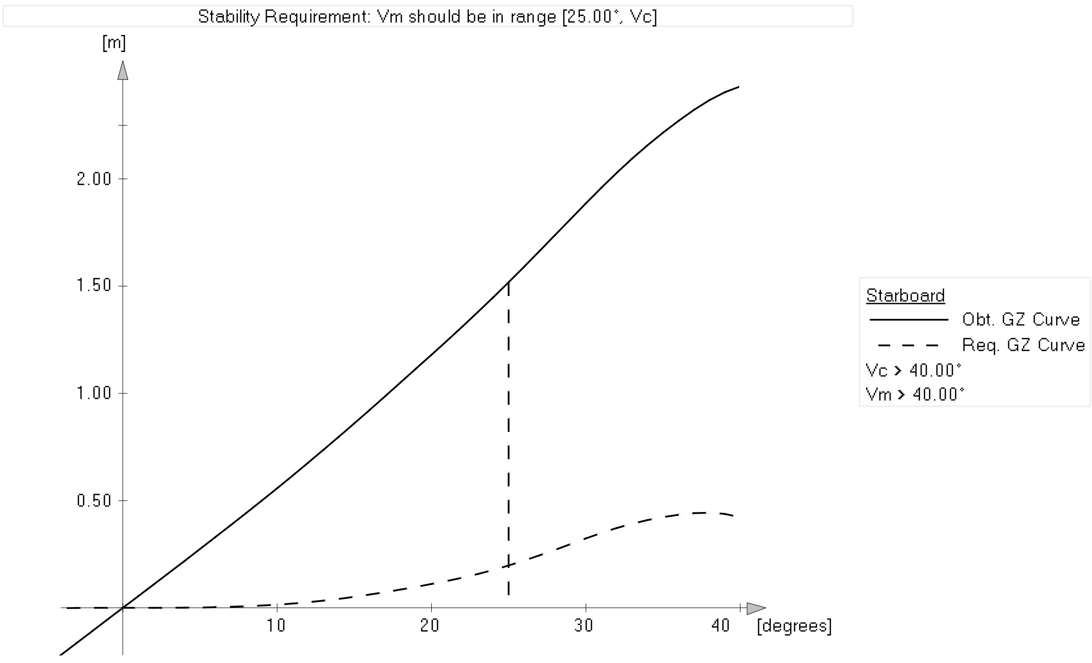
Stability Requirement: Vm should be in range [25.00°, Vc]
[m]
2.00
1.50
1.00
0.50
10
20
30
40
[degrees]
Starboard
Obt. GZ Curve
Req. GZ Curve
Vc > 40.00°
Vm > 40.00°

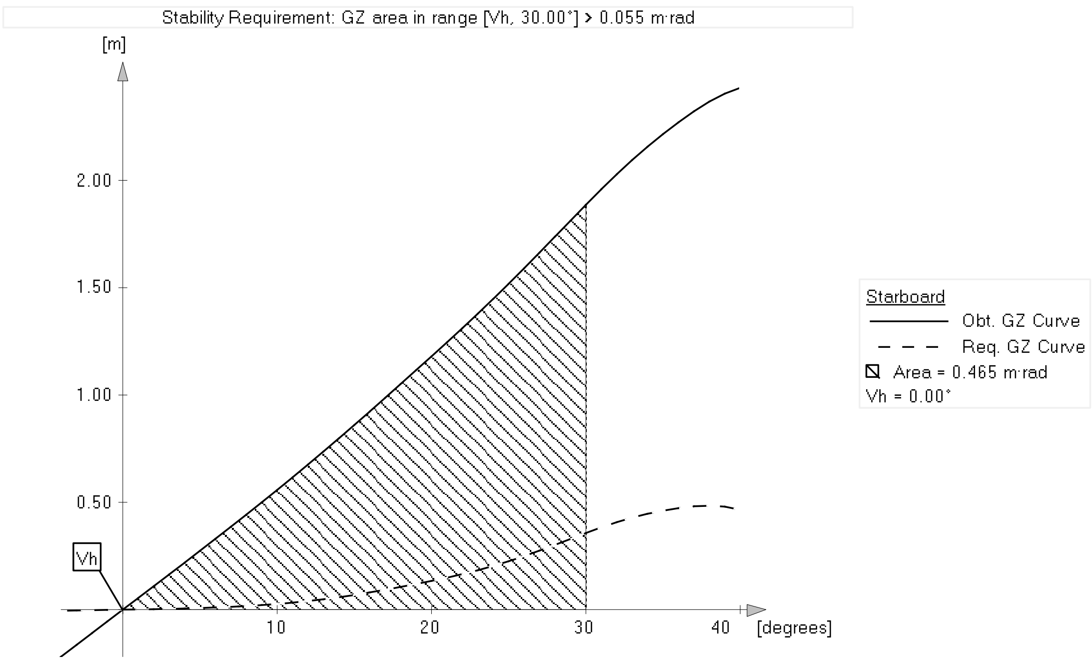
Stability Requirement: GZ area in range [Vh, 30.00°] > 0.055 m·rad
[m]
2.00
1.50
1.00
0.50
Vh
10
20
30
40
[degrees]
Starboard
Obt. GZ Curve
Req. GZ Curve
Area = 0.465 m·rad
Vh = 0.00°

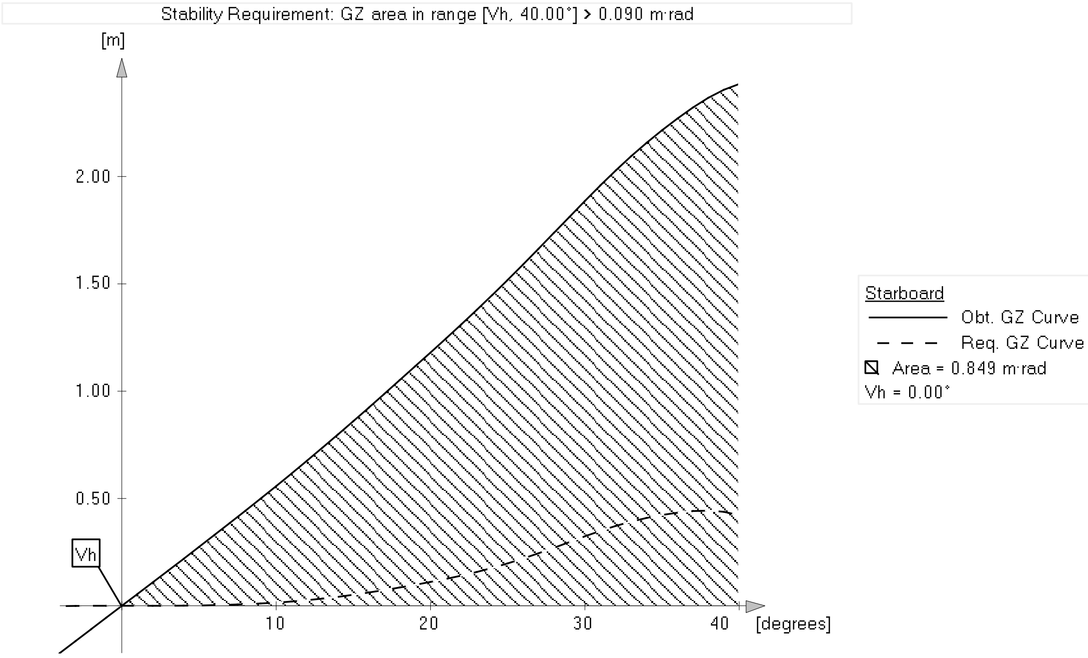
Stability Requirement: GZ area in range [Vh, 40.00°] > 0.090 m·rad
[m]
2.00
1.50
1.00
0.50
Vh
10
20
30
40
[degrees]
Starboard
Obt. GZ Curve
Req. GZ Curve
Area = 0.849 m·rad
Vh = 0.00°

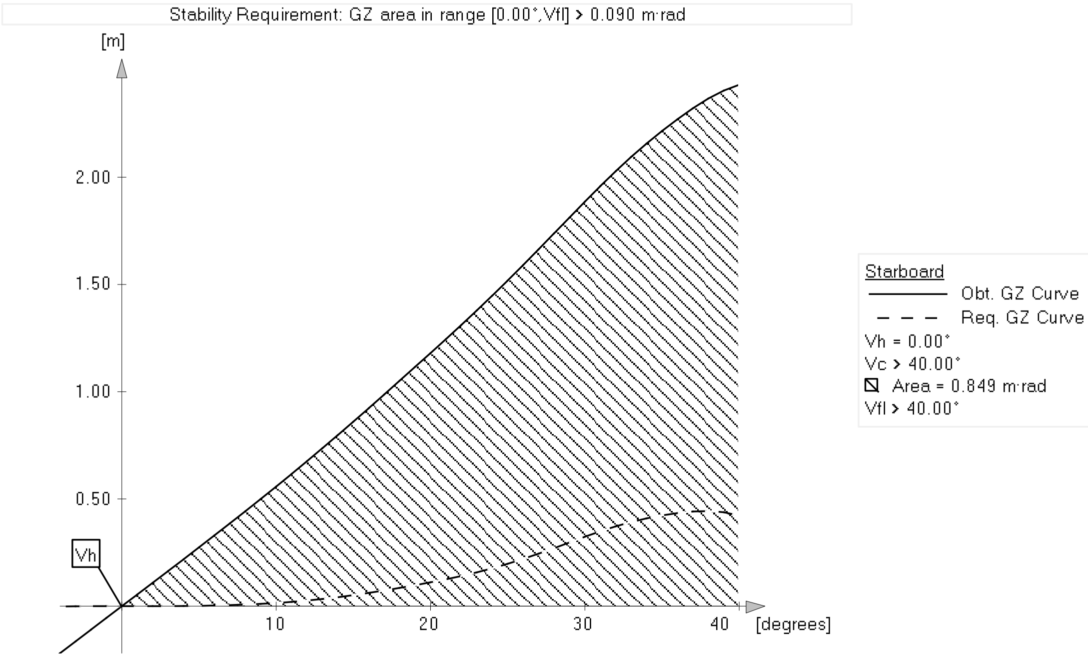
Stability Requirement: GZ area in range [0.00°,Vfl] > 0.090 m·rad
[m]
2.00
1.50
1.00
0.50
Vh
10
20
30
40
[degrees]
Starboard
Obt. GZ Curve
Req. GZ Curve
Vh = 0.00°
Vc > 40.00°
Area = 0.849 m·rad
Vfl > 40.00°

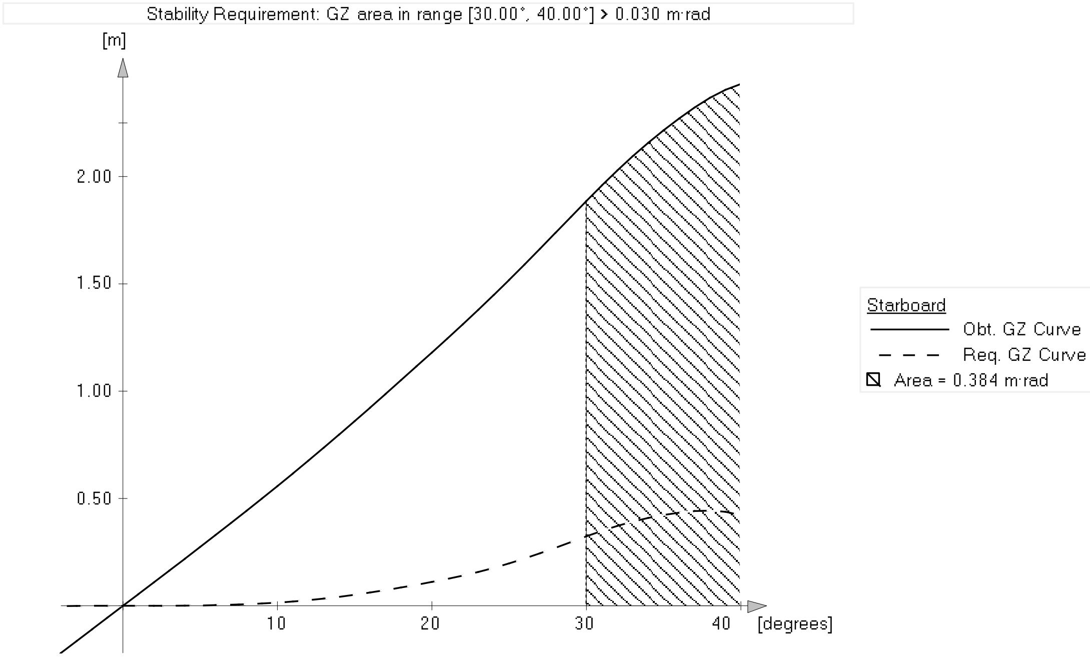

Stability Requirement: GZ area in range [30.00°, 40.00°] > 0.030 m·rad
[m]
2.00
1.50
1.00
0.50
10
20
30
40
[degrees]
Starboard
Obt. GZ Curve
Req. GZ Curve
Area = 0.384 m·rad

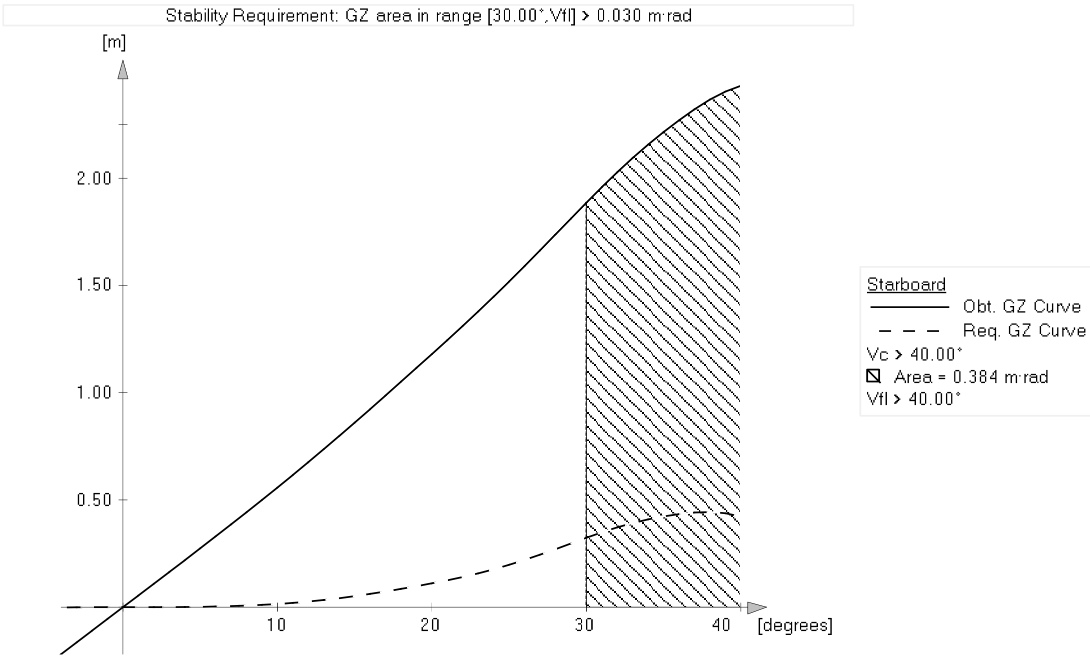

Stability Requirement: GZ area in range [30.00°,Vfl] > 0.030 m·rad
[m]
2.00
1.50
1.00
0.50
10
20
30
40
[degrees]
Starboard
Obt. GZ Curve
Req. GZ Curve
Vc > 40.00°
Area = 0.384 m·rad
Vfl > 40.00°

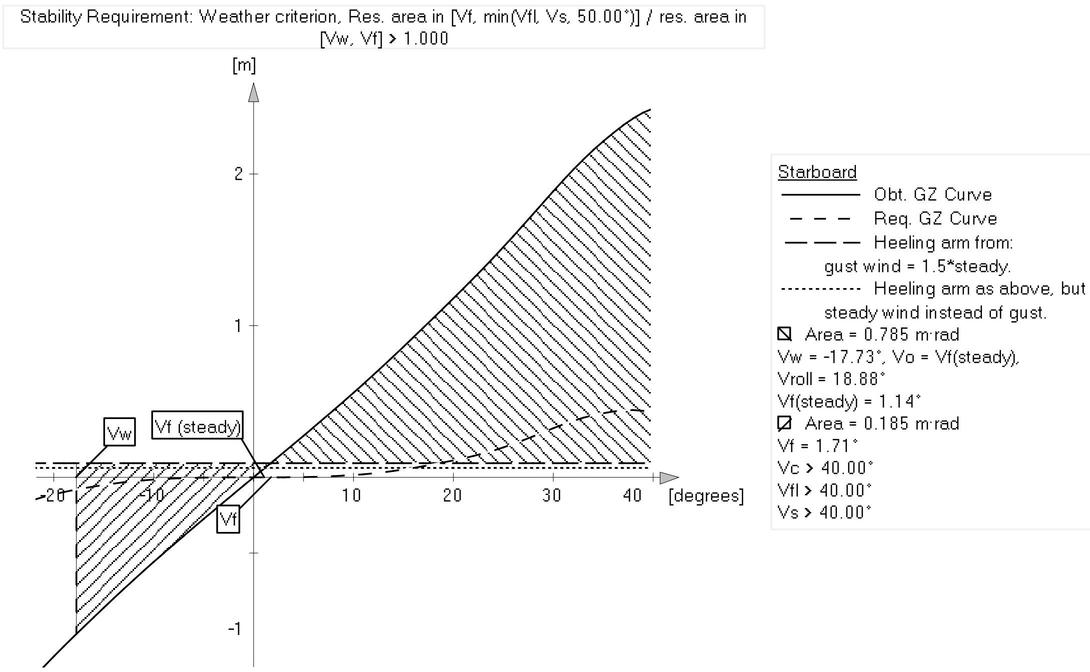
Stability Requirement: Weather criterion, Res. area in [Vf, min(Vfl, Vs, 50.00°)] / res. area in [Vw, Vf] > 1.000
[m]
2
1
-1
-20
-10
10
20
30
40
[degrees]
Vw
Vf (steady)
Vf
Starboard
Obt. GZ Curve
Req. GZ Curve
Heeling arm from:
gust wind = 1.5*steady.
Heeling arm as above, but
steady wind instead of gust.
Area = 0.785 m·rad
Vw = -17.73°, Vo = Vf(steady),
Vroll = 18.88°
Vf(steady) = 1.14°
Area = 0.185 m·rad
Vf = 1.71°
Vc > 40.00°
Vfl > 40.00°
Vs > 40.00°

B Thickness distribution due to M_y

From the moment of inertia around the y-axis of the pedestal, in combination with the requirement to fail at material yield stress, the thickness distribution along the height of the pedestal is given below.

$$I_{yy} = \frac{1}{12}HB^3 - \frac{1}{12}(H - 2t_H)(B - 2t_B)^3 \tag{1}$$

Or

$$I_{yy} = \frac{1}{12}HB^3 - \frac{1}{12}H(1 - \frac{2t}{H})(B^3(1 - \frac{6t}{B}) + 12B^3(\frac{t}{B})^2) \tag{2}$$

Thickness distribution for shape 1:

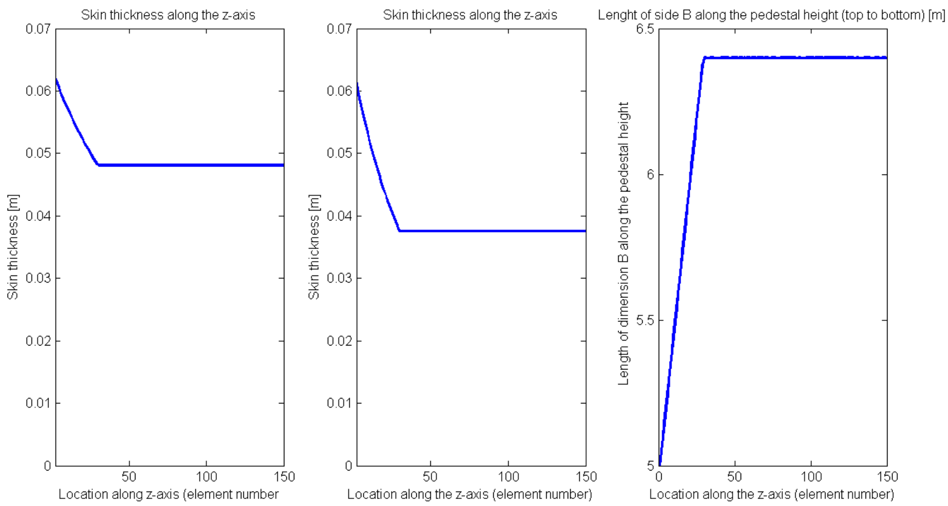

Figure 1: Thickness distribution and dimensions of lenght B

Thickness distribution for shape 2:

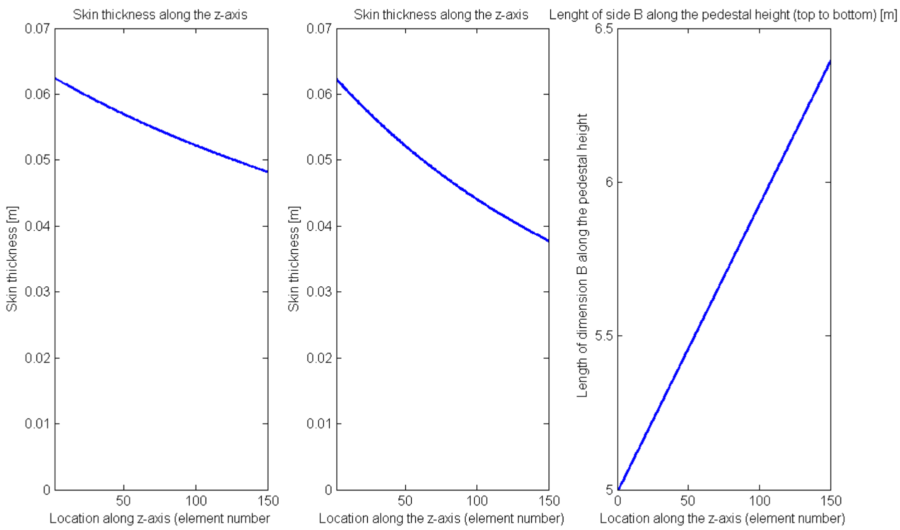

Figure 2: Thickness distribution and dimensions

C Numerical model explanation

In this appendix the basic principles of the program setup are explained. The Matlab code consists of 7 functions and one main script. The functions are listed below:

coordi_angle: Obtains x and y-coordinates of each node with angle β
connection: Relates each nodal connection with each element
feeldof: Extracting system DOF for each element
frame: Obtain stiffness and mass matrix for each element
asmb11: Assembly of element stiffness matrix into the global system matrix
asmbl1: Assemply of the element mass mattrix into the gloabl system matrix
feaplycs: Applying boundary conditions
Naturalfrequencies: Main script

Also, some attention should be spend on the relation between the numbering of the degrees of freedom of each element and the system degrees of freedom. The numbering is listed in the table below. An example of the spatial degrees of freedom of three elements is shown.

Local and global DOF's			
Local DOF	Global DOF element 1	Global DOF element 2	Global DOF element 3
1	1	4	7
2	2	5	8
3	3	6	9
4	4	7	10
5	5	8	11
6	6	9	12

Table 1: Global and local DOF's

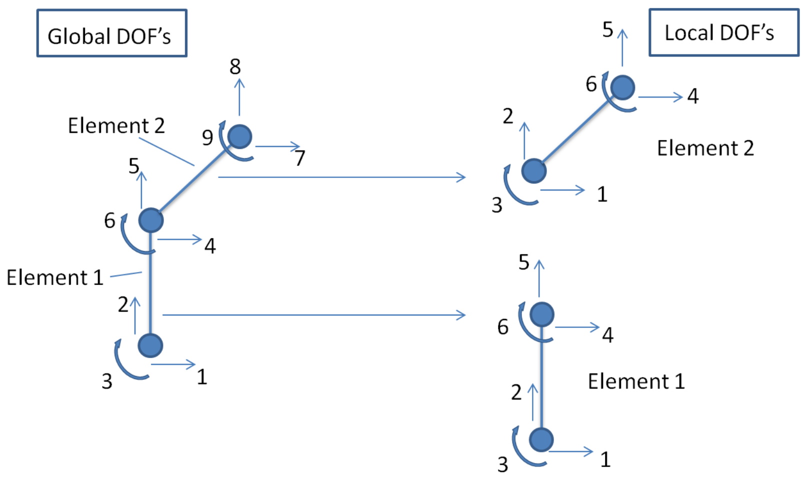

Figure 3: Global and local DOF's

The total finite element model is visualized in figure 4

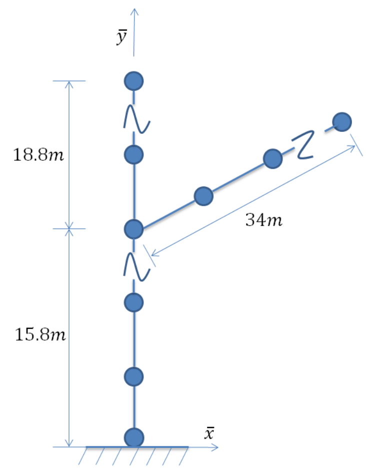

Figure 4: Total finite element model